TEL AVIV UNIVERSITY

SACKLER FACULTY OF MEDICINE

THE DR. MIRIAM AND SHELDON G. ADELSON

DEPARTMENT OF PHYSIOLOGY

Unsupervised characterization of human brain networks that are involved in emotional processing and regulation

THESIS SUBMITTED FOR THE DEGREE "DOCTOR OF PHILOSOPHY"

BY ADI MARON-KATZ

SUBMITTED TO THE SENATE OF TEL AVIV UNIVERSITY

October 2015

This work was carried out under the academic supervision of

Talma Hendler

Professor of Psychiatry and Psychology

School of Psychological Science, Sagol School of Neuroscience, Faculty of Medicine Tel-Aviv University

Director, Functional Brain Center , Wohl Institute for Advanced Imaging, Tel-Aviv Sourasky Medical Center

AND

Ron Shamir

Professor of Computer Sciences

Blavatnik School of Computer Science Tel-Aviv University

Dedicated with gratitude to my parents and entire family for their love and encouragement, and especially to Oded, Shachar and Ofek. Without your love and support I would not have completed this thesis.

Acknowledgements:

I wish to start by thanking my Yoga professor Orit Sen-Gupta, who by beautifully sharing her knowledge of the Yogic philosophy of the mind, inspired me to go on this quest. I wish to thank my advisors Prof. Talma Hendler and Prof. Ron Shamir who made it possible for me.

I also wish to thank my fellow students in the lab at Wohl Institute for Advances Imaging at the Tel-Aviv Sourasky Medical Center as well as in the lab for Computational Genomics at Tel-Aviv University for their help and support all through my PhD. Especially I would like to thank Michal Ballas-Gruberger and Haggai Sharon for their invaluable support and inspiration; Eti Ben Simon, David Amar, Sharon Vaisvase, Tamar Lin and Gadi Gilam for productive collaboration; Gal Raz, Shahar Jamshy, Ilana Podlipsky and Yael Yaakov for helpful discussions.

Thanks ☺

This work was supported by the Israeli ministry of Science and Technology

TABLE OF CONTENT

List of Figures and Tables

List of equations

Abbreviations and symbols

Brain regions: Anterior Cingulate Cortex (ACC); Amygdala (Amy); Basolateral Amygdala (BLA); Inferior Frontal Gyrus (IFG); Prefrontal Cortex (PFC); dorsolateral PFC (DPLFC); Superior temporal sulcus (STS); Posterior cingulate cortex (PCC); Visual network (VN); Default-mode network (DMN); Fronto-parietal control network (FPCN); Sub-lobular (SL); Auditory network (AN); Executive control network (ECN); Ventral attention network (VAN); Dorsal attention network (DAN); Sensory-motor network (SMN)

Brain imaging and physiology: Functional Magnetic Resonance Imaging (fMRI); Magnetic Resonance Imaging (MRI); Electroencephalogram (EEG); General Electric (GE); repetition time (TR); Region Of Interest (ROI); field potential (LFP); Heart rate (HR); Heart rate variability (HRV); Electrocardiogram (ECG);

Others: Post-traumatic Stress Disorder (PTSD); Functional Connectivity (FC), Resting State (rs); Leave-one-out cross validation (LOOCV); Ultimatum-game (UG); Trier Social Stress Test (TSST); Degree preserving permutation (DPP); Hypergeometric (HG); inter-subject correlation (ISC); Automated Anatomic Labeling (AAL)

1. ABSTRACT

Background

In the past decade and a half, the neuroscience community has learned that during rest, ongoing energy consuming activity takes place in the brain. When focusing on low frequencies, this activity is highly correlated within known functional networks. Although these correlated fluctuations are generally maintained over time, they were shown to vary with changes in cognitive and emotional states, and were suggested to hold information on individual history of interaction with the world as well as a priori cognitive and emotional biases.

Exploration of variability in resting-state (rs) neural functional connectivity (FC) through functional magnetic resonance imaging (fMRI) has been traditionally performed using hypothesis-driven analysis while focusing on one or a few pre-defined seed regions. This approach can reveal only a fraction of the actual phenomenon as it relies on prior knowledge of the putative functional network structure. An alternative approach is to conduct a whole-brain voxel-wise analysis, which is computationally expensive and sensitive to noise. A possible compromise is to define a set of regions of interest (ROIs) that provide good coverage of the brain. Such dimensionality reduction allows conducting whole-brain rsFC analysis while treating the data as a collection of independent connections and performing statistical analyses of each connection separately. Alternatively, multivariate techniques evaluate the relationship between the entire connectome matrices and their associated phenotypic variables in a single statistical test. While powerful, such analysis does not reveal information on the involvement of individual connections.

Despite the methodological progress in studying variability in rsFC patters, to date findings that are obtained from large-scale rsFC analysis are mostly interpreted by a qualitative comparison to known neural maps which are is based on existing literature. Such methodology does not use statistical tools for interpretation, and holds the risk of reporting false positive results and missing important findings. In order to perform this interpretation rigorously one

must address it statistically. A natural way to do this is by testing whether a link between two known brain regions or functional networks is significantly more prevalent in the results than would be expected by chance (i.e. enriched). Analysis of enrichment has long been used in the field of Bioinformatics, and is the acceptable way for characterizing large sets of genes that emerge from data driven genomic analysis.

This work uses rsfMRI to examine the way in which different types of emotionally challenging experiences affect patterns of neural coactivation in subsequent resting periods. This is done using several approaches for large-scale rsFC analysis in combination with enrichment analysis as an established manner for interpretation. Assuming that rsFC holds information on individual tendencies as well as on prior experience, we examined inter-individual differences in these patterns and their relation to various behavioral measures of emotional reactivity and regulation. We hypothesized that emotionally challenging experiences will induce large scale changes in patterns of fMRI rsFC. We further expected these changes to be associated with subjective measures of emotional experience.

Objectives:

1) Develop improved means for characterizing and interpreting large-scale changes in FC patterns of rsfMRI data.
2) Data-driven investigation of rsFC modulations following several different types of “emotional challenge”.
3) Identify inter-individual differences in rsFC modulations that correspond to inter-individual differences in measures of affective experience.

Methods

To evaluate enrichment within sets of neural positions we adopted the statistical hyper-geometric test. We used the same test to evaluate enrichment within sets of neural connections, however for this case we added an additional non-parametric permutation test, which accounts for uneven levels of FC in different brain areas. Both tests were integrated into the RichMind Matlab package. Given a collection of findings (neural positions or connections), and a known neural mapping, RichMind tests for enrichment in the input, and provides both statistical reports and brain visualization of the identified enrichments. The

software was validated on two previously published studies, the first conducted on healthy participants viewing emotion-inducing film clips, and the second on participants with amnestic mild cognitive impairment.

Next, we analyzed data recorded before and after three different emotionally–challenging paradigms: a social-stress induction task, an anger-provoking inter-personal conflict task (the ultimatum game; UG) and a night without sleep (i.e. sleep deprivation; SD). In all three cases a pre-defined functional parcellation was applied on the data before analysis for dimensionality reduction. We used a univariate analysis approach to identify rsFC changes. In the sleep deprivation study we used a combination of univariate analysis with multivariate approaches of leave-one-out cross validation (LOOCV) and modularity analysis, due to the small sample size. Large-scale findings were characterized using enrichment analysis. Emotional experience was measured using a number of self-reported questionnaires, and in some cases also using a physiological measure of heart-rate and heart-rate variability.

Main results

Following the Trier social stress test we identified a large-scale rsFC change across the brain, which included strengthening of thalamo-cortical connectivity alongside a weakening of cross-hemispheral parieto-temporal connectivity. These alterations were associated with change in subjective stress reports. Integrating report-based information on stress sustainment 20 minutes post induction revealed a single significant rsFC change between the right basolateral amygdala (BLA) and the precuneus, which inversely predicted the level of subjective recovery. A parcel centered in the right amygdala demonstrated differential rsFC also following the inter-personal conflict task. Specifically, it showed increased rsFC with a single parcel centered in the right inferior frontal gyrus. Baseline levels of overall rsFC of that parcel were positively correlated with subsequent subject gain in UG as well as reported anger following the game.

Following SD we identified a large-scale pattern of decreased thalamo-cortical rsFC and increased rsFC of the left frontal inferior operculum with a distributed set of cortical regions. The increased rsFC pattern was marginally associated with change in negative mood. Furthermore, the extent of rsFC change across

all differential connections was positively associated with trait-anxiety measured at the beginning of the experiment. LOOCV analysis revealed that this distributed pattern distinguishes between SD and baseline states with an accuracy level of 94.1%. Modularity analysis that was applied on the group-level average rsFC matrices, combined with enrichment analysis, revealed a pattern of network reorganization involving regions of the default-mode network (DMN), the Limbic network and the fronto-parietal control network. This change was associated with the change in reported mood.

Conclusions

The novel use of enrichment analysis, introduced here for studying changes in rsFC, allowed improved insight on experience-related neural modulations in cases where the induced effect is large and distributed. This type of improvement was observed when analyzing rsFC modulations induced by acute social stress as well as following SD. The changes that were identified following each of the tasks were different by nature, however, it can be said that they share a common mechanism in which inter-individual differences and past experiences affect the connectivity between the limbic system and the DMN, which, in turn, affects the subjective emotional experience.

From a methodological perspective, we believe that data-driven rsFC analysis combined with enrichment analysis comprises a productive tool with a diagnostic potential for investigating alterations in neural connectivity.

2. Introduction

2.1 The resting Brain

"Tis the great art of life to manage well the restless mind."

John Armstrong , *The Art of Preserving Health*, 1744

Although most cognitive neuroscience research has traditionally focused on mapping the details of task-induced activation patterns, in recent years it has become it became clear that even in the absence of a task – that is, in what appears to be a state of rest , ongoing activity takes place in the brain (Harmelech and Malach 2013, Kelly and Castellanos 2014). This activity has been shown to be a compulsive user of energy and resources (Raichle and Mintun 2006, Raichle 2010). In blood oxygen-level-dependent (BOLD) functional MRI (fMRI), these fluctuations appear to span the entire cortex and are of similar amplitude to those produced during task performance (Nir, Hasson et al. 2006). These patterns have also been documented in human single unit and local field potential (LFP) recordings (He, Snyder et al. 2008, Nir, Mukamel et al. 2008, Manning, Jacobs et al. 2009, Keller, Bickel et al. 2013, Foster, Rangarajan et al. 2015), revealing that their dynamics is far slower than typical task activations (Nir, Mukamel et al. 2008). When focusing on low frequencies, this activity demonstrates high correlations within known functional networks (Biswal, Zerrin Yetkin et al. 1995), correlations that extend beyond primary sensory and motor systems to circuits supporting higher order cognitive and social function (Greicius, Krasnow et al. 2003, Beckmann, DeLuca et al. 2005, Fox, Snyder et al. 2005). This correspondence between task-evoked and resting-state architectures suggests

that correlated activity at rest serves to maintain the integrity of neuronal networks, supporting cognition and action, even in the absence of processing demands. Patterns of resting-state functional connectivity (rsFC) are understood to constitute a trace of task-evoked coactivation among regions within an individual. By consequence, the complete set of resting state networks (RSNs) within an individual, also termed the functional connectome, can be seen to comprise of both universal and unique aspects (Biswal, Mennes et al. 2010, Kelly and Castellanos 2014). The universal aspects comprises of the set of phylogenetically determined functional networks that, in the absence of developmental aberration, emerge in all individuals (Buckner and Krienen 2013), and are evident in observations of precursory RSNs in infants and young children (Gao, Zhu et al. 2009, Dinstein, Pierce et al. 2011, Fransson, Åden et al. 2011), of homologous RSNs in other species (Vincent, Patel et al. 2007, Margulies, Vincent et al. 2009, Hutchison, Gallivan et al. 2012, Lu, Zou et al. 2012), in the reproducibility of RSNs across hundreds of studies and samples (e.g., (Biswal, Mennes et al. 2010)), and in the moderate-to-high test-retest reliability of RSNs over both short and long intervals (Shehzad, Kelly et al. 2009, Thomason, Dennis et al. 2011). The unique aspects of the functional connectome, on the other hand, appear to reflect the individual history of interaction each person has with the world, which sculpts patterns of evoked coactivation and thus fine-tunes the intrinsic brain architecture (Harmelech and Malach 2013). This aspect is demonstrated by studies linking differences in rsFC to genetic variation (Glahn, Winkler et al. 2010, Liu, Song et al. 2010, Wiggins, Bedoyan et al. 2012, Tunbridge, Farrell et al. 2013), environmental influences such as early life stress (Burghy, Stodola et al. 2012, Herringa, Birn

et al. 2013), and interindividual differences in a variety of behavioral characteristics including task performance, social competence, and personality (Hampson, Driesen et al. 2006, Tambini, Ketz et al. 2010, Adelstein, Shehzad et al. 2011). Together, these traces of previous coactivation patterns provide a predictive neural context, a preparatory state that anticipates future patterns of evoked coactivation (Fox and Raichle 2007, Deco and Corbetta 2011, Raichle 2011, Engel, Gerloff et al. 2013). That is, these spontaneous fluctuations capitalize on the individual's history of interactions with the world, i.e. past experience, to optimize the brain's readiness to respond to similar inputs in the future (Kelly and Castellanos 2014).

2.2 Experience related fingerprint in resting state fMRI

Assuming that an individual's past experience has an effect on personal biases and tendencies, the notion that rsFC patterns reflect these biases, is supported by the vast body of research showing traces of task-evoked coactivation patterns in successive resting state periods. This has been demonstrated for cognitive and motor tasks (Waites, Stanislavsky et al. 2005, Lewis, Baldassarre et al. 2009, Vahdat, Darainy et al. 2011, Wang, Liu et al. 2012, Harmelech, Preminger et al. 2013, Guidotti, Del Gratta et al. 2015) as well as for tasks that present an emotional challenge (Van Marle, Hermans et al. 2010, Eryilmaz, Van De Ville et al. 2011, Riedl, Valet et al. 2011, Veer, Oei et al. 2011, Vaisvaser, Lin et al. 2013). For example: Lewis et al. (2009) trained participants on performing a difficult perceptual target detection task for several days, leading to significantly improved performance. Comparing rs-fMRI data

acquired before and after training revealed that after training, negative rsFC between the trained portion of visual cortex and regions of the dorsal attention network (DAN), was strengthened, while negative correlations with the default mode network (DMN) were weakened. The former change was also associated with behavioral evidence of learning. The authors interpret the redistribution of rsFC observed to reflect the active decoupling of DAN and visual areas that occurs with the development of expertise on and automation of the trained task (Lewis, Baldassarre et al. 2009). In another study Eryilmaz et al. investigated the effect of emotionally joyful and fearful video clips on subsequent rsfMRI patterns in 15 healthy participants. They reported a strong enhancement of rsFC between ACC and insula as well as an increased level of activity in these regions following emotional context alongside a reduction in ventro-medial prefrontal cortex and amygdala rsFC that was selective to fearful context (Eryilmaz, Van De Ville et al. 2011).

2.3 Neural traces of Inter-individual differences in handling emotionally-challenging experiences

Emotion is a dynamic, complex psycho-physiological experience of an individual's state of mind as interacting with internal and external influences. As emotion is an inseparable part of human experience, its proper regulation has been acknowledged as a key function that is required for adapting to socially accepted norms as well as for maintaining well-being, and its dysregulation could lead to various forms of psychopathology (Cicchetti, Ackerman et al. 1995, John and Gross 2004).

In spite of the fact that emotional experiences are common to all humans, high inter-individual variability exists in the process that takes place between the occurrence of an event and the emotional response, as has been demonstrated with subjective (behavioral) as well as neurophysiological measures (Admon, Lubin et al. 2009, Admon, Leykin et al. 2013, Lin, Vaisvaser et al. 2015). These differences result from the fact that events impinge on different personality traits and concerns (Silvia, Henson et al. 2009, Smith and Kirby 2009), as well as different appraisal propensities in different individuals (Frijda 2009, Van Mechelen and Hennes 2009). For example, inter-individual differences have been demonstrated in stress vulnerability and tendency to develop post-traumatic stress disorder (PTSD) (McEwen 2004, Yehuda and LeDoux 2007). This variability has been associated with the tendency to attend to a threatening stimuli (Bar-Haim, Lamy et al. 2007), trait anxiety (McFarlane 1990) and neural activity in limbic regions and prefrontal cortex (Admon, Lubin et al. 2009, Admon, Milad et al. 2013). Another example is the individual tendency to use specific regulation strategies such as reappraisal or suppression. The frequent explicit use of reappraisal has been associated with lower levels of negative affect, greater interpersonal functioning, and greater psychological and physical well-being (Gross and John 2003). Moreover Greater use of reappraisal in everyday life has been associated to decreased amygdala activity and increased prefrontal and parietal activity during the processing of negative emotional facial expressions (Drabant, McRae et al. 2009).

In spite of the above, the question remains, to what extent are inter-individual differences in emotion generation, processing and regulation evident in the variability of rsFC patterns.

2.4 Methods for studying variability in resting state functional connectivity

Several approaches have been used to study changes in FC patterns. Analytic hypothesis-driven routines like seed based analysis (Biswal, Zerrin Yetkin et al. 1995) have been used in numerous studies investigating cognitive functions (Rissman, Gazzaley et al. 2004, Uddin, Clare Kelly et al. 2009, Mennes, Kelly et al. 2010). However, this approach is limited to revealing only a fraction of the actual phenomenon as it relies on prior knowledge of the putative functional network structure. An alternative approach is to conduct a whole-brain voxel-wise analysis, but such an approach is computationally expensive, sensitive to noise, and difficult to interpret. Furthermore, there is high redundancy in the representation of the data at the voxel scale, which makes it possible to significantly reduce the dimensionality of the fMRI data (Craddock, James et al. 2012). This can be done by defining a set of regions of interest (ROIs) that provide good coverage of the brain. The definition of ROIs is crucial both for the estimation of connectomes and for group comparison (Wang, Wang et al. 2009, Varoquaux and Craddock 2013). Several strategies exist for defining suitable ROIs. One popular approach is to use anatomic definitions (Shehzad, Kelly et al. 2009, Wang, Wang et al. 2009, Zeng, Shen et al. 2012) however, while the regions defined by these atlases are anatomically or cyto-architectonically homogeneous, they do not necessarily have homogeneous activity patterns. For example, it has been shown that adjacent regions of the

anterior cingulate cortex (ACC) have drastically different structural and FC patterns (Margulies, Kelly et al. 2007, Beckmann, Johansen-Berg et al. 2009), even though the ACC is typically represented as a single ROI in brain atlases (Talairach and Tournoux 1988). Another approach is to define a whole-brain functional parcellation using the fMRI signals, which results in more homogeneous regions that better represent connectivity present at the voxel level than anatomically-defined atlases such as the anatomic atlas labeling (AAL) or Harvard-Oxford (Craddock, James et al. 2012). This has been done using various clustering methods (Beckmann and Smith 2004, Thirion, Flandin et al. 2006, Bellec, Rosa-Neto et al. 2010, Craddock, James et al. 2012), and has been shown to identify well-known functional structures from rest data (Varoquaux and Craddock 2013). Notably, the most appropriate number of regions (i.e. resolution) for whole-brain connectivity analysis should be carefully considered. On one hand a sufficiently large number of regions is needed to ensure functional homogeneity within regions and adequate representation of FC information in the data. On the other hand too many regions reduce the power of statistical inference and increase computational complexity (Varoquaux and Craddock 2013). In order to estimate an optimal number of regions cross-validation methods can be employed (Blumensath, Behrens et al. 2012, Craddock, James et al. 2012). For example, Craddock et. al. (2012) used a spatially constrained spectral clustering algorithm on rsfMRI data recorded from 41 healthy subjects. Resulting parcellations, comprised of 200, 500 and 1000 parcels, were evaluated and compared against anatomic atlases and random parcellations on an independent dataset. Evaluation was based on homogeneity, the ability to reproduce connectivity information present at the

voxel scale, and the ability to obtain the same parcellations from independent data. The authors report that ROIs generated from their clustering approach outperformed anatomic atlas-based ROIs as well as random parcellations in all measures (Craddock, James et al. 2012). This reported ability to obtain a very similar parcellation from independent data allows such a parcellation to be used as a pre-defined template in other studies rather than repeat the parcellation process for each study. Thus, in all data driven analysis performed throughout this work, we defined ROIs using the parcellation templates generated in the above study. The choice of the template resolution depended on the number of subjects, to allow sufficient statistical power for data driven analysis.

After defining ROIs and extracting the BOLD signal for each ROI, a similarity measure (usually Pearson correlation coefficient) can be used to estimate the level of rsFC for each pair of ROIs, producing a whole-brain rsFC matrix. The simplest approach to compare such whole-brain rsFC matrices is to treat them as a collection of independent connections and perform statistical analyses of each connection separately, without accounting for interactions or relationships between them (Varoquaux and Craddock 2013). Such analysis results in a set of p-values (one for each connection), which can be obtained using t-tests, F-tests, regression, etc. that indicate the extent of identified difference for each connection. Such results are relatively easy to interpret. However, this approach involves many statistical tests, which require correction for multiple comparisons to adequately control for the number of false positives. Standard correction techniques such as false discovery rate (Genovese, Lazar et al. 2002) that do not model the dependencies between edges may result in overly liberal or conservative corrections (Efron 2008, Craddock, Jbabdi et al. 2013).

Alternatively, multivariate techniques evaluate the relationship between the entire connectome matrices and their associated phenotypic variables with a single statistical test (Craddock, Holtzheimer et al. 2009, Dosenbach, Nardos et al. 2010). Although powerful, such analysis does not reveal information on the involvement of individual connections; extracting such information requires a return to connection-specific tests, which necessitate multiple-comparison correction (Craddock, Holtzheimer et al. 2009, Craddock, Jbabdi et al. 2013) .

Regardless of the exact method used, data-driven analysis of variability in rsFC often produces large sets of neural positions or position pairs (i.e. functional connections). The interpretation of such sets is usually done by comparing them against an existing neural mapping based on previous literature. In some cases, where the number of results is large, they are filtered either by manual selection or by repeating the analysis with a stricter statistical threshold, to facilitate interpretation. As the interpretation is often done without a clear statistical justification, such methodology holds the risk of reporting false positive results and missing additional results. Thus, a more rigorous method of interpretation is required to allow improved inference of data-driven results.

3. Research Objectives

In this work we address two gaps that exist in the current literature. The first is a methodological gap: the lack of rigorous means for interpreting large-scale

changes in rsFC. The second is the following question: to what extent are inter-individual differences in affective experience evident in the variability of rsFC patterns? Accordingly, we define the following objectives:

Objective 1: Develop improved means for characterizing large-scale changes in connectivity patterns of task-free (resting state) fMRI data: Such means should facilitate the interpretation of large sets of modified functional connections and/or functional modules under previously established neural mapping schemes, and provide these sets with statistical significance. The approach will be validated on previously published large-scale neural results.

We hypothesize that this approach will allow interpreting large-scale results that were not interpreted in the original studies. We further hypothesize that it will statistically collaborate most of the claims made in the original studies, and possibly add additional insight.

Objective 2: Data-driven investigation of changes induced in resting-state fMRI patterns following different types of emotional challenges.

This will be done by investigation of existing rsfMRI data, recorded from three different groups of participants in three independent experiments. Analysis will involve a hypothesis-free parcellation-based whole-brain exploration, with no a-priori assumptions regarding the identity of the networks and the inference of their behavioral relevance to the specific emotional experience. We expect to find a unique effect of rsFC change across participants, following each challenge. We further expect some of these effects to be of large-scale, in

accordance with previous literature, and thus require special means for interpretation.

Objective 3: Identify inter-individual differences in rsFC modulations that correspond to inter-individual differences in affective behavioural measures

Inter-individual differences in the identified changes in rsfMRI patterns will be compared against several behavioral and physiological measures which have been validated as indicators of emotional experience. We hypothesize that some of the modulations identified across participants (i.e. objective 2) will be sensitive to inter-individual differences in affective behavioral measures.

4. General methods and materials

This section describes materials and methods that were applied for most or all of the studies included in this work. Specific adaptations made in certain cases are described in the specific context of each study in the next sections.

4.1 Functional MRI

4.1.1 Background - fMRI is a noninvasive neuroimaging method that is typically utilized to provide the blood-oxygen-level-dependent (BOLD) signal. This signal has been shown to reflect hemodynamic responses coupled with stimulus-induced neuronal activity, and thus it comprises an indirect index of such local activity. While neuronal activity affects the factors of blood volume and blood oxygenation (Fox, Raichle et al. 1988, Attwell, Buchan et al. 2010), it is mainly the coupled increased blood flow that enhances the BOLD signal. Following glutamate release during neural activation, neurons and astrocytes send molecular messengers inducing nitric oxide, prostaglandins to smooth muscles of the adjacent blood vessels. These messengers cause the dilation of the vessels and thus increase the blood flow (Attwell, Buchan et al. 2010).

The enhanced flow locally increases the ratio between red blood cells containing oxidized hemoglobin and those that have deactivated form of hemoglobin. Deoxidized hemoglobin has stronger magnetic influence on its surrounding than oxidized hemoglobin and it produces measurable inhomogeneity in the magnetic field. Its displacement by the increasing blood flow about two seconds after the onset of the stimulus-induced neuronal activity therefore increases inhomogeneity and therefore causes a rise in the BOLD signal[96]. Finally, it should be noted that comparative studies of fMRI and

intracranial recording indicate that BOLD mainly reflects local field potential, which is influenced by synaptic input to the local neurons (post-synaptic activity) and internal neural processing rather the by regional output.

4.1.2 fMRI acquisition - All of the MRI scans included in this work were performed in a 3 Tesla, General Electric scanner, Horizon echo speed scanner with an 8-channel head coil and a resonant gradient echoplanar imaging system (GE, Milwaukee, WI, USA) located at the Wohl Institute for Advanced Imaging at the Tel-Aviv Sourasky Medical Center.

4.1.3 fMRI preprocessing and parcellation

Preprocessing was performed using SPM software (http://www.fil.ion.ucl.ac.uk/spm). Head motions were detected and corrected using trilinear and sinc interpolations respectively, applying rigid body transformations with 3 translation and 3 rotation parameters. The criterion for data exclusion due to exaggerated head motions was deviations higher than 2.5 mm from the reference point. . Spatial smoothing with a 6 mm FWHM kernel was applied. Anatomical SPGR data were standardized to 1x1x1 mm and transformed into MNI space. SPGR images were then manually co-registered with the corresponding functional maps. Before further analysis, low frequency fluctuations (0.01–0.08Hz) in blood oxygenation level-dependent (BOLD) signals were filtered out using DPARSF toolbox [102].

In all studies we used whole-brain functional parcellations reported in (Craddock, James et al. 2012), which was generated by applying a correlation-based clustering procedure on rsfMRI data recorded from 41 healthy subjects,

and partitions the brain volume into either 200 or 517 parcels. Parcels were masked to include gray matter voxels only using the WFU Pick Atlas Tool (Maldjian, Laurienti et al. 2003, Stamatakis, Adapa et al. 2010) and parcels that had less than 5 voxels in common with the gray matter mask were excluded, leaving 182 and 463 parcels respectively. For each scan, average BOLD value across all gray matter voxels was calculated within each parcel at each time point. These time series were used as the parcel's signal.

4.1.4 Cross correlation functional connectivity analysis

In all studies, the level of rsFC between every two parcels was estimated separately for each subject and scan by calculating the Pearson correlation coefficient between the corresponding BOLD signals. The Pearson correlation coefficient is given by:

$$\textbf{(4-1)}\quad r_{x,y} = corr(X,Y) = E\left[(X-\bar{X})(Y-\bar{Y})\right]/\sigma_x\,\sigma_y$$

Before making statistic inference of these correlation values they were Fisher transformed to better fit a normal distribution, which is assumed in the parametric statistical student t-test. The Fisher transformation is given by:

$$\textbf{(4-2)}\quad Fisher\big(corr(X,Y)\big) = arctan[corr(X,Y)]$$

All p-values obtained in rsFC analysis were controlled for a false discovery rate (FDR) of 0.05 using the procedure suggested by Benjamini and Hochberg (Benjamini and Hochberg 1995).

4.2 Behavioral measures of affective response

Several behavioral and physiological measures were used in this work as indices of affective response. Of these, the *State-Trait Anxiety Inventory (STAI) (Spielberger 2010)* was collected and used in all three experiments. The other measures are described in the specific materials and methods sections of each experiment. STAI is a 40-item gold standard questionnaire for assessing anxiety. State Anxiety reflects subjective feelings of tension, nervousness, and arousal, and fluctuates in intensity over time as a function of perceived threat. Items are rated on a 4 -point frequency scale from 1 (not at all) to 4 (very much). Trait anxiety relates to stable individual differences in anxiety proneness, i.e. the tendency one has in perceiving stressful situations as dangerous and threatening (and thus reflects the disposition to respond to such situations with increased state anxiety). Items are rated on a 4 -point frequency scale from 1 (almost never) to 4 (almost always). The psychometric properties of these scales are well established (Spielberger and Sydeman 1994, Spielberger, Sydeman et al. 1999).

4.3 Comparing neural measures against behavioral and other physiological measures

In all studies, identified neural changes were compared against behavioral measures as well as physiological measures using Spearman's rank correlation coefficient, which is a nonparametric measure of statistical dependence, and thus makes no assumptions on the nature of the measured variables [106]. Spearman's rank correlation coefficient is given by:

$$r_{XY} = \boldsymbol{E}\left[\left(\boldsymbol{rank}(\boldsymbol{X}) - \overline{\boldsymbol{rank}(\boldsymbol{X})}\right)\left(\boldsymbol{rank}(\boldsymbol{Y}) - \overline{\boldsymbol{rank}(\boldsymbol{Y})}\right)\right] \Big/ \boldsymbol{\sigma}_{\boldsymbol{rank}(\boldsymbol{X})}\, \boldsymbol{\sigma}_{\boldsymbol{rank}(\boldsymbol{Y})} \quad \textbf{(4-3)}$$

5. IMPROVING INTERPRETATION OF LARGE-SCALE CHANGES IN RESTING STATE NETWORKS

In this chapter, we address the methodological gap that was introduced in chapter 2.4 (i.e. objective 1), namely, the lack of means for rigorous interpretation of large-scale changes in patterns of rsFC.

A paper describing this section was written and is currently under review

5.1 Background

As described in chapter 3, various methods exist for data-driven investigation of variability in rsfMRI patterns. Many of these methods identify large sets of neural positions (i.e. voxels or parcels) demonstrating an activity pattern of interest (e.g. increased/decreased nodal degree following a specific task). To date, functional interpretation of such large-scale neuroimaging findings is often done by associating the identified regions to known *classes* (e.g., anatomic structures or functional networks). This process of using previous knowledge to ascribe functional meaning to findings is commonly based on a subjective visual inspection or on percent of overlap with existing maps (Nummenmaa, Glerean et al. 2012, Jola, McAleer et al. 2013, Wang, Zuo et al. 2013, Lahnakoski, Glerean et al. 2014, Ames, Honey et al. 2015). Such methodology, which is not based on statistical justification, holds the risk of reporting false positive results and overlooking additional results. For example, Nummenmaa et al. (2012) analyzed fMRI signals recorded from 16 healthy participants, while viewing film clips depicting unpleasant, neutral, and pleasant emotions. They identified cerebral regions where inter-subject correlations (ISC) were significantly correlated with subjective reports of valence and arousal provided by the participants. In order to interpret the findings, the authors subjectively associated the identified regions to known functional networks. They reported that arousal was mostly associated with ISC in regions of the sensori-motor network (SMN), visual network (VN) and dorsal attention network (DAN) while valence was negatively associated with ISC in regions of the default mode

network (DMN) as well as regions known to be involved in emotional processing (Nummenmaa, Glerean et al. 2012). However, as in many neuroimaging studies, no quantitative statistical measure was presented to support this association of findings to functional networks. An even more complex case is the case where the identified findings are a collection of neural position pairs (i.e. connections). When this collection is very large, as may occur in data-driven studies (Finn, Shen et al. 2014, Sripada, Kessler et al. 2014, Tyszka, Kennedy et al. 2014), interpretation becomes challenging. In some cases, this challenge is faced by filtering the results either by manual selection or by repeating the analysis using a stricter statistical threshold. For example Wang et. al. (2013) reported a set of 363 functional connections (FCs) that differed between a group of amnestic mild cognitive impairment (aMCI) patients and healthy controls. These connections were identified using the network-based statistic approach (Zalesky, Fornito et al. 2010) using a predefined 1024 functional parcellation (Craddock, James et al. 2012, Wang, Zuo et al. 2013). Results significance was estimated using a permutation test. However, due to the complexity of interpreting such a large set of connections, analysis was repeated using a stricter statistical threshold**.**

An alternative approach to interpreting such a large set of findings is to test whether the results contain significantly more elements with a specific class than expected by chance. For instance, one can examine whether an identified set of weakened connections in terms of DMN-SMN connectivity, and explore whether aMCI is associated with a significantly large number of weakened connections linking the DMN with the SMN. If the answer is positive, we say that the corresponding class (i.e. DMN-SMN) is *enriched* in the identified

collection. Such enrichment (or over-representation) can be assigned with a statistical significance value under an appropriate null hypothesis (Rahnenführer, Domingues et al. 2004, Glaab, Baudot et al. 2012).

In this study we propose using *enrichment analysis* to facilitate and improve the interpretation process of large-scale fMRI studies. We focus on two possible cases. In the first, *position-group analysis,* the identified collection is a set of neural positions (e.g. following inter-subject correlation analysis). In the second, *connection group analysis*, the identified collection is a set of neural position pairs that represent connections between brain regions (e.g. following a data-driven functional connectivity analysis). We examined different models for detecting significant overrepresentation of known functional brain annotation using simulated and real data.

We implemented our methods in RichMind, a computational tool that provides both statistical significance reports based on our suggested enrichment analysis methods, as well as brain visualizations. We demonstrate the abilities of RichMind by reanalyzing two previous fMRI studies: the first of subjects viewing emotion-inducing film clips (Nummenmaa, Glerean et al. 2012), and the second of subjects suffering from aMCI (Wang, Zuo et al. 2013). We show that by using enrichment analysis, we were able to provide statistical validation to most of the conclusions drawn in the original studies, while revealing additional statistically significant results. In addition we show how enrichment analysis allows interpreting a large set of results without having to apply additional filters, as often applied in studies, thus, allowing more accurate interpretation of the results.

5.2 METHODS

Neural annotation

A *neural annotation* is a mapping of neural positions to known classes. The annotation is based on previous knowledge, and can contain anatomic structure (E.g. Anatomic atlas labeling (Tzourio-Mazoyer, Landeau et al. 2002)), known functional mapping (E.g. functional networks identified in previous studies (Greicius, Krasnow et al. 2003, Yeo, Krienen et al. 2011)), previously known pathology association, etc.

In the current study we used two sets of annotations that are based on functional neural mapping. The first was used in (Nummenmaa, Glerean et al. 2012) and it consists of 6 functional networks, and the second annotation was used in (Wang, Zuo et al. 2013) and it consists of 5 functional brain networks. In our simulation, we used a made-up dummy annotation.

The Hypergeometric test

In this study, we use the hypergeometric (HG) test calculate the significance of the overlap of two sets. Let's assume that we have two sets A and B of sizes N and K respectively. Let x be the size of the intersection between the two sets. Let M be the total number of items in the background set from which the two sets were selected. Suppose that B is fixed. The null hypothesis of the HG test is that the N items in A were sampled randomly and independently from the population without replacement. Therefore, the significance of the intersection is the probability of having x or more elements in the intersection, which can be calculated using the hyper-geometric distribution as follows:

$$\textbf{5-1)} \quad p = F(x \vee M, K, N) = \sum_{i=x}^{min(N,K)} \frac{\binom{K}{i}\binom{M-K}{N-i}}{\binom{M}{N}}$$

Position group enrichment analysis using the HG test

Here, we are given a group of neural positions A^p and a class B. We also know the background set of neural positions from which A^p and B were taken. When using the HG test N is the number of neural positions in A^p, M is the number of all neural positions in the background set and K is the number of neural positions in B. The number of positions that are both in A^p and B is x.

Connections group enrichment analysis

Here we are given a group of connections (i.e. pairs of neural positions) $A^c = \{(x_1,y_1),\ldots,(x_n,y_n)\}$, where each x_i and y_i is a neural position. This set can also be viewed as a graph G(V,E), where V is the set of all neural positions, and $E=A^c$. In addition we are given two subsets of V, B and C. Our goal is to decide whether the number of observed edges between B and C in E, denoted as a(E,B,C), is larger than expected by chance. In this work, we test two approaches for this task: (1) a parametric approach that uses the HG test; and (2) a non-parametric test based on permutations. In the next two sections we use the same notation described above.

Parametric connection group analysis using the HG test

Here, we use the HG test with the following parameters. N is the number of pairs in A^c. M (i.e., the background set size) is the number of all possible neural pairs: $|V|(|V|-1)/2$. $K=|B|*|C|$ is the number of possible pairs between B and C. Finally, x is the observed number of pairs between B and C - a(E,B,C).

Non-parametric degree-preserving analysis

The HG approach for connection groups does not account for the degree distribution in the graph G. The importance of this distribution has been previously observed in brain networks (Rubinov and Sporns 2010, Sporns 2011). We therefore propose an additional non-parametric test. Here, our null hypothesis is that the graph G was randomly selected from the set of all graphs with the same node degrees - S. Formally, S={G'=(V,E') | |E'|=|E| and $deg_G(v)=deg_{G'}(v)$ for all v in V}, where $deg_G(v)$ is the number of pairs in E that contain v as one of the end points.

We calculate the p-value empirically by drawing graphs from S using a heuristic rewiring step: remove two disjoint edges in the current graph and replace them by two others so that node degrees remain unchanged. A long chain of such steps leads to a near-random sampling from S (Milo, Kashtan et al. 2003). The method has been successfully used in multiple bioinformatics applications (Pradines, Farutin et al. 2005, Franceschini, Szklarczyk et al. 2013). Given a set of graphs generated using this process we calculate for each one the number of observed edges between B and C. This step produces a vector of scores $a=a_1,\ldots,a_m$ (by default we generate m=1000 randomized graphs). The final empirical p-value is the fraction of scores in a greater than or equal to a(E,B,C).

Multiple testing correction

Since enrichment is tested for each combination of an identified collection and a class, the output contains multiple p-values. Therefore, we correct for multiple testing at a false discovery rate (FDR) of 0.05 using the procedure suggested by Benjamini and Hochberg (BH) (Benjamini and Hochberg 1995).

5.3 RESULTS

In this study we propose using enrichment analysis to facilitate and improve the interpretation of results obtained from large-scale fMRI studies. We address two cases: In the first case the large-scale analysis produces a set of neural positions. For example, these positions could be a set of voxels that demonstrate increased activation under a specific condition. In this case, we call the enrichment analysis *position-group analysis.* In the second case, the identified results are a set of neural position pairs (i.e. neural connections). For example, they can be pairs of neural positions demonstrating increased functional connectivity under a specific experimental condition (Finn, Shen et al. 2014, Sripada, Kessler et al. 2014, Tyszka, Kennedy et al. 2014). In this case, we call the enrichment analysis *connection-group analysis.* In both cases, in addition to the study results we are given an annotation of the brain that maps neural positions to classes representing known neural functions (e.g. (Damoiseaux, Rombouts et al. 2006, Yeo, Krienen et al. 2011, Shirer, Ryali et al. 2012)), or anatomic structures (e.g. (Talairach and Tournoux 1988, Lancaster, Woldorff et al. 2000, Maldjian, Laurienti et al. 2003)). For position-group analysis we use the hyper-geometric (HG) test, and for connection-group analyses we propose two different tests (See Methods for details). The first test is based on the HG score and is easy to compute. However, this test ignores the degree distribution in the graph represented by the neural connections. The second test uses permutations to create a large set of random graphs with the same node degrees.

Figure 5-1 shows a toy example that illustrates the difference between these tests. Graph A is very sparse, and the degree of “red” and “green” nodes is high relative to the rest of the graph. As a result, its HG p-value is significant, but its degree preserving permutation (DPP) p-value is not. In contrast, graph B is denser, and the degree of red and green nodes is relatively low, so its HG p-value is not significant but its DPP p-value is.

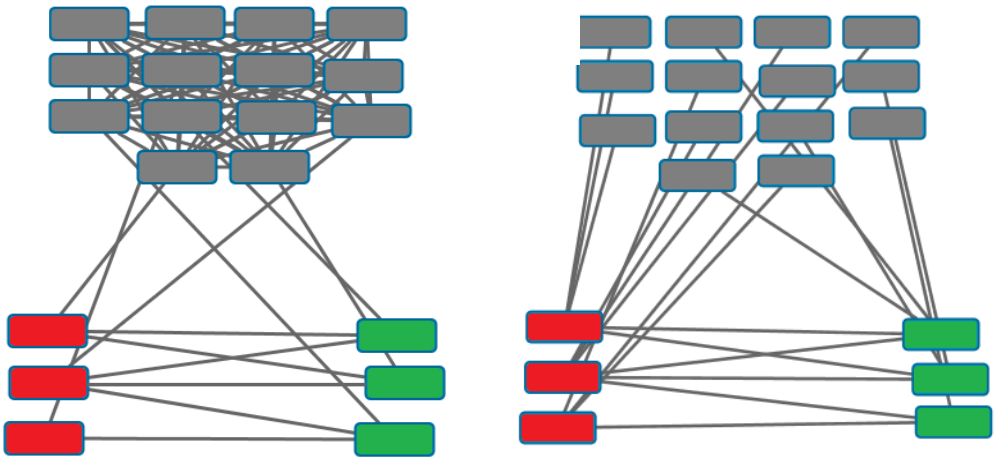

FIGURE 5-1: TWO EXAMPLES THAT DEMONSTRATE THE DIFFERENCE BETWEEN THE TWO APPROACHES TO CONNECTIVITY ENRICHMENT SIGNIFICANCE

Each of the graphs contains 20 nodes, of which three are labeled “green” and three are labeled “red”. The number of connections between green nodes and red nodes is 6 in both cases, however, the number of connections and consequently the degree of the nodes varies greatly between the two cases. Graph A was found to be enriched with red-green connections using HG-test (FDR q=4.4*10-5) but not using DPP (FDR q=0.22). On the other hand, graph B was found to be enriched with red-green connections using DPP (FDR q<0.001) but not using HG test (FDR q=0.34).

We implemented the two approaches in a matlab-based tool called RichMind. Below, we first give a brief explanation on the input and output of the tool. Next, we show two case studies in which we apply RichMind to real data from fMRI studies.

RichMind – a toolbox for analysis of enrichment of fMRI results:

RichMind receives as input either (1) one or more sets of neural positions for position-group analysis, or (2) a set of neural position-pairs for connection-group analysis. In addition, the collection of all positions considered in the experiment is required. RichMind uses an established neural annotation, attributing neural positions to meaningful terms. These classes reflect prior knowledge of brain function or anatomic structure, so they can be anatomic labels, functions, pathology association, etc. By default, RichMind uses as annotation the functional neural mapping provided in (Yeo, Krienen et al. 2011). Alternatively, it provides an option to use the anatomic mapping provided in (Fischl, Salat et al. 2002), or any other mapping provided by the user. In each type of analysis RichMind calculates the p-values for over-representation of the classes (see Methods for details). All p-values are corrected for multiple testing using the false discovery rate (FDR) q-value (Benjamini and Hochberg 1995). Alternatively, the user can choose the more stringent Bonferroni correction. Finally, RichMind reports a list with all significant enrichments (0.05 FDR by default), and also produces bar plots that display the p-value and an additional measure of enrichment level called the “frequency ratio”. The frequency ratio is the ratio between class representation within the tested set and its representation in the background set (see Figure 5-2 A for example). For each reported result, brain 2D and 3D views overlaying the neural positions (or connections) are available by clicking on the result (see Figures 5-2 B, and 5-3 B for examples). In addition, one can export these overlay graphs into files that can be loaded to the BrainNet viewer (Xia, Wang et al. 2013) (see right hand panels in Figures 5-2 B and 5-**3b** for examples).

Case Study 1: Inter-subject correlation identified while watching emotion inducing film clips

Nummenmaa et al. (2012) analyzed fMRI signals recorded from 16 healthy participants, while viewing film clips depicting unpleasant, neutral, and pleasant emotions. They identified cerebral regions where inter-subject correlation (ISC) was reported to be significantly correlated with self-reported valence and arousal scores provided by the participants. ISCs were derived by calculating, for each voxel, the Pearson correlation coefficient of the BOLD time series recorded in each pair of subjects. This was done both for the entire time frame and for sliding windows of 17 time points. Ongoing measures of self-reported valence and arousal provided by participants were used as regressors in a general linear model (GLM), to identify significantly associated ISCs. Results were interpreted by the authors in the context of six functional networks extracted using seed-based FC analysis on the same data – the VN, SMN, AN, DMN, DAN and the executive control network (ECN). The authors reported that arousal was mostly associated with ISC in the SMN, VN and DAN while valence was negatively associated with ISC in the DMN as well as in regions involved in emotional processing, such as midbrain, thalamus, ventral striatum, insula, and anterior cingulate cortex (ACC) (Nummenmaa, Glerean et al. 2012). No quantitative statistical measure was presented to support this interpretation.

We ran RichMind position group analysis on two sets of cerebral regions: one where ISC was inversely associated with self-reported valence, and another where ISC was positively associated with self-reported arousal. All gray matter voxels were used as background for enrichment test. The mapping of voxels to the six functional networks was taken from the original paper. The results are presented in Table 5-1 and Figure 5-2. RichMind identified arousal associated

ISC to be enriched with regions involved in AN (q=1.28E-10), SMN (q=1.85E-10), DAN (q=9.28E-09), and VN (q=9.26E-11), and valence associated ISCs to be enriched with DMN (q=9.26E-11), SMN (<1.4E-37) and ECN (q=6.59E-09). These results recapitulate the results of the original paper. However, they add additional findings of AN enrichment within arousal associated ISCs, and ECN and SMN enrichment within valence associated ISCs. These finding reinforce the claim made in the original study, by which high arousal serves to direct individuals' attention to features of the environment. Identifying ECN and SMN enrichment within valence associated ISCs, is in line with the authors' suggestion by which negative valence synchronizes brain circuitries, supporting emotional sensations across individuals.

TABLE 5-1 – RICHMIND RESULTS FOR CASE STUDY 1

DAN=dorsal attention network, AN=auditory network, SMN=sensori-motor network, VN=visual network, DMN=default-mode network, ECN=executive control network

ISCs set	Enriched attribute	HG-based q-values	Frequency Ratio	# Voxels
Arousal	DAN	9.28E-09	2.9	4560
Arousal	AN	1.28E-10	1.6	2358
Arousal	SMN	1.85E-10	1.4	5018
Arousal	VN	9.26E-11	6.9	2901
Valence	DMN	9.26E-11	3.5	1357
Valence	ECN	6.59E-09	4.3	2684
Valence	SMN	0	1.3	2056

A)

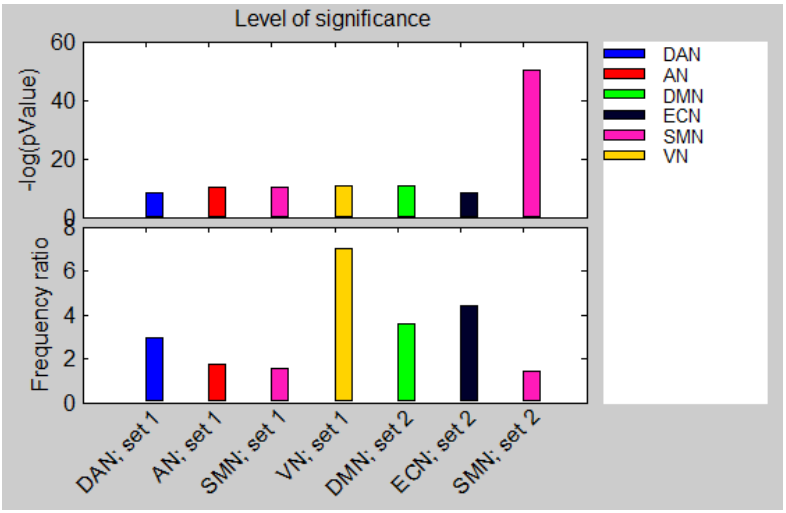

B)

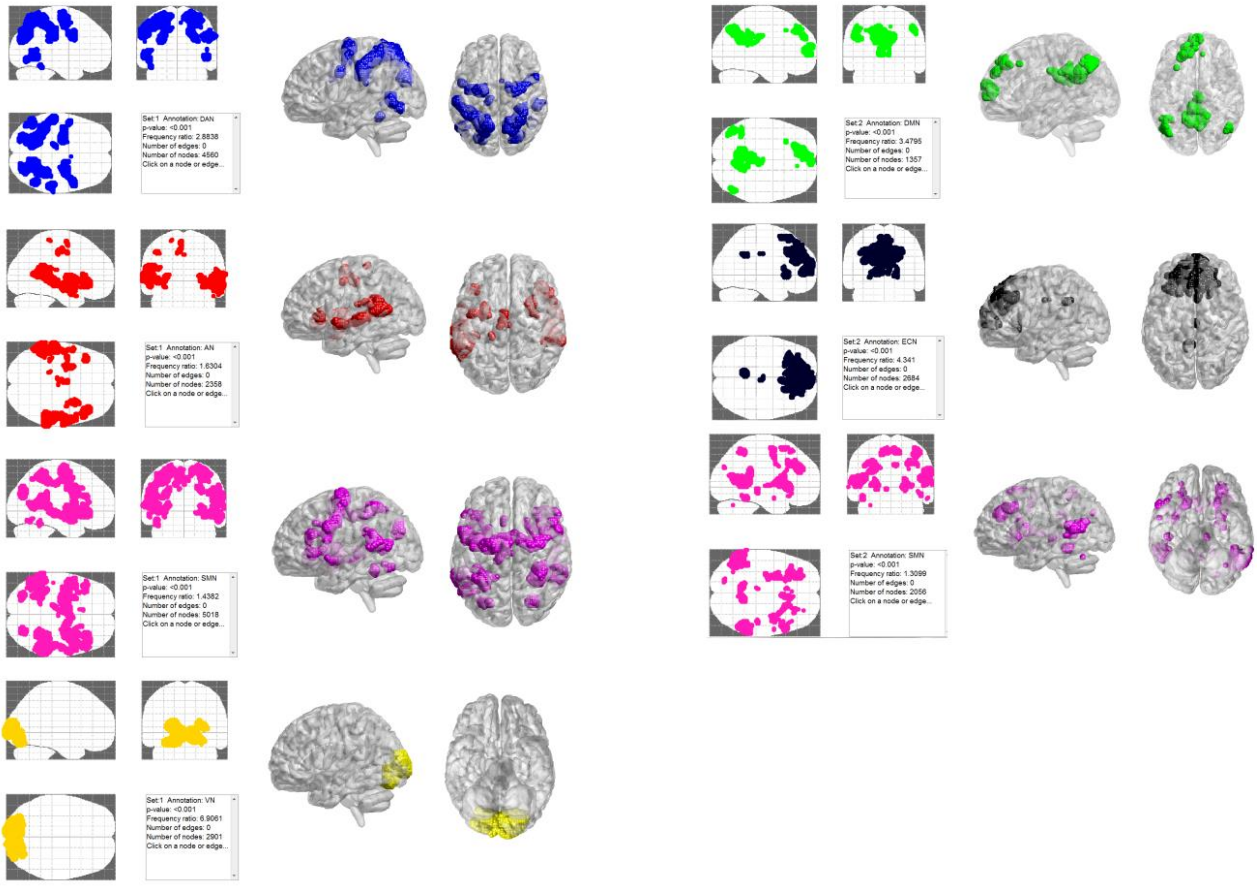

FIGURE 5-2: RICHMIND RESULTS VISUALIZATION FOR CASE STUDY 1

(A) Bar plots displaying the p-values and frequency ratios of enrichment analysis results. Each bar is colored according to the attribute which corresponds to the enriched attribute. (B) 2D and high-resolution 3D brain visualization, which shows, for each enriched attribute, all neural positions that are both in the SOI and in the attribute. Positions are colored according to the corresponding attributes. High resolution 3D images were generated using BrainNet viewer (Xia, Wang et al. 2013).

Case Study 2: fMRI FC differences identified in cases of amnestic mild cognitive impairment

Wang et. al. (2013) analyzed resting state (rs) fMRI data recorded from 37 subjects with aMCI, and 47 healthy controls. The analysis produced functional connections (FCs) that differed between the groups. These connections were identified using the network-based statistic approach (Zalesky, Fornito et al. 2010) on a predefined functional parcellation containing 1024 parcels (Craddock, James et al. 2012, Wang, Zuo et al. 2013). The approach identified connected components (CCs) that are composed of FCs for which the inter-group difference exceeded a pre-defined threshold. Component significance was estimated using a permutation test. This analysis detected a single CC of 363 reduced FCs when using a p-value threshold of $5*10^{-4}$. We call this set CC363. In addition, two CCs of 65 and 22 reduced FCs were discovered using a p-value threshold of 10^{-4}, denoted as CC65 and CC22, respectively.

In the original study, due to the large number of connections in CC363, only CC65 and CC22 were further interpreted. This was done in the context of a modular architecture derived from the control group, which includes five modules corresponding to the VN, the SMN, the DMN, the ventral attention network (VAN) and the auditory network (AN). CC65 was reported as comprised mainly of inter-module connections (46/65, 70.8%), which linked regions in the SMN module, the VN module, and the AN module. CC22 was reported to contain predominantly intra-module connections (15/22, 68.2%) within the DMN module (Wang, Zuo et al. 2013).

We used RichMind to analyze CC363. All 1024 parcels were used to generate the background for the enrichment analyses. A mapping of nodes to functional

modules was taken from the original paper. The results are presented in Table 5-2 and Figure 5-3. The HG-based analysis identified CC363 as enriched with inter-modular FCs that link regions of the SMN module, the VN module, and the AN module ($q_{(SMN-VN)}$= 0.011, $q_{(SMN-AN)}$= 6.54E-08; $q_{(AN-VN)}$=1.2E-09), and with intra-modular connections within the DMN module (q=0.003). These results reproduce the main conclusions of the original study, but were obtained on the larger CC, which was not discussed in the original study due to its size. In addition, the test revealed enrichment in connections within the VN module (q=0.00014), which was not reported in the original study. The degree preserving permutation test did not identify FC enrichment within the VN nor did it identify FC enrichment between the SMN and the VN. However, it recovered the other three inter-module links (see **Table 5-2**).

TABLE 5-2: RICHMIND RESULTS FOR CASE STUDY 2 ; CLASS ABBREVIATIONS: VN=VISUAL NETWORK, AN=AUDITORY NETWORK, SMN=SENSORI-MOTOR NETWORK, DMN=DEFAULT-MODE NETWORK

Enriched inter-class connection	HG- based q-value	Permutation based q-value	Frequency ratio	# Connections
VN-AN	6.8E-10	0.0325	2.8	72
SMN-AN	3.9E-08	0.00075	2.3	54
VN-VN	8.4E-05	0.79	1.9	41
DMN-DMN	0.0019	<0.00075	1.6	49
SMN-VN	0.0066	0.79	1.4	55

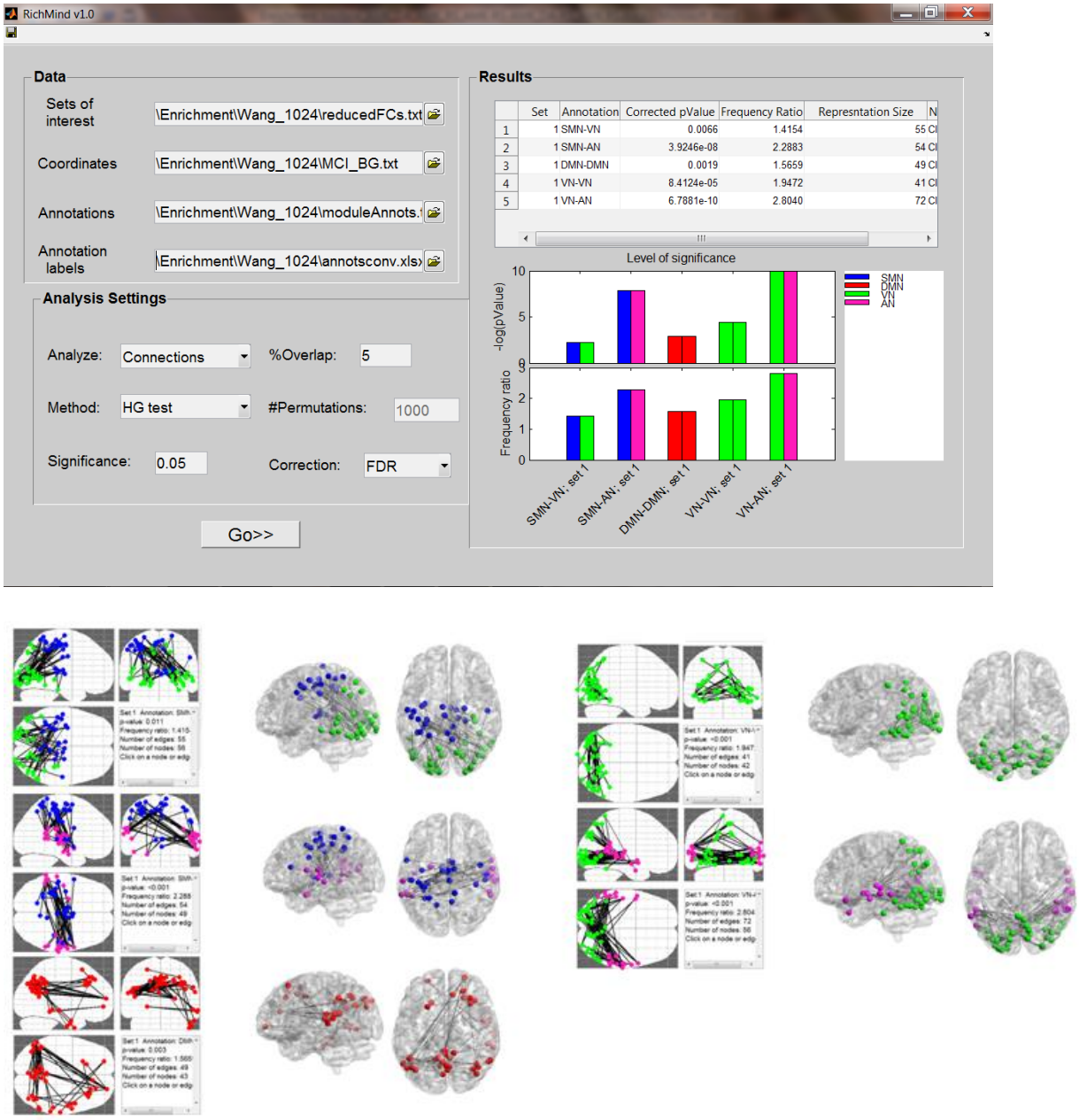

FIGURE 5-3: RICHMIND RESULTS VISUALIZATION FOR CASE STUDY 2

(A) Bar plots displaying the p-values and frequency ratios of enrichment analysis results. Each bar is composed of two rectangles colored by the two classes that constitute the enriched class. (B) 2D and high-resolution 3D brain visualization, showing, for each enriched class, all neural connections that are both in CC363 and in the class. Parcels are colored according to the corresponding classes. High resolution 3D images were generated using BrainNet viewer (Xia, Wang et al. 2013).

Repeating case analyses with an external annotation

The above analyses were conducted using the same annotations that were used by the authors of the original papers for interpretation. In both cases, these

were functional brain networks that were extracted from the same experiment. However, to validate the results of a new experiment, it is preferable that enrichment analysis is conducted using an independent annotation. Another advantage of using such an external annotation is that it allows the results to be comparable across studies. Accordingly, we repeated both case analyses using an annotation reported in (Yeo, Krienen et al. 2011), which includes a partition of the cortex into seven functional brain networks. This annotation was selected because it is based on a thorough analysis of a very large cohort of 1000 subjects. When we repeated the analysis of RichMind using this annotation two of the 5 results in our previous analysis of case study 2 were identified (VN-SMN and VN-VN connectivity). In case study 1, the results remained similar to those obtained in our previous analysis, however, slight differences were identified. For example, valence associated ISC was enriched with SMN using the original annotation but not the external one. This difference results from discrepancies in the mapping of voxels to network.

5.4 Discussion

In this work we describe RichMind, a Matlab-based, easy-to-use computational tool that tests for enrichment of known classes in large-scale neural results. It provides both statistical reports and brain visualizations of the identified enrichments. Statistical reports state the probability of getting the observed representation of each annotation in the tested set by chance.

We applied RichMind totwo case studies, and in both of them RichMind reinforced the main claims made in the original papers, while adding new

findings. In case study 1, the involvement of the ACC in the valence-associated ISCs seems to contribute most to the identified ECN enrichment within that group (Figure 5-2B shown in black), in accordance with the statement in the original study. However, regions of the SMN were reported in the original study only in association with arousal ISCs and not with valence ISCs. Using RichMind we reveal SMN enrichment within valence associated ISCs, a finding with extremely low q-value, indicating that it is highly significant. Notably, this enrichment was not identified using the external annotation that was based on (Yeo, Krienen et al. 2011), due to differences between the mappings. This inconsistency demonstrates the need for an established functional mapping of the brain that is acknowledged in the field as “common ground”.

While enrichment analysis is standard in genomic and genetic studies (Sherman and Lempicki 2009, Ulitsky, Maron-Katz et al. 2010), few previous fMRI studies addressed the issue of large-scale interpretation by calculating the relative frequency of specific classes. For example, in case study 2 Wang et al. used maps of known functional brain networks extracted from the set of healthy controls through modularity analysis, and then calculated the percent of the results that link each pair of networks (Wang, Zuo et al. 2013). However, such an approach does not take into consideration the spatial coverage of each class, which has a major effect on the frequency of its representation in the results. Furthermore, it does not provide statistical significance of the reported findings.

Unlike the simple case where results contain sets of neural positions, when examining sets of neural connections, the null hypothesis of random independent sampling, which underlies the hyper-geometric test, may not be

suitable. This is due to a non-uniform distribution of the degrees in the brain network (Rubinov and Sporns 2010, Sporns 2011). Instead, empirical p-values can be calculated using a permutation test, in which the random background model preserves the degrees of the nodes in the graph. Such degree-preserving permutation test has been previously used for analyzing enrichment within protein-protein interaction networks (Pradines, Farutin et al. 2005, Franceschini, Szklarczyk et al. 2013). In our tests, when comparing HG to the degree preserving permutation test, we observed that the latter was often much more stringent and produced less results.

Shortcomings and future plans: Using a data-driven approach, which considers all possible classes, while correcting for multiple tests, is very strict, and thus may increase the rate of false negative findings. In addition, the analysis is conducted under the assumption of specific null models, which, in some cases, may not hold. Other null models can be added to RichMind in the future based on user requests.

The use of enrichment analysis is always based on some previously established mapping that is used as an annotation. For this purpose, it would be ideal to use an established functional mapping of the brain that is accepted in the field as “common ground”. Such annotation systems exists in other fields for this type of analysis, e.g. the Gene Ontology system (Consortium 2004) or the KEGG pathway database (Kanehisa and Goto 2000), which are used as standard gene annotations in computational genomics analysis. However, due to the lack of such a common ground in neuroscience, we adopted a functional annotation that was based on a previously published study, conducted on the 1000 connectomes data, and an anatomic annotation of lobe-laterality

information that was based on the TD atlas. We believe that established mapping systems will be available in the near future, and will encourage and improve the use of enrichment analysis in the field.

Availability: RichMind package and sample data is freely available for academic use at http://acgt.cs.tau.ac.il/RichMind. A technical user manual is available at http://acgt.cs.tau.ac.il/RichMind/help.html .

In the coming chapters of this work, enrichment analysis was applied whenever there was a need to interpret large-scale changes in rsFC. This was done using the RichMind toolbox.

6. CHARACTERIZING CHANGES IN RESTING-STATE NETWORKS INDUCED BY A PSYCHOLOGICAL PERTURBATION

6.1 BACKGROUND

The dynamics of interpersonal interactions often evoke strong emotions, some perceived as positive and pleasant, while others as unpleasant or negative. Of the latter, social stress and anxiety are associated with appraisals of uncertainty, risk, and relative weakness (Smith and Ellsworth 1985, Mackie, Devos et al. 2000, Lerner and Keltner 2001) and are considered emotions that discourage confrontation (i.e. flight/avoidance) (Smith and Lazarus 1990, Blanchard and Blanchard 2003), whereas anger is associated with appraisals of certainty, low risk, and relative strength (Smith and Lazarus 1990, Blanchard and Blanchard 2003), and is more likely to motivate one to take action (i.e. fight /approach) (Berkowitz 1989, Berkowitz 1993, Lazarus 1994, Harmon-Jones and Sigelman 2001). This difference is further supported by evidence for two different biological profiles of stress hormonal response. The same study demonstrates how individual tendencies affect levels of reported anger and anxiety provoked by the same stressor (Moons, Eisenberger et al. 2010).

These two behavioral patterns of approach vs. avoidance were shown to be associated with differences in functional lateralization in the prefrontal cortex, as indicated by frontal asymmetry measured with electroencephalography (EEG) (Heller 1993, Davidson 2004, Harmon-Jones, Gable et al. 2010, Quaedflieg, Meyer et al. 2015). However, little is known on differences in patterns of neural network reorganization that underlie these two behaviors.

In this section we present two case studies in which we explore changes in patterns of rsFC induced by established paradigms involving social interactions that were used to generate an emotional challenge: the first of acute social stress and the second of inter-personal social conflict that is known to provoke anger. In both cases the study was conducted on a cohort of healthy young male subjects. We assumed that both challenges would have a large-scale effect on patterns of neural FC, which would be evident in subsequent rsfMRI. We further expected that the identified changes in rsFC would differ between the two case studies due to the difference in type of challenge.

6.2 Case study 1: Characterizing changes in resting-state networks induced by acute social stress

In this section we describe the data-driven investigation of rsFC changes identified following exposure to acute social stress. A paper describing the results was submitted to a journal, and is now under peer review.

6.2.1 Specific Background

Acute stress calls for an adequate immediate response, followed by recovery processes and homeostasis restoration once the stressor has terminated

(Cannon 1929, De Kloet, Joëls et al. 2005, Hermans, Henckens et al. 2014). While the neural basis of the stress response at the time of induction has been widely investigated (Wang, Rao et al. 2005, Pruessner, Dedovic et al. 2008, Ulrich-Lai and Herman 2009), much less is known about the neural processes that underlie successive recovery in human subjects. Characterizing individual variability in recovery from stress is of particular interest since it has been associated with several stress-related psychopathologies, including Post Traumatic Stress Disorder (PTSD) and depression (McEwen 2003, Yehuda and LeDoux 2007).

One approach to study post-processing of prior events, such as stress, is by inspecting the spontaneous neural activity that takes place during rest after the event occurred. This post-processing has been shown to support prior experience consolidation (Lewis, Baldassarre et al. 2009, Tambini, Ketz et al. 2010, van Kesteren, Fernández et al. 2010), and thus, may play a central role in regaining mental and physiological homeostasis and is expected to involve large scale brain network reorganization (Eryilmaz, Van De Ville et al. 2011, Wang, Liu et al. 2012, Hermans, Henckens et al. 2014). Accordingly, using post-stress resting-state functional magnetic resonance imaging (rsfMRI) to investigate network reorganization following stress may provide a vital insight into the large-scale neural mechanism that underlies affective recovery from acute stress.

Few previous fMRI studies investigated changes in resting-state functional connectivity (rsFC) following acute stress (Van Marle, Hermans et al. 2010, Veer, Oei et al. 2011, Vaisvaser, Lin et al. 2013). For example, van Marle et al. reported increased amygdala rsFC immediately following acute stress with

anterior cingulate cortex, anterior insula, and a dorso-rostral pontine region (Van Marle, Hermans et al. 2010). In another study Veer et al. reported increased amygdala rsFC with the posterior cingulate cortex, precuneus and medial prefrontal cortex an hour following stress, suggesting that these effects could be related to top-down control of the amygdala and consolidation of self-relevant information following a stressful event (Veer, Oei et al. 2011). Lastly, Vaisvaser et al. examined changes in rsFC patterns seeded at the posterior cingulate cortex (PCC) and hippocampus, both immediately after social stress induction and two hours later (Vaisvaser, Lin et al. 2013). Unlike the two aforementioned studies, here rsFC alterations were examined with respect to the pre-stress resting period. Immediately after stress induction several rsFC changes were reported including altered coupling within the default mode network (DMN) and between hippocampus and amygdala**.** Intriguingly, two hours later all rsFCs returned to pre-stress levels with the exception of a sustained increase in rsFC found between the hippocampus and amygdala. Notably, these studies used a hypothesis-driven fMRI analysis approach, exploring connectivity changes involving one or few predefined seed regions. Alongside the clear statistical advantages of such a seed-based approach lies the disadvantage of revealing only that fraction of the actual phenomena that involves the preselected seed, and possibly missing other relevant findings, which can be identified using a data-driven approach. Such a data-driven approach was taken by Hermans et al. who used group independent component analysis (ICA) in combination with inter-subject correlation analysis to identify large-scale stress-related FC changes induced during exposure to fear-related movie clips. They reported an increase in interconnectivity within a

salience network, which positively correlated with the subjective stress response magnitude (Hermans, van Marle et al. 2011). This network included cortical (frontoinsular, dorsal anterior cingulate, inferotemporal, and temporoparietal) and subcortical (amygdala, thalamus, hypothalamus, and midbrain) regions. Accordingly, it has been suggested that exposure to acute stress prompts the recruitment of a salience network, at the expense of a fronto-parietal executive control network involving dorso- frontal and parietal areas, and that this resource allocation is reversed after stress subsides (Hermans, Henckens et al. 2014). Nonetheless, large scale alterations after exposure to stress require further identification and deeper characterization.

In this study we aimed to gain a broader perspective on rsFC modulations following acute social stress, and examine their correspondence to individual subjective experience. To this end we adopted a data-driven approach for analyzing rsfMRI data recorded from healthy male subjects before and after performing the arithmetic task from the well-established Tier Social Stress Test (Kirschbaum, Prüssner et al. 1995), adapted to the scanner (Wang, Rao et al. 2005, Vaisvaser, Lin et al. 2013). In addition, in order to study the relation between stress-induced rsFC modulations and subjective experience of recovery, we divided our participants according to their reported stress sustainment.

Data analysis was conducted using a fine-grained predefined functional parcellation (Craddock, James et al. 2012) that allowed dimensionality reduction on one hand, while maintaining a relatively coherent per-parcel BOLD

signal on the other hand. The parcellation contained 517 parcels, of which 463 survived after gray-matter masking. In this parcellation most anatomic structures are covered by more than one parcel. This redundancy in regional representation along with the expected large-scale effect of stress induction may lead to a large number of identified changes even after controlling for type-I error. In such cases an additional means is required in order to pinpoint the most robust rsFC changes. To this end we applied *enrichment analysis*, which is described in section 5, and is commonly used in the field of Bioinformatics for interpreting a large number of noisy results (Sherman and Lempicki 2009, Ulitsky, Maron-Katz et al. 2010). In the current study enrichment analysis was conducted based on parcel anatomic positions, seeking pairs of lobes that were over-represented (i.e. significantly more prevalent than would be expected by chance) in the set of identified modulations.

We hypothesized that using a whole-brain data-driven approach would reveal a large-scale effect of stress-induced rsFC modulations, which corresponds to changes in the subjective experience of stress. We expected some of these changes to involve rsFC that had been previously associated with stress reactivity, such as connections within the salience network and executive control network, as suggested in (Hermans, Henckens et al. 2014), and rsFC previously associated with post-stress processing, e.g. within the DMN or between the DMN and limbic regions (Veer, Oei et al. 2011, Vaisvaser, Lin et al. 2013). Furthermore, we expected some of these stress-induced rsFC robust changes to be sensitive to inter-individual differences in subjective stress recovery measured 20 minutes after the stress eliciting experience.

6.2.2 Specific materials and methods

Participants

We used fMRI data from a study conducted at our lab, on a cohort of 61 healthy male participants (age 19–22) (Vaisvaser, Lin et al. 2013). The data were previously analyzed using a different methodological approach of exploring changes in rsFC of a-priori preselected seed regions. Participants had no reported history of psychiatric or neurological disorders, no current use of psychoactive drugs, no family history of major psychiatric disorders, and no previous exposure to abuse during childhood and/or potentially traumatic events before entering the study. In addition, all participants had normal or corrected-to-normal vision and provided written informed consent approved by Tel Aviv Sourasky Medical Center Ethics Committee and conformed to the Code of Ethics of the World Medical Association (Helsinki Declaration). Of the 61, four individuals were excluded from the current analysis due to signal artifacts; therefore the final study group consisted of 57 participants.

Experimental procedure

Each participant underwent a 65 minutes MRI scan that consisted of 6 phases: acclimation and anatomical scan (15 minutes), a rest condition ("rest1", 5 minutes), control task (6 min), a social stress task (6 minutes), a second rest condition ("rest2", 5 minutes) and another anatomical scan (15 minutes). Acute stress was induced using a serial subtraction arithmetic task (Kirschbaum, Prüssner et al. 1995, Wang, Rao et al. 2005), fully described in (Vaisvaser, Lin et al. 2013). Briefly, participants were instructed to continuously subtract 13

from 1022 for a period of 6 minutes, responding verbally, while monitored on-line by an experimenter. The stress task was preceded by a non-stressful condition of backward counting for a period of 6 minutes, without external monitoring. The experimental timeline is shown in Figure 6-2 A**.** During the rest conditions participants were instructed to keep their eyes open and stare at a fixation point. Psychological effect of stress (on a 9 point Likert scale) and salivary cortisol were evaluated at four time points: after the first rest scan (Stress Reprot_1; SR1), after the control task (SR2), right after the stress task (SR3) and 20 minutes after the stress task, following the second anatomical scan (SR4) (Figure 6-2 A). In addition, the STAI questionnaire described in section 4.2 was administered and Electrocardiography (ECG) was recorded continuously during scanning via a BrainAmp ExG MRI-compatible system at a sampling rate of 5000Hz, and used to extract heart-rate measure.

Physiological data analysis

Preprocessing of the ECG signal and RR interval analysis was performed similarly to (Raz, Winetraub et al. 2012). Briefly, gradient artifacts were removed using FASTR algorithm (Niazy, Beckmann et al. 2005), implemented in FMRIB plug-in for EEGLAB (Delorme and Makeig 2004). R peaks of ECG were detected using the FMRIB toolbox, and corrected for mis-detection (maximum correction rate over participants was 5.95%) and presence of ectopic beats. Finally, RR intervals were used to derive a beats-per minute HR index. Due to motion artifacts, 42 participants, for whom a reliable R peak signal could be detected in all conditions, were included in the final HR analysis. The

Kubios software tool (Tarvainen, Niskanen et al. 2009) was used to extract the high frequency component of HRV from the ECG channel.

fMRI data acquisition information

Functional imaging was acquired with gradient echo-planar imaging (EPI) sequence of $T2^*$-weighted images (TR/TE/flip angle: 3000/35/90; FOV: 20 × 20 cm; matrix size: 96 × 96) in 39 axial slices (thickness: 3 mm; gap: 0 mm) covering the whole cerebrum.

fMRI preprocessing and parcellation

fMRI data preprocessing was performed with SPM5 (Wellcome Department of Imaging Neuroscience, London, UK). The procedure is described in section 4.1.3.

We used the whole-brain functional parcellation reported in (Craddock, James et al. 2012), as described in section 4.1.3 to partition the brain into 463 parcels for which average BOLD values across all gray matter voxels were calculated at each time point. These time series were used as the parcel's signal. In order to reduce the effect of physiological artifacts and nuisance variables, the whole-brain mean signal, six motion parameters, cerebrospinal fluid, and white matter signals were regressed out of these parcel signals.

Parcel-based univariate functional connectivity analysis

The procedures of rsFC analysis and statistical characterization are illustrated in Figure 6-1. We used a univariate analysis approach, in which a model is

fitted independently to each connection to assess evidence for experimental effects.

Level of rsFC between every two parcels was estimated by calculating the Pearson correlation coefficient between the corresponding signals. This was done for each subject and each rest condition separately. Correlation values were next Fisher transformed to better fit a normal distribution. FC level estimates of "rest1" were then subtracted from the corresponding estimates in "rest2", resulting in a single FC change value (denoted ΔFC) for each pair of parcels and for each subject. To identify parcel-pairs that demonstrated significant rsFC change following the stress task, we applied a one-sample t-test on the ΔFC values of each pair across all subjects.

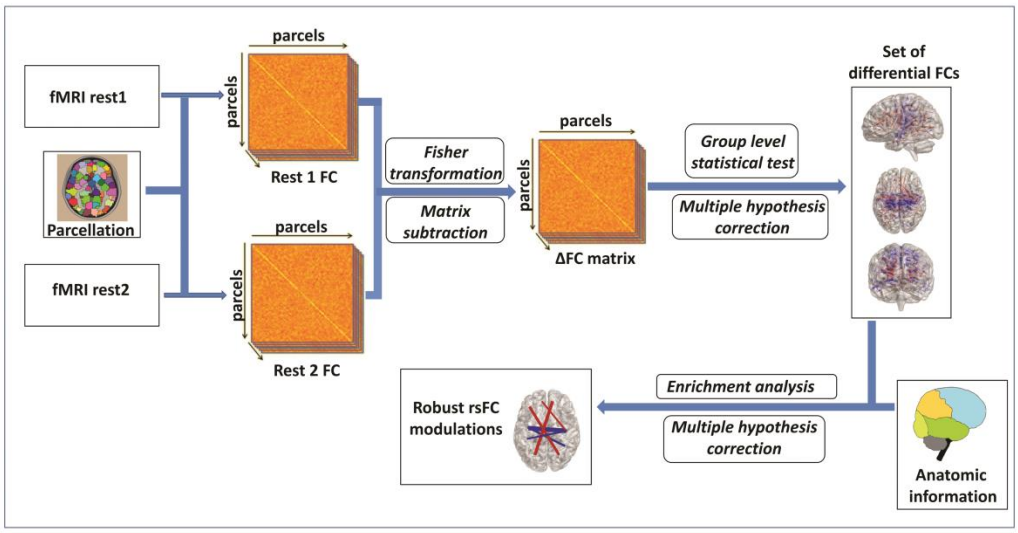

Figure 6-1: **An illustration of data-driven univariate rsFC analysis**. Following parcellation, cross-correlation matrices were calculated for each subject and resting-state session. A paired t-test was applied on the Fisher-transformed rsFC values to identify parcel-pairs for which rsFC changed significantly. An FDR procedure was used to correct for multiple testing. Next, anatomy-based enrichment analysis was used to characterize the

Statistical characterization of identified connections using enrichment analysis

In order to characterize the identified changes, we conducted enrichment analysis on the two sets of connections that were identified as differential: the

set of weakened connections, and the set of strengthened connections. This was done using the RichMind toolbox described in section 5.2. Each parcel was annotated according to the lobe and hemisphere in which it was located. Lobes were identified by mapping parcel spatial centers into the TD lobe map provided with the WFU Pick Atlas Tool (Maldjian, Laurienti et al. 2003, Stamatakis, Adapa et al. 2010), combined with laterality information, i.e., left($x<-6$), midline ($-6<x<6$) or right ($x>6$). This resulted in a unique mapping of each of the 463 parcels to one of 18 possible annotations. Consequently each connection was given a pair of annotations according to the location of the two parcels comprising it.

The Hyper-geometric cumulative distribution function (HG-CDF) was used to assess the enrichment levels of the lobe representation of identified connections (see section 5.4 for details). The probabilities were corrected for multiple comparisons using Bonferroni correction.

Since the null hypothesis that underlies the HG-CDF is that parcel-pairs were obtained randomly and independently. As an additional filtering, to rule out dependency biases in the enrichment results, we used a random permutation test (see section 5.4 for details).

For each identified enrichment result, an additional measure called “enrichment factor” (EF) was calculated. For each pair of annotations (a1,a2) EF corresponds to the ratio between the relative frequency of a1-a2 links in the sample (e.g. parcel-pairs with increased rsFC) and their relative frequency in the background (i.e. all possible parcel-pairs). This descriptive measure was

not used to identify the results; rather it allowed additional assessment of the extent of each of the identified enrichment results.

6.2.3 RESULTS

Behavioral and physiological indications of stress

As reported by Vaisvaser et al., both subjective reports and HR (beats per minute) measures showed a significant elevation in stress in measure SR3 as compared to the two previous measures (SR1 and SR2), and a decrease to initial levels during the second rest period. For salivary cortisol, a marginally significant main effect of time was reported, with a peak in cortisol level in the final sample (SR4) as compared to post “rest1” sample.

Stress sustainment versus recovery group division: The SR4-SR1 value distribution is shown in Figure 6-5 A. Out of 57 participants, 23 demonstrated elevated reported stress levels 20 minutes post stress induction (i.e. SR4-SR1>0), and were thus assigned in the current study to the “sustained stress” group. The rest of the subjects (n=34) were assigned to the “recovered stress” group. For the “recovered stress” group a significant decline in stress ratings was identified 20 minutes following stress-induction (SR4) relative to ratings immediately after stress induction (SR3, Tukey’s HSD $p < 0.0001$). This decline was not evident in the "sustained stress" group (Figure6-2 B).

Notably, no association was found between state and trait anxiety measured by STAI questionnaire at the beginning of the experiment and level of stress sustainment as measured by SR4-SR1 value ($p > 0.15$) or increase of reported stress following the task as measure by SR3-SR1 value ($p > 0.5$).

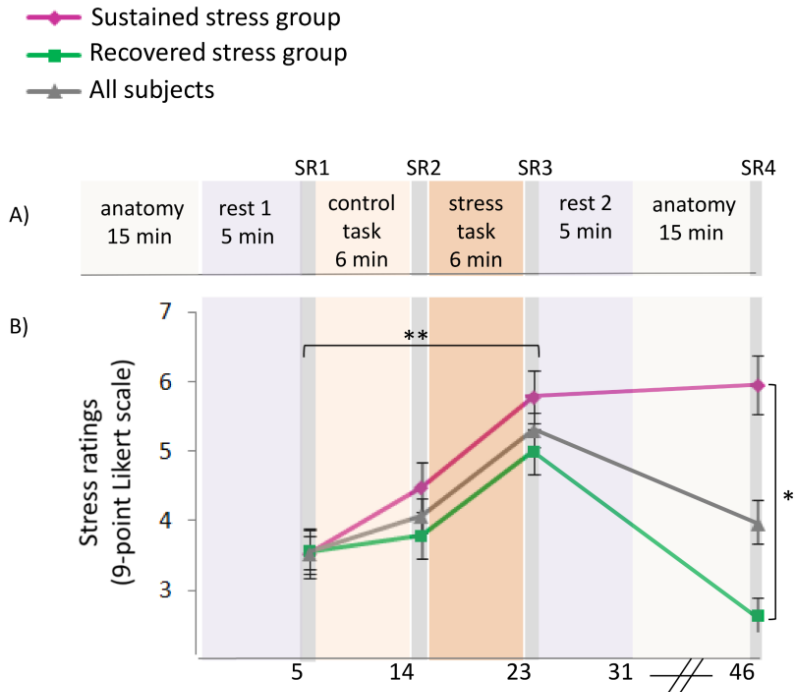

Figure 6-2: **Psychological response to stress on experimental timeline.** Subjective ratings of stress (B) are presented in reference to the time course of the experiment (A). Time 0 indicates the start of the first rest condition. The orange columns represent control and stress tasks (6 min each), violet

Stress-induced rsFC alterations

In order to identify post-stress rsFC changes we conducted a univariate statistical analysis on the Fisher-transformed cross-correlation matrices. This was done by subtracting the "rest1" matrix from the "rest2" matrix, and then applying a one-sample t-test on the resulting ΔFC values of each parcel pair. A significant rsFC change (FDR<0.05) was identified in 490 out of 106953 possible parcel-pairs. Of these, 189 pairs demonstrated rsFC increase and 301 demonstrated rsFC decrease. Pairs are presented as connections/edges on a 3D brain image in Figure 6-3.

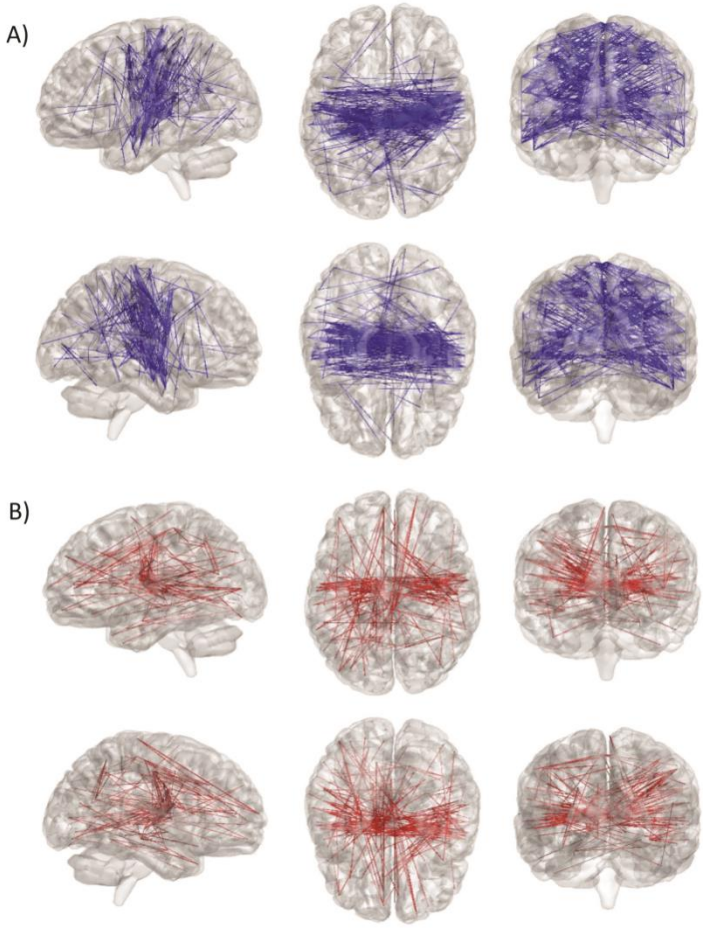

Figure 6-3:: **Significant rsFC changes following stress**

Using FDR of 0.05, 490 parcel-pairs demonstrated a significant ΔFC between "rest1" and "rest2". Of these, 301 demonstrated rsFC decrease (A - shown in blue) and 189 demonstrated rsFC increase (B - shown in red). Visualization was generated using Brain Net Viewer (Xia, Wang et al. 2013).

This large-scale effect required a second-level analysis in order to highlight the main findings. To this end, we conducted enrichment analysis.

Using the lobe and laterality annotation of each parcel, we searched for pairs of annotations that were significantly over-represented (i.e. "enriched") in the set of connections identified as affected by the stress task across all subjects. Enrichment analysis was applied separately on the set parcel-pairs demonstrating rsFC increase (i.e. "strengthened set") and on the set parcel-

pairs demonstrating rsFC decrease (i.e. “weakened set”). Results are summarized in Table 6-1 and illustrated in Figure 6.4-A. The strengthened set was found to be enriched with thalamo-frontal (right), thalamo-temporal (bilateral) and thalamo-parietal (right) connections, while the weakened set was found to be enriched with cross-hemispheral temporo-parietal connections, including regions of the inferior, middle and superior temporal gyri along with regions of the pre- and post central gyri and the superior and inferior parietal lobule. Table 6-2 contains information on enrichment-inducing pairs (i.e. parcel-pairs that were both modulated by the task and link lobe pairs that were found to be enriched).

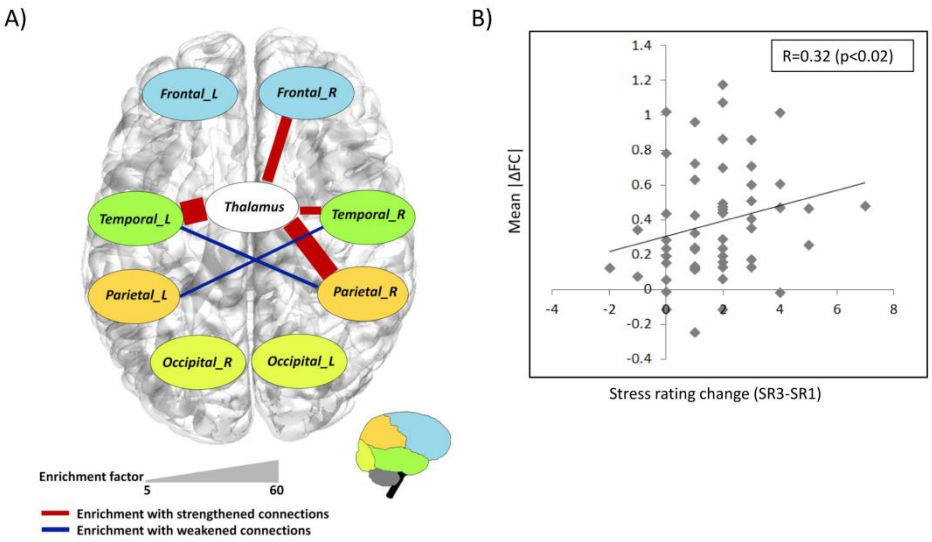

Figure 6-4: **A graph representation of the enrichment analysis results**
(A) Lobe distribution of connections that demonstrated significant ΔFC from "rest1" to "rest2". Each node corresponds to a lobe in the analysis. An edge indicates significant over-representation of the corresponding lobe pairs in the set of strengthened connections (red) and the set of weakened connections (blue). Edge width reflects the enrichment factor (EF) of the identified connections. (B) A scatter plot presenting the mean ΔFC across all parcel-pairs that were involved in the identified enrichments against the (SR3-SR1) change in subjective stress rating. Each spot shows the two values for one subject. A significant correlation is identified (r=0.32, p<0.02).

TABLE 6-1 – LOBE-BASED ENRICHMENT ANALYSIS RESULTS

Results of lobe-based enrichment analysis of significantly strengthened and weakened connections (p-value<=0.05, Bonferroni corrected). The enrichment factor is the ratio between the fraction of pairs with the specified lobe representation in the set of increased/decreased ΔFC pairs, and that fraction in the set of all possible connections. R=right, L=left.

Lobes	ΔFC	#connections	Corrected p-value	% of connections	Enrichment factor
Temporal L;	↑	17	1.13E-08	9%	60.1
Temporal R;	↑	7	2.46E-05	3.7%	20.2
Parietal R;	↑	10	4.51E-07	5.3%	47.2
Frontal R;	↑	12	6.94E-08	6.3%	28.3
Temporal L;	↓	30	5.76e-08	10%	8.88
Temporal R;	↓	27	6.04e-08	9%	7.83

TABLE 6-2 – ENRICHMENT-INDUCING PARCEL PAIRS:

A specification of all parcels-pairs that demonstrated differential rsFC following stress, and link enriched lobe pairs. Rows are sorted according to t-values.

Parcel1	x	y	z	Parcel2	x	y	z	p-value	Fdr q	t-value
453_	54	-9	-15	524_	-39	-54		2.28E-07	0.007	-5.3
93_	-45	-36	54	453_	54	-9	-15	4.86E-07	0.007	-5.2
93_	-45	-36	54	188_	63	-12		7.78E-07	0.007	-5.1
196_	51	-24	54	258_	-60	-9	-24	9.79E-07	0.007	-5.1
11_	48	-27	42	102_	-54	0		1.55E-06	0.01	-5
196_	51	-24	54	399_	-60	-15		3.13E-06	0.014	-4.8
11_	48	-27	42	258_	-60	-9	-24	3.24E-06	0.014	-4.8
3_	63	-12	-21	93_	-45	54		6.17E-06	0.015	-4.7
102_	-54	-33	0	508_	54	45		7.02E-06	0.015	-4.6
3_	63	-12	-21	549_	-60	30		7.72E-06	0.016	-4.6
158_	-54	-24	-3	233_	27	66		1.08E-05	0.018	-4.5
79_	39	-36	45	102_	-54	0		1.17E-05	0.018	-4.4
158_	-54	-24	-3	345_	63	18		1.31E-05	0.019	-4.4
258_	-60	-9	-24	508_	54	45		1.49E-05	0.019	-4.3
151_	-12	-66	57	453_	54	-9	-15	1.56E-05	0.019	-4.3
258_	-60	-9	-24	393_	39	-57		1.90E-05	0.02	-4.3
37_	-42	-36	42	453_	54	-9	-15	1.95E-05	0.02	-4.2
399_	-60	-12	-15	508_	54	45		2.09E-05	0.02	-4.2
3_	63	-12	-21	180_	-54	42		2.10E-05	0.02	-4.2
102_	-54	-33	0	345_	63	18		2.36E-05	0.021	-4.2

393_	39	-39	57	399_	-60	-	-15	2.55E-05	0.022	-4.59
102_	-54	-33	0	286_	63	-	30	2.66E-05	0.022	-
192_	-54	-3	-18	508_	54	-	45	3.05E-05	0.024	-
11_	48	-27	42	158_	-54	-	-3	3.18E-05	0.024	-
102_	-54	-33	0	393_	39	-	57	4.12E-05	0.028	-
11_	48	-27	42	341_	-54	-	6	4.63E-05	0.028	-
140_	-57	-18	-24	196_	51	-	54	4.71E-05	0.028	-
3_	63	-12	-21	151_	-12	-	57	4.87E-05	0.028	-
11_	48	-27	42	399_	-60	-	-15	4.93E-05	0.028	-
151_	-12	-66	57	496_	36	-	-21	5.87E-05	0.031	-
265_	-54	-42	45	453_	54	-9	-15	6.05E-05	0.031	-
79_	39	-36	45	258_	-60	-9	-24	6.66E-05	0.033	-4.31
158_	-54	-24	-3	508_	54	-	45	6.67E-05	0.033	-4.31
498_	63	-3	-18	549_	-60	-	30	6.76E-05	0.033	-
188_	63	-18	-12	219_	-57	-9	15	8.51E-05	0.036	-
151_	-12	-66	57	326_	27	-	-18	8.52E-05	0.036	-
192_	-54	-3	-18	196_	51	-	54	9.48E-05	0.037	-
180_	-54	-27	42	316_	54	-3	-27	9.49E-05	0.037	-
93_	-45	-36	54	316_	54	-3	-27	9.89E-05	0.037	-
214_	-30	-42	63	264_	63	-	3	9.97E-05	0.038	-
180_	-54	-27	42	453_	54	-9	-15	0.000102	0.038	-
56_	-57	-60	9	79_	39	-	45	0.000103	0.038	-4.18
11_	48	-27	42	192_	-54	-3	-18	0.000112	0.039	-
3_	63	-12	-21	37_	-42	-	42	0.000124	0.04	-
318_	-27	-57	57	453_	54	-9	-15	0.000128	0.041	-
93_	-45	-36	54	498_	63	-3	-18	0.000132	0.041	-
79_	39	-36	45	325_	-51	6	-27	0.000134	0.041	-
11_	48	-27	42	145_	-63	-	3	0.000137	0.041	-
158_	-54	-24	-3	286_	63	-	30	0.00015	0.043	-
219_	-57	-9	15	498_	63	-3	-18	0.000156	0.043	-
188_	63	-18	-12	549_	-60	-	30	0.00017	0.045	-4.03
3_	63	-12	-21	524_	-39	-	54	0.000173	0.045	-
303_	-66	-39	-3	393_	39	-	57	0.000178	0.045	-
63_	-27	-72	36	288_	54	9	-12	0.000191	0.047	-
102_	-54	-33	0	233_	27	-	66	0.0002	0.048	-3.98
180_	-54	-27	42	498_	63	-3	-18	0.000215	0.049	-
19_	-21	-78	42	288_	54	9	-12	0.000217	0.049	-
72_	-60	-12	3	242_	6	-9	6	0.000228	0.05	3.941
45_	12	-63	21	420_	3	-	9	0.000224	0.05	3.945
242_	6	-9	6	550_	63	-	12	0.000223	0.05	3.947
248_	60	0	18	420_	3	-	9	0.00021	0.049	3.965
24_	-6	-6	9	204_	54	0	45	0.000204	0.048	3.974
24_	-6	-6	9	173_	-66	-	9	0.000201	0.048	3.979
35_	-3	-3	3	248_	60	0	18	0.0002	0.048	3.981
196_	51	-24	54	242_	6	-9	6	0.000183	0.046	4.008
11_	48	-27	42	242_	6	-9	6	0.000141	0.041	4.087

242_	6	-9	6	345_	63	-	18	0.000138	0.041	4.094
159_	51	-30	21	242_	6	-9	6	0.000127	0.041	4.117
158_	-54	-24	-3	242_	6	-9	6	0.000123	0.04	4.129
24_	-6	-6	9	196_	51	-	54	0.000119	0.04	4.139
102_	-54	-33	0	242_	6	-9	6	0.000107	0.038	4.169
35_	-3	-3	3	152_	51	-9	36	0.000106	0.038	4.173
264_	63	-15	3	420_	3	-	9	8.79E-05	0.036	4.228
89_	54	-33	0	420_	3	-	9	8.48E-05	0.036	4.239
229_	-48	-30	9	420_	3	-	9	8.48E-05	0.036	4.239
28_	54	6	33	242_	6	-9	6	8.33E-05	0.035	4.244
35_	-3	-3	3	508_	54	-	45	8.14E-05	0.035	4.251
242_	6	-9	6	264_	63	-	3	7.93E-05	0.035	4.259
115_	54	-15	15	242_	6	-9	6	6.62E-05	0.033	4.312
24_	-6	-6	9	501_	-45	-	21	6.59E-05	0.033	4.314
103_	54	-24	-3	242_	6	-9	6	5.72E-05	0.031	4.355
35_	-3	-3	3	68_	63	-6	30	5.50E-05	0.03	4.367
145_	-63	-27	3	242_	6	-9	6	5.35E-05	0.03	4.375
152_	51	-9	36	242_	6	-9	6	4.52E-05	0.028	4.424
24_	-6	-6	9	72_	-60	-	3	3.07E-05	0.024	4.536
242_	6	-9	6	321_	63	-	0	2.35E-05	0.021	4.613
102_	-54	-33	0	420_	3	-	9	2.00E-05	0.02	4.66
24_	-6	-6	9	152_	51	-9	36	1.90E-05	0.02	4.674
24_	-6	-6	9	145_	-63	-	3	1.69E-05	0.019	4.708
103_	54	-24	-3	420_	3	-	9	1.48E-05	0.019	4.746
24_	-6	-6	9	102_	-54	-	0	1.44E-05	0.019	4.753
242_	6	-9	6	413_	60	-3	6	1.40E-05	0.019	4.761
145_	-63	-27	3	420_	3	-	9	7.28E-06	0.015	4.946
24_	-6	-6	9	229_	-48	-	9	6.74E-06	0.015	4.967
72_	-60	-12	3	420_	3	-	9	6.09E-06	0.015	4.995
158_	-54	-24	-3	420_	3	-	9	5.82E-06	0.015	5.008
24_	-6	-6	9	158_	-54	-	-3	5.51E-06	0.015	5.023
24_	-6	-6	9	68_	63	-6	30	5.17E-06	0.015	5.041
68_	63	-6	30	242_	6	-9	6	4.05E-06	0.014	5.109
242_	6	-9	6	508_	54	-	45	3.84E-06	0.014	5.124
24_	-6	-6	9	508_	54	-	45	3.12E-06	0.014	5.181
24_	-6	-6	9	269_	-60	-	21	8.23E-07	0.007	5.546
242_	6	-9	6	248_	60	0	18	2.27E-07	0.007	5.893

Relation between stress-induced rsFC changes and subjective stress reports

Examination of the relation between the mean ΔFC magnitude across all 103 enrichment-inducing pairs and the reported change in stress immediately after induction (i.e. SR1 vs SR3) across all subjects, revealed a significant positive correlation (Spearman $r=0.32$, $p<0.02$; Figure 6-4 B). When conducting the same test separately for the 46 parcel-pairs involved in strengthened rsFC enrichment (the "strengthened subset", Table 6-1) and the 57 parcel-pairs involved in weakened rsFC enrichment (the "weakened subset"), a significant correlation was found for the strengthened subset (Spearman $r=0.265$, $p<0.05$), but not for the weakened subset (Spearman $r = -0.21$, $p=0.115$). Nevertheless, the mean ΔrsFC within the weakened subset was found to be significantly anti-correlated with the mean ΔrsFC within the strengthened subset (Pearson $r=-0.47$, $p<0.0005$). Notably, no association was found between the extent of ΔFC across all 103 enrichment-inducing pairs and STAI-trait or state measures ($p>0.45$).

In order to identify functional connections for which the change induced by stress was associated with affective stress sustainment, we used the SR4-SR1 stress-rating-based group partition (described above), and applied a two-sample t-test on ΔFC values of enrichment-inducing parcel-pairs. No significant inter-group difference was identified in ΔFC of any of the pairs separately (FDR $q>0.99$). Additionally, there was no significant difference in the mean ΔFC magnitude of all 103 enrichment-inducing pairs ($p>0.6$). Following this lack of association, we conducted a similar two-sample t-test on the entire set of 106,953 parcel-pairs in the data. Once again, an FDR procedure was used to correct for multiple hypothesis testing. Only one parcel pair demonstrated a

significant inter-group difference in ΔFC between groups (with an FDR of 0.05). Parcels of the identified pair were anatomically mapped to the right basolateral amygdala (BLA) and to the precuneus, based on parcel spatial centers (x=6, y=-54, z=48 and x=27, y=-3, z=-21 respectively) (Figure 6-5 B).

We further examined the relationship between this BLA-precuneus rsFC modulation and the longer term change in subjective stress ratings (SR4-SR1) across all subjects, and found a negative association between them (Spearman r=-0.526, p<0.00005, Figure 6-5 C). Additionally, a repeated measures ANOVA conducted on the corresponding Fisher-transformed rsFC values at both conditions ("rest1" and "rest2"), revealed an interaction between condition and group [F(1,55)=32.6, p <0.001]. Finally, Tukey's HSD post-hoc analyses revealed that only the "sustained stress" group showed a significant BLA-precuneus rsFC decline following stress ("rest2") as compared to "rest1" (p<0.001). The means and standard deviation (in parenthesis) of "rest1" and "rest2" were -0.12 (0.24) and -0.18 (0.23) respectively, for all subjects, -0.024 (0.23) and -0.289 (0.24) for the "sustained stress" group and -0.18 (0.22) and -0.11 (0.2) for the "recovered stress" group. Results are shown in Figure6-5 D.

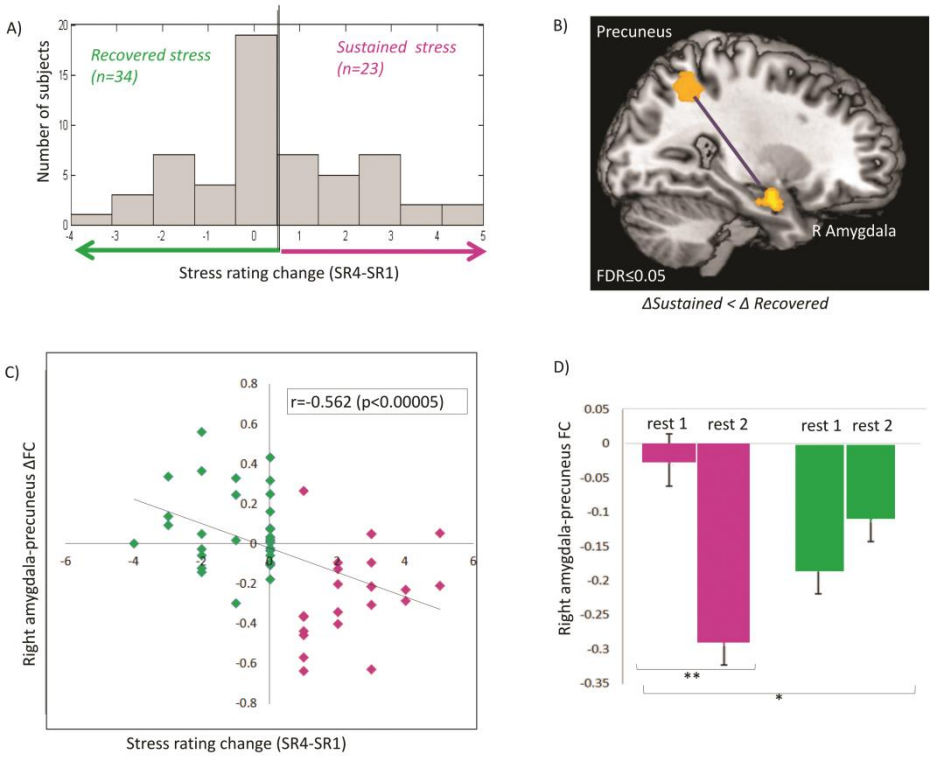

Figure 6-5: Results of inter-group rsFC change comparison. (A) Group partition marked on the distribution of change in subjective stress ratings. (B) A connection between the right BLA and the precuneus that was identified in the inter-group ΔFC analysis. (C) A scatter plot presenting the right amygdala - precuneus ΔFC against the (SR4-SR1) change in subjective stress rating. Each spot shows the two values for one subject and is colored by group assignment (green – "recovered stress", purple – "sustained stress"). A significant anti-correlation is identified (r=-0.562, p<0.00005) (D) right BLA-precuneus rsFC patterns of "sustained stress" group (purple) and "recovered stress" group (green). Bars indicate standard error. ∗ p<0.001, ∗∗ p<0.0005

The change in rsFC between right BLA and precuneus was further found to be significantly correlated with change in the high frequency component of HRV across all 34 subjects for which a valid HR signal was extracted from both restring-state scans (Spearman r=0.4, p<0.02). However, no association was found between the extent of this change and STAI-trait or state measures (p>0.5).

6.2.4 Discussion – study 1

In this work we conducted a data-driven investigation of stress-induced rsFC alterations and their correspondence to the subjective experience of stress, among a cohort of 57 healthy male participants. In line with our hypothesis, our analysis revealed a large-scale effect of rsFC modulations following acute social stress induction. Pinpointing the most significantly prevalent rsFC modulations, our enrichment analysis unraveled a pattern of decreased cross-hemispheral temporo-parietal connectivity along with increased thalamo-cortical (frontal, temporal and parietal lobes) connectivity. Importantly, as we predicted, these patterns of change in connectivity strength were associated with the change in subjective stress reports across subjects. Specifically a larger mean increase in reported stress immediately after the task was associated with a larger absolute rsFC change across all parcel-pairs forming both the strengthened and the weakened enriched connectivity alterations.

Network reorganization following acute stress

Our work extends previous studies investigating post-stress rsFC modulations in a hypothesis-driven manner (Van Marle, Hermans et al. 2010, Veer, Oei et al. 2011, Vaisvaser, Lin et al. 2013), by providing a broader unbiased picture. Identifying the thalamus as a central node of stress-induced rsFC increase is consistent with its known role in arousal regulation (Schiff 2008) and in mediating the interaction of attention and arousal in humans humans (Portas, Rees et al. 1998). Notably, the thalamus was found to be involved in post-stress rsFC alteration in our previous seed-based study, increasing its connectivity with the PCC (Vaisvaser et al., 2013). Increased rsFC of the thalamus with several cortical regions including the Insula and IPL was also reported following fearful in comparison to neutral movies (Eryilmaz, Van De Ville et al. 2011).

In addition, a larger increase in thalamo-cortical rsFC was associated with a larger decrease in temporo-parietal rsFC, suggesting that both patterns are part of a joint mechanism of dominance-shift induced by acute stress. The identified pattern of stress-induced rsFC weakening involved regions of the inferior, middle and superior temporal gyri along with regions of the pre- and post-central gyri and the superior and inferior parietal lobule. Most of these regions were reported to exhibit reduced BOLD activation in a within-subject analysis comparing high-stress task to a control task using a similar experimental paradigm (Wang, Rao et al. 2005) and have been repeatedly reported to increase activity in attention-driven goal-directed tasks (Hopfinger, Buonocore et al. 2000, Culham and Kanwisher 2001, Behrmann, Geng et al. 2004, Culham and Valyear 2006, Raz and Buhle 2006).

These findings are in overall agreement with the recently suggested model by which exposure to acute stress prompts a reallocation of resources to a salience network, involving several subcortical regions including the thalamus, and several cortical regions in the frontal , temporal and parietal lobes, at the cost of an executive control network , involving dorsal frontal areas and dorsal posterior parietal areas (Hermans, Henckens et al. 2014).

Post-stress rsFC modulations associated with inter-individual differences in subjective recovery

In addition to the above large-scale pattern of rsFC alterations, which were evident across subjects, we were interested in neural modulations that underlie inter-individual differences in the sustainment versus recovery of the stress experience. We identified a single modulation of rsFC between the right BLA and the precuneus that differed between individuals with self-reported

“sustained stress” and individuals with “recovered stress”. Importantly, this single statistically significant rsFC modulation was identified out of over 100,000 possible parcel-pairs without making any a-priori assumptions. This modulation was further associated with change in heart rate variability (HRV) measure from the first to the second resting state session. HRV is an established measure of regulated emotional responding, and has been used for this purpose in multiple studies (reviewed in (Appelhans 2006)). The physiological basis of this measure is that high-frequency (0.15 to 0.4 Hz) component of the power spectrum of heart rate variability (HF-HR) is considered to represent an autonomic parasympathetic vagal influence on the sino-atrial node of the heart (Malik, Bigger et al. 1996). The BLA had been acknowledged as an important locus for integrating the various hormonal and neurotransmitter systems that are involved in consolidation following exposure to acute stress (Roozendaal, McEwen et al. 2009). Moreover, previous evidence points to casual involvement of the right amygdala in generation of the subjective experience of fear and mark it as a potential therapeutic target in anxiety disorder (Fredrikson and Furmark 2003). The precuneus is a node of the DMN known to play a central role in a wide range of complex tasks, including self-referential processing and an experience of agency (Cavanna and Trimble 2006). Abnormal precuneus activity and connectivity patterns have been previously reported in PTSD patients (Bluhm, Williamson et al. 2009, Lanius, Bluhm et al. 2010, Patel, Spreng et al. 2012, Sartory, Cwik et al. 2013, Yan, Brown et al. 2013). Importantly, spontaneous BOLD activity in the BLA has been shown to be negatively associated with the activity in the posterior cingulate cortex and precuneus in healthy subjects (Roy, Shehzad et al. 2009, Zhang and Li 2012),

and abnormal patterns of precuneus-BLA rsFC have been previously reported in anxiety disorders (Bluhm, Williamson et al. 2009, Liao, Qiu et al. 2010, Pannekoek, Veer et al. 2013). In the current study we found a stress-induced enhancement of the BLA-precuneus anti-correlation in "rest2" as compared to "rest1" only in individuals who reported a sustained stress experience, i.e., the "sustained stress" group. Furthermore, when accounting for inter-individual differences, we found that the extent of this single modulation predicted the level of affective recovery reported 20 minutes later across all subjects, suggesting that it may underlie the individual tendency and dynamics of subjective stress recovery.

In conclusion, using our robust data-driven approach we were able to characterize stress-induced large-scale rsFC modulations, that were further associated with subjective experience. In addition, our group-based analysis pinpointed stress-induced rsFC change between right BLA and precuneus as a neural predictor of affective recovery. This specific connection may serve as a potential biomarker and target for future treatment in stress-related disorders.

6.3 Case study 2: Characterizing changes in resting-state networks following an anger inducing social interaction

6.3.1 Specific Background

Anger is regarded as one of the most prototypical of all emotions (Fehr and Russell 1984, Scherer and Tannenbaum 1986, Shaver, Schwartz et al. 1987), and is reported by healthy people to be experienced on a daily basis (Averill 1983, Kassinove, Sukhodolsky et al. 1997). It may be caused by a wide variety of triggers, and though it has negative consequences on health and well-being, it has a central role in motivating to take action and approach rather than avoid

a confrontation. Although anger is considered to be a survival response inherent in all living creatures, humans are normally equipped with the mental ability to control and regulate their anger, and adapt it to socially accepted norms. Anger is thus a complex multidimensional construct that poses theoretical and operational difficulties in defining it as a single psycho-biological phenomenon.

Previous neuroimaging studies investigated anger-related patterns of neural activity, under a few types of anger-inducing paradigms. These include depicting angry faces as static stimuli (Blair, Morris et al. 1999, Kesler, Andersen et al. 2001, Whalen, Shin et al. 2001), self-generation of anger by recollecting personal autobiographic angry experiences (Dougherty, Shin et al. 1999, Kimbrell, George et al. 1999, Damasio, Grabowski et al. 2000, Fabiansson, Denson et al. 2012), and generating an interpersonal situation that evokes an angry experience within the fMRI setting (Denson, Pedersen et al. 2009, Gilam, Lin et al. 2015). Of these, the latter approach accounts for the ecological and naturalistic dynamics of anger that are typically rooted in social interactions. An example to such an ecological approach is the Ultimatum Game (UG) (Güth, Schmittberger et al. 1982), which has been regarded as an interpersonal induction of angry experience (Güth, Schmittberger et al. 1982, Ochsner, Bunge et al. 2002, Etkin, Egner et al. 2006, Banks, Eddy et al. 2007, Srivastava, Espinoza et al. 2009). In the UG, a proposer offers to split a sum of money, between himself and a responder who in turn decides whether to accept or reject the offer. If he accepts, both players receive the designated sum of money but if he rejects, both receive nothing. Replicated by countless studies, people tend to reject offers of 25% and below of the total sum (Camerer

2003). The common explanation is that these are unfair offers that elicit anger, which results in a rejection and thus no money is gained (Pillutla and Murnighan 1996, Van't Wout, Kahn et al. 2006, Rotemberg 2008, Andrade and Ariely 2009). Several studies using the UG point to emotion regulation (ER) as the capability which enabled participants to overcome the anger evoked by the unfair offers and decide to accept them after all in order to increase monetary reward (Kirk, Carnevale et al. 2006, Koenigs and Tranel 2007, Kirk, Downar et al. 2011, Grecucci, Giorgetta et al. 2013). Thus it reasonable to assume that a participant who gains more money in a UG has employed some form of ER strategy which enabled to down-regulate the anger and accept more unfair offers, compared to a participant who gained less money.

A few neuroimaging studies investigated neural activation patterns induced over the course of UG. These identified the involvement of the insula, dorsolateral PFC (DPLFC), ACC, superior temporal sulcus (STS) and inferior-frontal gyrus (IFG) when people are confronted with unfair offers (Sanfey, Rilling et al. 2003, Kirk, Downar et al. 2011, Feng, Luo et al. 2015). However, patterns of functional connectivity induced by UG have not yet been explored. In addition, all these studies investigated data recorded during course of UG. The sustained neural effect of UG in subsequent resting-state is still unexplored.

In this project we examined the effect of UG on subsequent resting state rsFC patterns, with respect to behavioral measures of gain and reported levels of anger. We expected to find alterations in rsFC patterns that would be associated with behavioral measures.

6.3.2 Specific materials and methods

Participants

We used fMRI data collected at our lab, on a cohort of 60 healthy male participants (age 18-20). Participants had no reported history of psychiatric or neurological disorders, no current use of psychoactive drugs, no family history of major psychiatric disorders, and no previous exposure to abuse during childhood and/or potentially traumatic events before entering the study. In addition, all participants had normal or corrected-to-normal vision and provided written informed consent approved by Tel Aviv Sourasky Medical Center Ethics Committee and conformed to the Code of Ethics of the World Medical Association (Helsinki Declaration). Of the 60, 9 individuals were excluded from the current analysis due to signal artifacts and additional 7 were removed due to excessive head movements; therefore the final study group consisted of 44 participants.

Experimental procedure

Each participant underwent two 6 min. resting state scans ("rest1", and “rest2” respectively), interleaved by 10 rounds of anger-inducing task (10 minutes). Anger was induced using a modified version of the Ultimatum game (UG), fully described in (Gilam, Lin et al. 2015). Briefly, participants underwent 10 rounds, which included a money partition offer, a participant decision, a display of the resulting sums and a 30 seconds negotiation between the participant and a putative participant who is in fact a professional actor trained with scripted improvisations to further intensify the negative emotional experience. The experimental timeline is shown in Figure 6-6**.** During the rest conditions participants were instructed to keep their eyes open and stare at a fixation point.

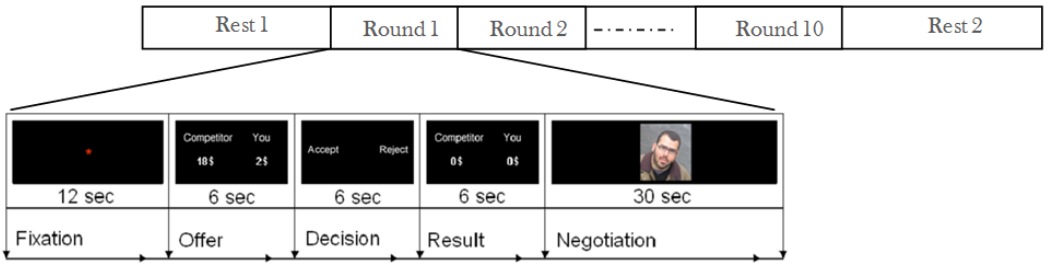

Figure 6-6: Experimental procedure of case study 2: Two sessions of 6 min. resting-state fMRI were recorded before and after 10 rounds of ultimatum game performed in the scanner, which included staring at a fixation cross, an offer made by the actor, a decision made by the participant, a display of the resulting partition and a negotiation period.

Behavioral measures

Subjective emotional reports were obtained using the Geneva Emotion Wheel (Gilam, Lin et al. 2015) (GEW) scheme. The GEW presents 16 types of emotion arranged in a circular pattern based on two axes, control (high/low coping potential) and valence (positive/negative): Pride, Elation, Happiness, Satisfaction, Relief, Hope, Interest, Surprise, Anxiety, Sadness, Boredom, Shame/Guilt, Disgust, Contempt, Hostility and Anger. The GEW has been shown to be a valid instrument to measure emotions within a decision making context. In our adapted-GEW (aGEW), participants were instructed to rate each emotion on a 7-point intensity scale from 0 (zero) to 6 (very high). In addition, the aGEW is an iterated version in which participants have a specific emotional wheel for each offer, result and negotiation periods of the game, thus reaching 30 wheels (3 wheels for each of the 10 UG-rounds). The participants were instructed to rate these wheels consecutively and dynamically, with each wheel being referenced to the emotion ratings of the previous wheel. This allows both the participant and the researchers a complex overview of all the emotions, with each their own intensity value, experienced in each period of the mUG.

State-Trait Anxiety Inventory (STAI) described in section 4.2 was administered at the beginning of the experiment.

fMRI data acquisition information

fMRI was acquired with standard gradient-echo echo-planar imaging (GE-EPI) sequence of T2*-weighted images (TR/TE/flip angle: 3,000/35/90; FOV: 20 * 20 cm1; matrix size: 96*96) divided into 39 axial slices (thickness: 3 mm; gap: 0 mm) covering the whole cerebrum. Each scanning session also includes high-resolution anatomical imaging which was acquired by a 3D spoiled gradient echo (SPGR) sequence with high-resolution 1mm slice thickness (FOV: 25*18; matrix: 256*256; TR/TE:7.3/3.3 ms).

fMRI preprocessing and parcellation

Preprocessing and parcellation procedures are identical to the ones described in chapter 6.2.2 .

Parcel-based univariate global functional connectivity analysis

To assess evidence for experimental effects we applied the same univariate analysis approach described in section 6.2, in which a model is fitted independently to each connection. In addition, we conducted global FC analysis in which for each parcel, the sum of functional connections with all other parcels was computed. This procedure was performed also for positive and negative FCs separately. We next calculated the change in these overall rsFC values for each subject and parcel by subtracting global FC level estimates of "rest1" from the corresponding estimates in "rest2", resulting in three rsFC change values (denoted ΔrsFC, $\Delta rsFC^{s}$ and $\Delta rsFC^{-}$) for each parcel and for each subject. To identify parcels that demonstrated significant change in overall rsFC following

UG, we applied a one-sample t-test on the ΔrsFC values of each parcel across all subjects.

The procedure is described in Figure 6-7.

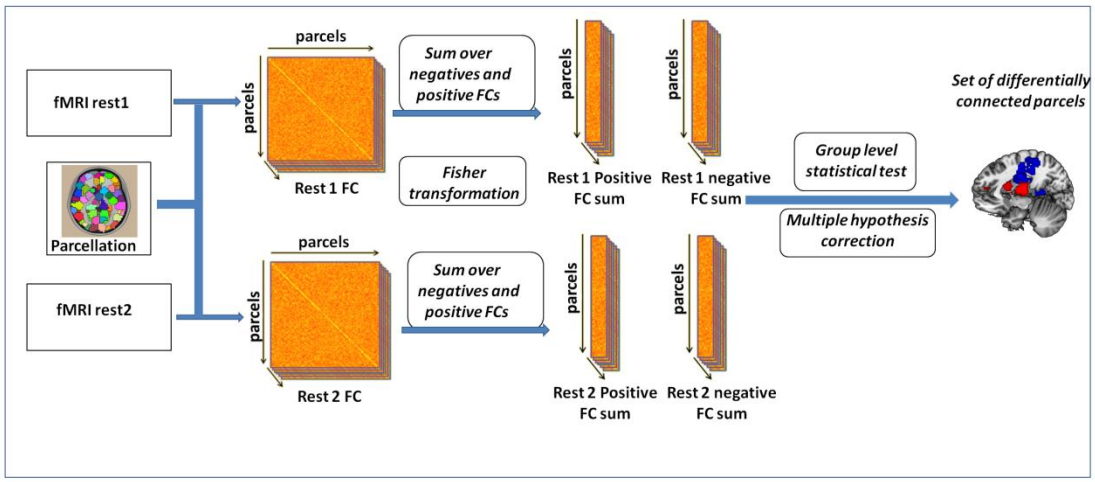

Figure 6-7: An illustration of the global rsFC analysis steps: Following parcellation, cross-correlation matrices were calculated for each subject and resting-state session. A paired t-test was applied separately on the sum of all positive rsFC values and of the sum of all negative rsFC values to identify parcels for which rsFC changed significantly. An FDR procedure was used to correct for multiple testing.

6.3.3 Results

Though it is not part of the findings of the current study, it should be noted that during UG, unfair offers were associated with increased levels of reported anger, and with a decrease in positive emotions compared to fair offers. Notably this association increased in the second half of the game, in which even fair offers seemed to have become more irritating, pointing at the effect of the anger-infused social dynamics both in subjective reports and skin conductance measure (Gilam, Lin et al. 2015).

STAI-trait measures were associated with both reported anger and gain achieved in subsequent UG task. Specifically, a positive correlation was found between STAI-trait and achieved gain (Spearman r=0.35, p=0.019) and a negative correlation was found between STAI-trait and reported anger (Spearman r=-0.33, p=0.027).

rsFC alterations following anger-inducing ultimatum game

In order to identify anger-induced rsFC changes we conducted a univariate statistical analysis on the Fisher-transformed cross-correlation matrices. This was done by subtracting the "rest1" matrix from the "rest2" matrix, and then applying a one-sample t-test on the resulting ΔFC values of each parcel pair. This analysis did not reveal any significant rsFC change (FDR q>0.5). We next conducted a global functional connectivity analysis, by calculating, for each parcel, the sum of functional connections with all other parcels. This was repeated also for positive and negative FCs separately. We then applied a one-sample t-test on the resulting ΔrsFC, $\Delta rsFC^{+}$ and $\Delta rsFC^{-}$ values of each parcel. This analysis revealed a single parcel centered in the right amygdala (18,-3,-18) for which positive rsFC significantly increased following the task (FDR q<0.05, t=4.34). We next repeated the rsFC univariate analysis focusing only on functional connections that involve this specific parcel. This analysis revealed a single connection with the right inferior frontal gyrus (rIFG) (28,18,-18), which was significantly strengthened following the task (FDR q< 0.05, t=4.29). This connection is shown in Figure 6-8 C.

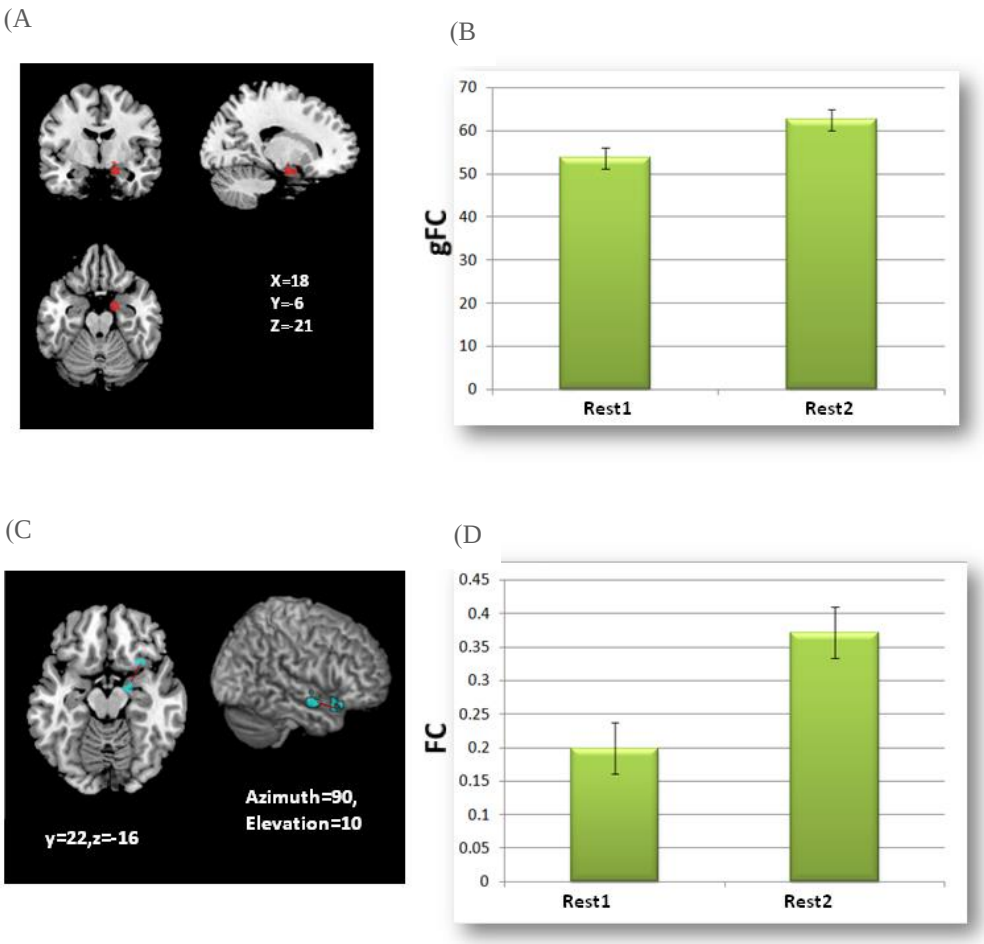

Figure 6-8: rsFC changes identified flowing UG: A parcel centered in the right amygdala (shown in A) demonstrated a significant increase in overall positive rsFC following UG (level of increase is shown in B). When examining rsFC change involving that parcel only, a significant increase was identified with a single parcel centered in the right IFG (Connection is shown in C). The extent of identified change is shown in D.

Relation between identified rsFC change and behavioral measures

Examination of the relation between the identified rsFC change and our behavioral measures, namely: reported anger, gain achieved in the game and trait-anxiety, revealed a significant positive correlation between the aforementioned rAmy-rIFG rsFC change and STAI-trait measure, estimated at the beginning of the experiment (Spearman r=0.48, p=0.0015). However, no association was found between reported anger or gain and Amy-rIGF rsFC

(p>0.5) nor was there an association between these measures and overall change in rAmy rsFC (p>0.3).

We further examined the relation between rsFC values during rest 1 and rest 2 and the same behavioral measures and found a significant association between overall rsFC of the rAmy-centered parcel during “rest1” and reported anger level (Spearman r=-0.33,p<0.03; Figure 6-9 A), as well as with gain (Spearman r=0.353,p<0.02; Figure 6-9 B). Notably, a non-significant anti-correlation was found between reported anger, and gain achieved in UG (Spearman r=-0.27, p>0.07).

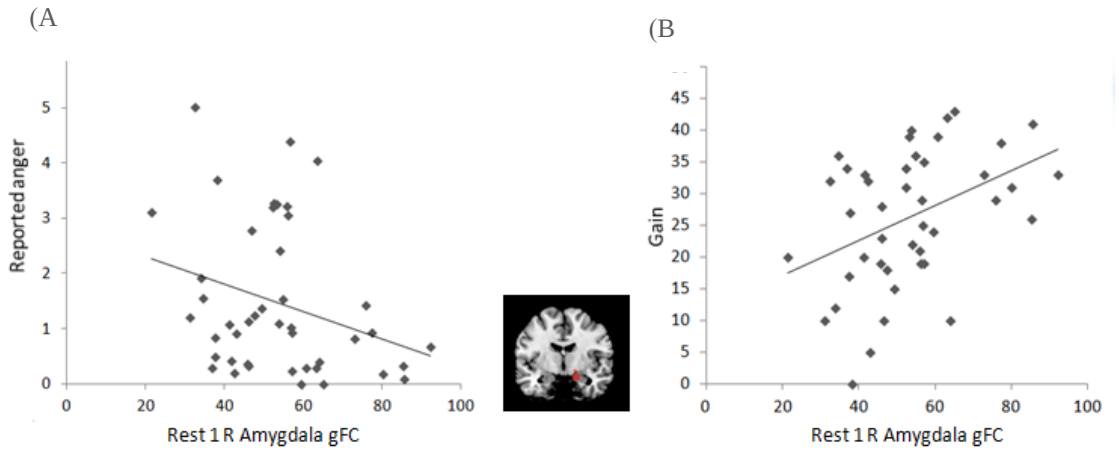

Figure 6-9: Scatter plots presenting the reported level of anger following UG (A) and the gain achieved during the game (B) against overall positive rsFC (denoted as gFC) of parcel 363 centered in the right amygdala during rest1. Each spot shows the two values for one subject. A significant anti-correlation is identified with reported anger (Spearman r=-0.33, p<0.03), while a significant correlation is identified with gain (Spearman r=0.353,p<0.02)

6.3.4 Discussion- study 2

As we hypothesized, UG induced a change in patterns of rsFC in subsequent resting-state. However, rather than a large-scale effect, our analysis in this case revealed a specific increase in rsFC of the right amygdala, which was mostly driven by an increase in rsFC with the right IFG. The right IFG has been acknowledged for its central involvement in response inhibition (Aron, Robbins et al. 2004, Aron, Robbins et al. 2014), and was reported to exhibit anti-

correlated activity with the amygdala during an emotion-regulation task. Furthermore the extent of this anti-correlation was reported as one of a few variables, explaining inter-individual variance in inhibition of emotional response (Depue, Orr et al. 2015). Interestingly, in the current study we identified an increased positive correlation between these regions in post-task resting state, rather than an anti-correlation. However, positive correlation has been demonstrated before between the amygdala and several frontal regions including dorsolateral, dorsal medial, anterior cingulate and orbital during emotion-regulation tasks (Banks, Eddy et al. 2007). Notably, in the current study the extent of rAmy-rIFG change positively correlated with anxiety tendency measured at the beginning of the experiment by STAI-trait questionnaire. STAI-trait measure was also positively correlated with gain and negatively correlated with reported anger, indicating that individuals with a higher trait anxiety gained more in the game and experienced less anger during UG task, after which they showed a higher increase in rsFC between the right amygdala and the right IFG. These results support the hypothesis that the increased FC in right amygdala – right IFG is part of an anger regulation mechanism.

In contrast to previous literature on the involvement of amygdala-rIFG FC in emotion-regulation, in this case, findings were obtained on rsfMRI data and without making any a priori decisions on seed ROIs. To the best of our knowledge, this is the first attempt to investigate changes in rsFC following induction of anger. Thus our findings extend previous literature by indicating that the neural effect of UG task is sustained in subsequent rsFC patterns. Notably, the overall functional connectivity level of amygdala before the task (but not its connectivity with right IFG), was associated with the gain achieved

during the task as well as the levels of reported anger, supporting the claim that information on individual tendencies of emotion-processing and regulation exists in baseline coactivation patterns of rsfMRI.

6.4 Joint Discussion

In this chapter we presented the analysis of alterations in rsFC patterns induced by two different types of psychological challenges that involve social interactions: acute-social stress (TSST) and inter-personal conflict that is known to provoke anger (UG). Notably, in both studies data was recorded from healthy young male participants. The number of participants was similar in the two studies. In addition, analysis steps (namely preprocessing steps, parcellation and rsFC analysis) were very similar between studies. In spite of this similarity, there was a substantial difference in the rsFC effect that was identified in each experiment. While acute stress induced a large-scale distributed effect, a very specific small-scale effect was identified following anger-provoking UG.

In both cases connectivity patterns of the right amygdala were associated with individual differences in subjective experience induced by the task. However, while in the case of UG, its overall rsFC at baseline was associated with elicited anger following the task, in the case of acute social stress the decrease in its rsFC with the precuneus was associated with the sustainment of stress 20 min post induction.

Interestingly, in study 2, anxious individuals demonstrated a more regulated behavioral as well as neural response to UG. This is in line with neural findings

showing opposed neuroendocrine responses in stress vs. anger (Moons, Eisenberger et al. 2010) as well as studies showing opposite patterns of frontal alpha asymmetry in approach vs. avoidance emotional response (Heller 1993, Davidson 2004, Harmon-Jones, Gable et al. 2010, Quaedflieg, Meyer et al. 2015).

While the current chapter deals with emotional challenges that are introduced by a psychological load generated via social interactions, the following chapter deals with the emotional challenge that is introduced by a physiological challenge (sleep deprivation), which is known to induce allostatic load.

7. Characterizing changes in resting-state networks following a physiological perturbation

7.1 Background

The state of sleep deprivation (SD) has consistently been associated with subjective reports of negative emotions and emotional difficulty (Horne 1985, Zohar, Tzischinsky et al. 2005, Goldstein and Walker 2014), as well as with difficulty to process, express and regulate emotions. Studies assessing objective physiological and neural measures of affect have provided additional verification of, and explanatory mechanisms for, emotional dysregulation following sleep deprivation (Gujar, Yoo et al. 2011, Goldstein and Walker 2014)

Previous fMRI studies reported that SD also disrupts task-induced deactivation within the DMN (Gujar, Yoo et al. 2010, De Havas, Parimal et al. 2012). These findings suggest that SD has a significant effect on the intrinsic functional organization of the brain, an effect that should be detected when examining rsFC patterns. Indeed, several previous studies examined rsFC alterations induced by SD. These mainly focused on the DMN and its anti-correlation with the attention and control networks (Sämann, Tully et al. 2010, De Havas, Parimal et al. 2012). Other studies reported increased FC within dorsal prefrontal cortex (Bosch, Rihm et al. 2013) and decreased thalamocortical FC (Shao, Wang et al. 2013) following SD. Notably, all the above studies used a hypothesis driven approach and did not find any association with behavioural measures. In a recent study, Yeo et al. conducted a data-driven rsFC analysis of 68 healthy subjects that underwent SD and reported a predictive association between baseline levels of anti-correlation between the DMN and attention networks and task performance under SD (Yeo, Tandi et al. 2015). However, none of the above studies reported an association between SD induced rsFC modulations and affect-related behavioral measures.

In an attempt to expand our understanding on the SD-induced rsFC modulation that underlie subsequent emotional dysregulation, we used both univariate and multivariate analysis approach to investigate fMRI data recorded from 17 healthy subjects during normal rest and in a state of sleep deprivation (after a night without sleep).

We hypothesized that SD would significantly impact connectivity patterns in the human brain and that these changes would be associated with affective impairments known to occur without sleep.

7.2 Specific materials and methods

7.2.1 Participants

17 adults (age range: 23-33 years, mean 26.9 ± 3 years; 10 females) completed a repeated measures crossover design. Participants were healthy with no prior history of sleep, neurologic or psychiatric disorders (assessed using a pre-screening questionnaire). Recent use of psycho-stimulants (e.g. Ritalin), psychiatric or hypnotic drugs also excluded subjects from participation in the study. The study was approved by the Tel-Aviv Sourasky Medical Center ethical review board and all participants provided written informed consent.

7.2.2 Experimental procedure

Each participant underwent two experimental sessions under two rest conditions, a sleep deprived (SD) condition, which took place after a night without sleep, and a sleep-rested (SR) condition, which took place after a night of normal sleep. In each experimental session a resting state scan was acquired prior to task performance for a total time of 6:50 minutes. Subjects were instructed to stay awake and keep their eyes open in front of a fixation

cross. To verify wakefulness, subjects' eyes were continuously monitored via a dedicated camera during the entire scan. As reported in (Simon, Oren et al. 2015) cognitive and behavioral changes following SD were monitored across both experimental sessions.

7.2.3 Behavioral measures

Psychomotor Vigilance Task (PVT) (Drummond, Bischoff-Grethe et al. 2005) was used to assess changes in cognitive performance. A 10-minutes version of the PVT, adopted from the PEBL task library (Mueller and Piper 2014) was performed every two hours during the SD night (from 23:00 until 7:00 am) as well as in the morning of the sleep-rested session (~8:00 am).

Positive and Negative Affective Scale (PANAS) (Watson 1988) and the visual analogue scale (VAS) were used to track mood changes. The PANAS consists of two 10-item questionnaires assessing either positive or negative mood. PANAS was administered every 4 hours across the SD night as well as upon arrival at the sleep-rested session. Participants were asked to rate each item on a scale ranging from 1 to 5.

In addition to the PANAS questionnaires, participant were asked to rate their mood ranging from terrible to excellent on a 10cm visual analogue scale (VAS).

STAI-trait questionnaire described in section 4.2 was administered at the beginning of the experiment to evaluate individual differences in anxiety proneness.

7.2.4 fMRI acquisition information

Functional whole-brain scans were performed in interleaved order with a T2*-weighted gradient echo planar imaging pulse sequence (time repetition [TR]/TE = [2,500-3,000]/35 ms, flip angle=90º, FOV = 200×200 mm, slice thickness = 4 mm, 32-39 slices per volume). Structural scans included a T1-weighted 3D axial spoiled gradient echo (SPGR) pulse sequence (TR/TE = 7.92/2.98 ms, flip angle = 15º, pixel size = 1 mm, FOV = 256×256 mm, slice thickness = 1 mm).

7.2.5 fMRI preprocessing and parcellation

fMRI preprocessing and parcellation procedures are described in section 4.1.3. Notably, in the current study, the low-resolution 200 parcels template was selected order to compensate for low sample size. As explained in section 4.1.3, parcels were masked to include gray matter voxels only using the WFU Pick Atlas Tool (Maldjian, Laurienti et al. 2003, Stamatakis, Adapa et al. 2010) and parcels that had less than 5 voxels in common with the gray matter mask were excluded, leaving 182 parcels. In order to reduce the effect of physiological artifacts and nuisance variables, the whole-brain mean signal, six motion parameters, cerebrospinal fluid, and white matter signals were regressed out of these parcel signals.

7.2.6 Parcel-based univariate functional connectivity analysis

Level of rsFC of each pair of parcels was estimated by calculating the Pearson correlation coefficients between the signals of the corresponding parcels. This was done for each subject and each rest condition separately. rsFC levels were next Fisher transformed to better fit a normal distribution. Baseline FC level estimates were then subtracted from the corresponding estimates in the SD

condition, resulting in a single FC change value (denoted ΔFC) for each parcel-pair and for each subject.

To identify parcels-pairs that demonstrated significant rsFC change following SD, we applied a one-sample t-test on the ΔFC values of each pair across all subjects.

To identify parcels that demonstrated significant overall rsFC change following SD, we calculated, for each parcel, the sum of ΔFC values with all other parcels, and applied a one-sample t-test on this sum across all subjects.

7.2.7 Parcel-based multivariate functional connectivity analysis

State-prediction using leave-one-out cross-validation analysis

In order to further examine the overall effect of SD on rsFC, we applied a leave-one-out cross validation (LOOCV) analysis on the data in the following manner: for each subject s, we calculated the Euclidian distance between subject–specific SR and SD rsFC values and the group average rsFC values (where subject s is excluded), across the k top ranking features (i.e. parcel pairs). Features were ranked according to the difference in group-level values between the two states (subject s excluded). Analysis was performed with k=1 to 500. Each subject-specific scan was assigned a state (SR or SD) based on the closest group-level rsFC data. Accuracy levels were defined as the number of correct assignments divided by the number of scans. Sensitivity was defined as the fraction of correctly assigned SD scans, while specificity was defined as the fraction of correctly assigned SR scans.

For each subject s, a success function was defined as follows:

7-1)

$$Success(s) = \begin{cases} 0 \; if \; dist(FC_s^{BS}, FC^{BS}) > dist(FC_s^{BS}, FC^{BS}) \wedge dist(FC_s^{SD}, FC^{SD}) > dist(FC_s^{SD}, FC^{BS}) \wedge \\ 2 \; if \; dist(FC_s^{BS}, FC^{BS}) \leq \wedge \; dist(FC_s^{BS}, FC^{BS}) \wedge dist(FC_s^{SD}, FC^{SD}) \leq \wedge \; dist(FC_s^{SD}, FC^{BS}) \\ 1 \qquad\qquad otherwise \end{cases}$$

Total accuracy level (acc) was defined as:

7-2)

$$acc = \sum_{s=1}^{subs} Success(s)$$

The significance of success levels was evaluated using the binomial cumulative distribution function, with p=0.5, n=2*subs:

7-3)

$$p(acc \geq k) = \sum_{i=k}^{n} \binom{n}{i} 0.5^n$$

Examining SD induced changes in graph modular organization

Group level rsFC matrices were constructed by averaging state-specific rsFC matrices across subjects. State-specific modularity structures were evaluated separately for SR and for SD by applying the weight-conserving Louvain modularity algorithm (Rubinov and Sporns 2011) on the group-level rsFC matrices. Due to some randomized steps in the algorithm implementation, this step was repeated 100 times for each graph, and the results were merged using the BCT implementation of the algorithm for detection of consensus clustering in complex networks as described in (Lancichinetti and Fortunato 2012).

SR modules were compared with SD modules using the Jaccard overlap score. The Jaccard score is given by:

$$\textbf{7-4)}\quad jac(m_1, m_2) = \frac{|p_1 \cap p_2|}{|p_1 \cup p_2|}$$

Where m_i stands for module I, and p_i stands for the set of parcels that constitute module i.

Modules were characterized by analysis of enrichment with seven predefined functional brain networks reported in (Yeo, Krienen et al. 2011). This analysis was conducted using the RichMind toolbox (http://acgt.cs.tau.ac.il/RichMind) described in 5.2.

7.3 Results

Although it is not part of the current study, it should be noted that as expected, SD induced a significant elevation in negative mood (M=1.3±0.28 to M=1.59±0.56; p<0.05), reduction in positive mood (M=2.86±0.65 to M=2.01±0.85; p< 0.0005) and in overall mood assessment via VAS (M=8.1±1.14 to M=5.7±2.37; p< 0.005), and reduction in task performance (M=2.94±2.49 to M=10.06±6.86; p<0.0005) (Simon, Oren et al. 2015).

7.3.1 rsFC alterations identified following sleep deprivation

In order to identify SD-induced rsFC changes we conducted a univariate statistical analysis on the Fisher-transformed cross-correlation matrices. This was done by subtracting the SR matrix from the SD matrix, and then applying a one-sample t-test on the resulting ΔFC values of each parcel pair. In this pairwise analysis, when correcting for all possible parcel-pairs no significant rsFC change was identified.

We next calculated a sum of ΔFC values for each parcel p, and applied a one-sample t–test to evaluate the level of change in overall parcel FC. This analysis revealed two parcels demonstrating significant change in overall rsFC. Parcel 165, centered in (-57,9,18) and mapped to the left frontal inferior operculum, and parcel 148, centered in (0,-6,6) and mapped to the thalamus. Results are presented in Table 7-1

TABLE 7-1– RESULTS OF UNIVARIATE OVERALL RSFC ANALYSIS

Parcel	MNI center	AAL position	t-value	p-value	FDR q-value
165	**-57,9,18**	**Front_Inf_Oprc_L**	**5.77**	**2.8e-5**	**0.0052**
148	**0,-6,6**	**Thalamus_L**	**-4.667**	**2.6e-4**	**0.0314**

We next performed the pairwise rsFC univariate analysis while considering only rsFC changes involving the above two parcels (i.e. treating these two parcels as seed-parcels), and correcting only for 2*n comparisons (n = 182; number of parcels). This resulted in 28 parcel-pairs demonstrating significant change in rsFC. Results are specified in Table 7-2 and shown in Figure 7-1 A and B. When examining the relationship between these two patterns of thalamus rsFC decrease and left operculum rsFC increase (Figure 7-1 C), we detected a marginally significant anti-correlation between them (r=-0.41, p=0.051 one tailed) .

TABLE 7-2– RESULTS OF PAIRWISE UNIVARIATE RSFC ANALYSIS SEEDED IN PARCELS 165 AND 148

Parcel	AAL positions	FDR q-value	p-value	t-value	MNI center
Significant ΔFC change with parcel 165					
19	Calcarine_L	0.0441	0.0022	3.65	-48, -72, 9
53	Frontal_Inf_Orb_R	0.0441	0.001	4.01	48, -72, 12

71	Frontal_Inf_Orb_R	0.0446	0.0032	3.46	-9 , -69 , 21
91	Frontal_Sup_Medial_L	0.0446	0.0032	3.46	45 , 30 , -12
139	Frontal_Sup_Medial_R	0.0441	0.0018	3.73	27 , 24 , -15
186	Frontal_Sup_Medial_R	0.0475	0.0037	3.4	0 , 51 , 27
193	Frontal_Sup_Medial_R	0.0441	0.0009	4.09	12 , 63 , 9
112	Insula_L	0.0441	0.0018	3.73	12 , 45 , 45
105	Lingual_R	0.0446	0.0032	3.47	12 , 57 , 30
97	Occipital_Mid_L	0.0441	0.0012	3.94	-30 , 12 , -18
115	Precentral_R	0.0441	0.0007	4.19	15 , -57 , 3
58	Precuneus_L	0.0446	0.0031	3.48	-36 , -84 , 27
2	Temporal_Mid_L	0.0441	0.0022	3.65	45 , 0 , 48
150	Temporal_Mid_L	0.0446	0.0027	3.55	0 , -54 , 15
85	Temporal_Mid_R	0.0446	0.0029	3.51	-51 , -63 , 21
Significant ΔFC change with parcel 148					
5	Cingulum_Ant_L	0.0441	0.002	-3.7	-6 , 45 , 6
160	Cingulum_Ant_L	0.0446	0.0031	-3.48	0 , 21 , -9
22	Cingulum_Ant_R	0.0441	0.0013	-3.88	6 , 42 , 6
109	Frontal_Med_Orb_L	0.0441	0.0017	-3.76	0 , 57 , -9
127	Frontal_Mid_R	0.0441	0.0019	-3.72	30 , 18 , 51
104	Frontal_Sup_Medial_L	0.028	0.0001	-5.26	-9 , 63 , 12
139	Frontal_Sup_Medial_R	0.0441	0.0003	-4.52	12 , 63 , 9
189	Fusiform_L	0.0446	0.0033	-3.45	-27 , -51 , -12
3	Precuneus_R	0.0441	0.0009	-4.08	9 , -66 , 24
173	Supp_Motor_Area_L	0.0441	0.002	-3.68	-9 , 18 , 60
43	Temporal_Inf_L	0.0441	0.002	-3.69	-42 , 6 , -39
72	Temporal_Mid_L	0.0441	0.0007	-4.2	-60 , -15 , -18
101	Temporal_Mid_L	0.0446	0.0029	-3.52	-54 , 0 , -30

A)

B)

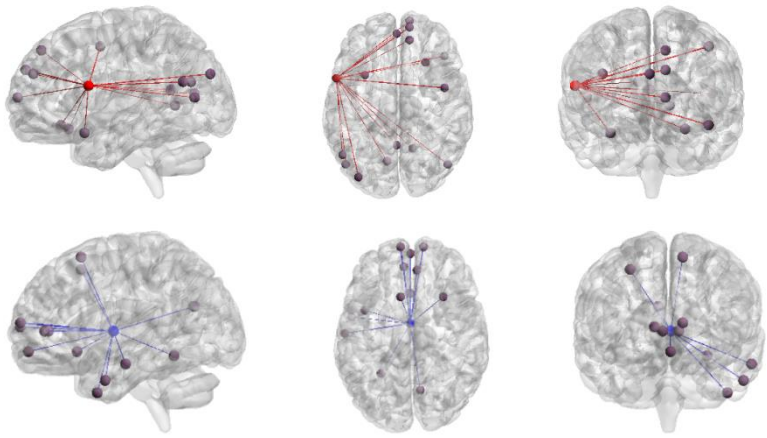

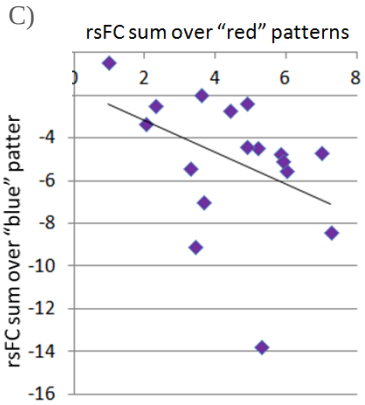

Figure 7-1: **Results of pairwise univariate rsFC analysis seeded in parcels 165 and 148.** Using FDR of 0.05, 28 parcels demonstrating significant change in rsFC between baseline and SD. Of these, 15 demonstrated rsFC increase with parcel 165 (A - shown in red) and 13 demonstrated rsFC decrease with 148 (B - shown in blue). Visualization was generated using Brain Net Viewer (Xia, Wang et al. 2013). A negative association between the "red" and the "blue" patterns is shown in C, where each point represents one subject.

We next examined the extent of rsFC change across parcel pairs identified in the above analysis against changes in task performance, mood and STAI reports. Results are shown in Figure7-2. Overall rsFC change across 15 strengthened connections with parcel 165 was marginally associated with change in negative PANAS score (Spearman r=-0.47, p=0.057), overall rsFC change across 13 weakened

connections with parcel 150 was associated with task performance (Spearman r=0.61,p=0.009) and lastly, the extent of rsFC change across all 28 differential connections was positively associated with STAI-trait measured at the beginning of the experiment (Spearman r=0.48, p=0.053).

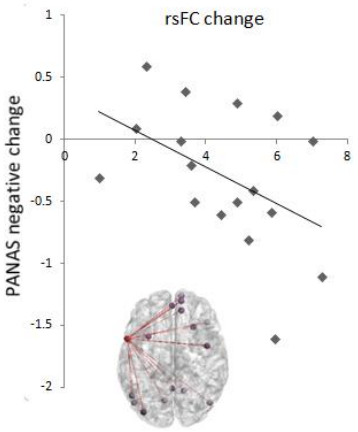

Figure 7-2: association between SD –induced rsFC change and behavioral measures. The “red” pattern was marginally associated with change in negative mood measured with PANAS (Spearman r=-0.47,p<0.06)

rsFC-based state prediction using LOOCV

In order to examine the extent to which rsFC patterns reflect SD, we applied a LOOCV procedure, so that for each subject s, group rsFC matrices were calculated after s had been excluded from the data. The analysis was performed 500 times using k=1 to 500 most differential functional connections. Figure 7-3 shows the accuracy achieved using subject-group Euclidean distance as a function of k. A maximum accuracy of 85.29% ($p=1.93*10^{-5}$, Binomial distribution) was achieved using only 24 FCs as features. 8 out of 24 features were repeatedly selected in all 17 iterations, and these are listed in Table7-3 and shown in Figure7-4.

Notably, only two of these features were identified in the previously described univariate rsFC analysis seeded in parcel 148 (Centered in the Thalamus). When examining the relationship between the “blue” (rsFC decrease) features and “red” (rsFC increase) features, (Figure 7-4), we detected a significant anti-correlation between them (r=-0.65, p=0.005). In contrast to the rsFC alterations identified in the univariate analysis, here we did not find any association between the extent of rsFC change across features and affective measures (p>0.1) nor did we find such an association with task performance.

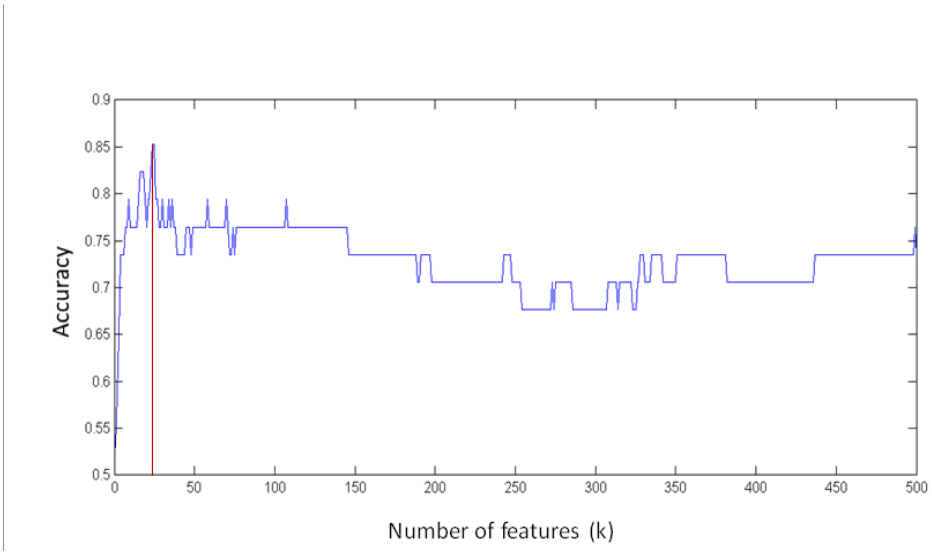

Figure 7-3: Accuracy rates of LOOCV analysis presented as a function of number of used features (k). The red vertical line indicates k=24, the value for which the highest accuracy (85.29%, $p=1.93*10^{-5}$, Binomial distribution) was achieved.

Table 7-3: Parcel pairs that were selected as features in all 17 iterations of LOOCV (k=24) analysis

ID 1	MNI center	ID 2	MNI center	SR rsFC	SD rsFC
11	(-63,-30,-3)	24	(-60,-27,15)	-0.172	0.305
64	(27,-3,57)	65	(12,-45,66)	0.354	-0.086
17	(48,9,33)	90	(-27,12,54)	-0.374	0.159
11	(-63,-30,-3)	119	(57,3,6)	-0.223	0.256
34	(-51,6,33)	127	(30,18,51)	-0.226	0.245
104	(-9,63,12)	148	(0,-6,6)	0.319	-0.148
139	(12,63,9)	148	(0,-6,6)	0.427	-0.048
119	(57,3,6)	197	(-42,-30,15)	0.343	-0.204

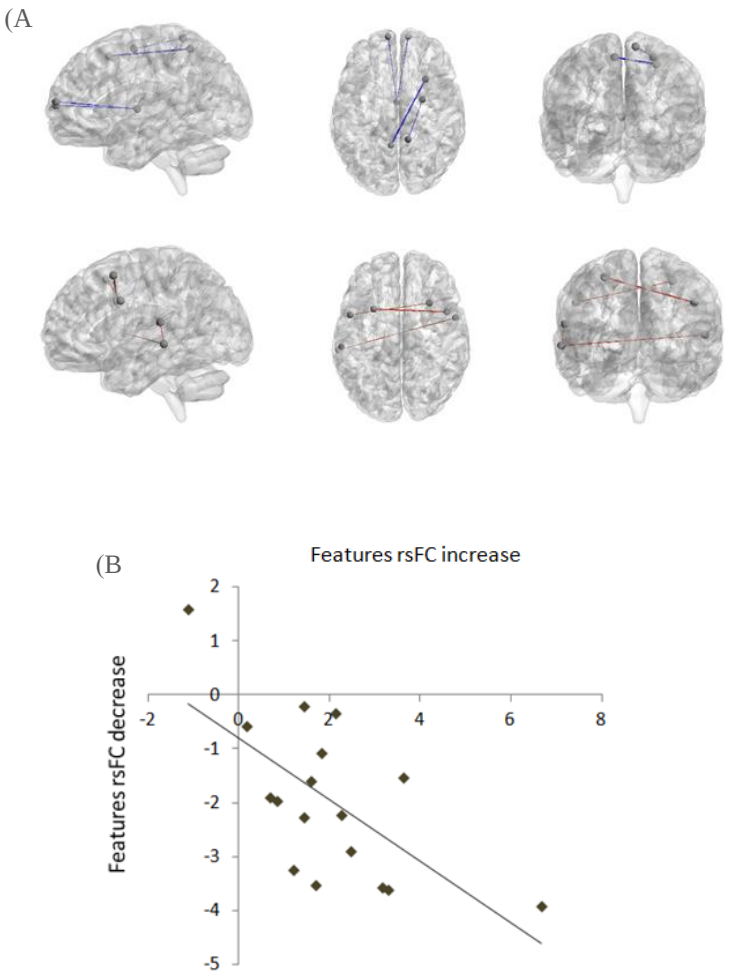

Figure 7-4: (A) 8 parcel pairs that were selected as features in all 17 iterations of LOOCV (k=24) analysis presented on a 3D brain image. Edge color indicates the direction of change in rsFC across group (red=rsFC increase, blue=rsFC decrease), edge width is proportional to the extent of change. Image was generated using Brain Net Viewer (Xia, Wang et al. 2013). (B) A scatter plot showing the rsFC change across "blue" features against rsFC change across "red" features in A. Each point represents one subject. A significant anti correlation was identified (r=-0.65, p=0.005)

In addition to the above feature selection process, we conducted the same LOOCV analysis using all 28 parcel-pairs identified in the rsFC univariate analysis as features. Classification accuracy was then raised to 94.1% ($p=3.47*10^{-8}$, Binomial distribution) with sensitivity =94.1% and specificity =94.1%.

SD induced changes in rsFC modular organization

To gain a broad perspective on changes in network organization following SD, we applied modularity analysis on group-level graphs that were generated by averaging state-specific matrices across subjects. This analysis revealed 4 modules in each of the two state graphs. In order to characterize the differences in modular organization in a statistically sound manner, we analyzed the enrichment of 7 predefined functional brain networks reported in (Yeo, Krienen et al. 2011) within each module. The 7 networks are shown in Figure 7-5. Results are shown in Table 7-3.

Table 7-4: Modules identified via modularity analysis on group-level rsFC matrices. Enrichment results are shown for each module, and include the FDR corrected significance (q-value), the enrichment score and the size of overlap between the module and the enriched network. Network name abbreviations: VS=visual network, FPCN=fronto-parietal control network, DMN=default mode network, SMN=somato-motor network, VAN=ventral attention network, DAN=dorsal attention network, Limb=limbic

ID	SR size	SD size	Overlap (jaccard)	SR enrichments			SD enrichments		
				Network	qValue	No. of parcels	Network	qValue	No. of parcels
1	26	41	0.558	VN	$4.8E^{-12}$	23	VN	$6.54E^{-}$	24
2	82	48	0.547	FPCN	$1.08E^{-}$	21	FPCN	$1.12E^{-7}$	19
				DMN	$5.27E^{-}$	26	DMN	$2.23E^{-5}$	19
				Limb	0.0236	8			
3	60	63	0.732	SMN	0.0125	12	SMN	$3.20E^{-8}$	19
				VAN	$5.27E^{-}$	16	VAN	$7.62E^{-5}$	16
4	14	30	0	DAN	$7.19E^{-4}$	5	LIMB	$4.11E^{-7}$	9
							DMN	0.0329	10

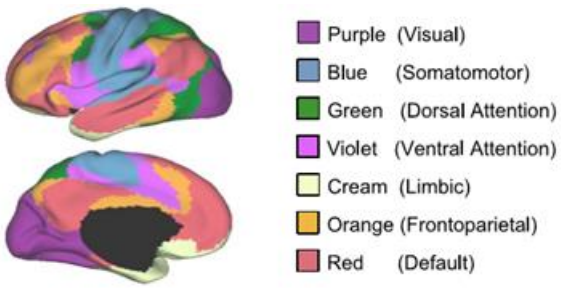

Figure 7-5: Annotations used in enrichment analysis: 7 network parcellation of the human cerebral cortex based on 1,000 Subjects. Adapted from (Yeo, Krienen et al. 2011)

Our analysis revealed several changes in the modular organization of the brain following SD: following SD: first, the VN-enriched module (module 1) showed an increase in size. Second, the DMN-FPCN-Limb enriched module (module 2) showed a decrease in size due to DMN and Limb parcels (including bilateral amygdala) that were reassigned to a separate module that was enriched with Limbic and DMM parcels. Lastly, a module that was enriched with DAN parcels (baseline module 4) was not detected following SD. Instead DAN parcels were distributed among several modules including VN enriched module and SMN_VAN- enriched module. These changes are shown in Figure 7-6 A.

Following these finding we examined the change in connectivity strength within modules that were enriched with Limbic-annotated parcels against affective behavioral measures. We identified a significant anti-correlation between the connectivity strength within SD module 4 and the change in positive mood as measured by the PANAS questionnaire (Spearman r=-0.67, p=0.0031), whereas the change in connectivity strength among parcels of the same module was positively correlated with the change in overall mood as measured by VAS (Spearman r=0.64, p=0.0056). In addition a marginally significant association was found between change in connectivity strength of baseline module 2 and change in negative mood as measured by the PANAS questionnaire (Spearman r=0.46, p=0.06). Results are shown in Figure7-6 B.

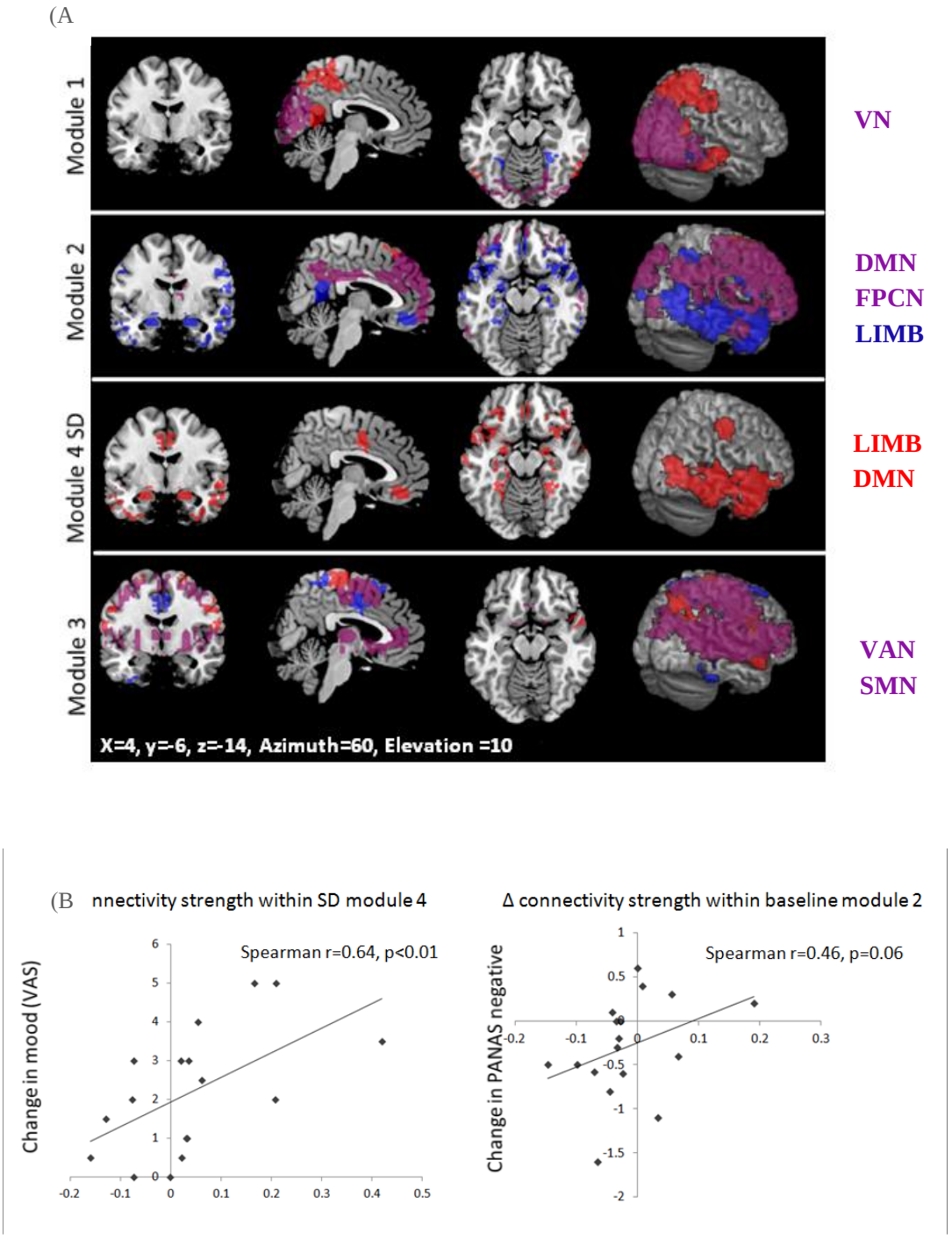

Figure 7-6: (A) SD-induced module alterations shown as overlays in MRICroN visualization. Baseline modules are shown in blue, SD modules are shown in red, overlaps are shown in purple. Enrichment based functional association is presented on the right; VN=visual network, DMN=default mode network, FPCN=fronto-parietal control network, LIMB=limbic network, VAN=ventral attention network, SMN=somatomotor network (B) The changes in connectivity strength of baseline module2 (right plot) as well as SD module 4 (left plot) were associated with change in reported mood across subjects.

7.

Following sleep deprivation we identified a large-scale distributed effect of decrease in thalamo-cortical rsFC and increase in rsFC of the operculum with

several cortical regions. These patterns were associated with changes in both task performance and reported mood. The use of a two-stage univariate analysis procedure assisted in overcoming the limitation of a relatively small sample size, by decreasing the number of statistical tests. For that same purpose we adopted, in this case, a relatively coarse parcellation of the brain into ~200 parcels instead of the ~500 parcels that were used for the other two datasets analyzed in this work.

The left frontal operculum is part of the left IFG, which is known for its role in language comprehension and generation (Friederici, Rüschemeyer et al. 2003, Vigneau, Beaucousin et al. 2006). This region has also been implicated in evaluating affective meaning of speech intonation (Wildgruber, Hertrich et al. 2004). However, its central involvement in SD induced neural modulations and the relation of these modulations to change in subjective affective experience is surprising. The thalamus is known for its central role in arousal regulation (Schiff 2008) and in mediating the interaction of attention and arousal in humans (Portas, Rees et al. 1998). Furthermore, reduced thalamo-cortical rsFC following SD has already been reported in previous literature (Shao, Wang et al. 2013). Modularity analysis performed on group-level rsFC matrices provided additional insight on SD induced network reorganization, by pinpointing the SD induced decomposition of a functional module involving DMN, limbic and FPCN regions into two functional modules, one enriched with DMN and FPCN parcels and the other enriched with limbic and DMN parcels. That change was further associated with subjective affective measures. Notably, this change was not revealed by our univariate analysis, which demonstrates the advantage of such a combined analysis. A breakdown in

connectivity within the DMN following SD has been documented before (De Havas, Parimal et al. 2012). However, to the best of our knowledge, this is the first time it has been associated with affective behavioral measures.

8. Concluding Discussion

8.1 Overview of the results

In this work the sustained effect of several types of emotionally challenging experiences on subsequent resting-state neural pattern was investigated, as well as the way these patterns reflect inter-individual differences in emotion processing and regulation.

The novel use of enrichment analysis introduced here for studying changes in rsFC provides improved means for exploring experience-related neural modulations in cases where the induced effect is large and distributed. This type of distributed effect was found following acute social stress as well as following SD. However, while acute stress induced an increase in thalamo-cortical functional connectivity, and a decrease in functional connectivity among various cortical regions, the opposite effect was identified following SD. Notably, in both cases, the extent of rsFC increase correlated with the extent of identified rsFC decrease, suggesting that these patterns are part of a joint mechanism.

The central involvement of the thalamus in the identified large scale neural modulations following stress and under SD may be attributed to its central role in arousal regulation (Schiff 2008) and in mediating the interaction of attention and arousal in humans (Portas, Rees et al. 1998).

The fundamental difference in the direction of rsFC modulation is in line with the suggestion that SD acts as a chronic stressor resulting in allostatic load (i.e. cumulative wear and tear on body systems), in which the system is low on resources, and thus differs by nature from acute stress (McEwen 2006) in which the saliency system is recruited at the expense of higher cognitive functions (Hermans, Henckens et al. 2014). Interestingly, in both cases, the extent of the

two rsFC patterns (increase vs. decrease) was correlated across subjects, suggesting that they are both part of a joint mechanism of dominance shift. Furthermore, the extent of this change was associated with subjective measures of affective experience.

In both SD and UG, trait anxiety was predictive of rsFC change effect. Specifically a higher STAI-t was associated with a larger change in rsFC following SD as well as UG. This indicates that individuals with a lower trait anxiety were less affected by the different challenges in the neuronal level and were thus more “resilient” to them. This finding extends previous literature on the relation between trait anxiety and stress resilience (McFarlane 1990). However, in contrast to our expectations, this indication was not found in the case of social stress, where no association was found between state or trait anxiety and the identified rsFC changes.

In all three cases examined, rsFC patterns of the amygdala seemed to underlie individual differences in coping with the introduced challenges: (1) In the case of anger provoking UG, the overall baseline rsFC of the amygdala predicted gain as well as elicited anger. (2) Following acute stress, rsFC change between the BLA and precuneus was associated with subjective affective recovery 20 minutes later. (3) Change in connectivity strength within a limbic-DMN functional module, which includes amygdala, was associated with change in affective state following SD. These findings extend previous literature by demonstrating again the relation between amygdala FC and individual differences in emotion processing and regulation.

Our findings can be summarized in a model by which the conditions of the environment (e.g. social conflict) as well as by individual tendencies effect the interaction between the limbic system and regions of the default-mode network, which in turn affects the emotional experience. This model is illustrated in Figure 8-1.

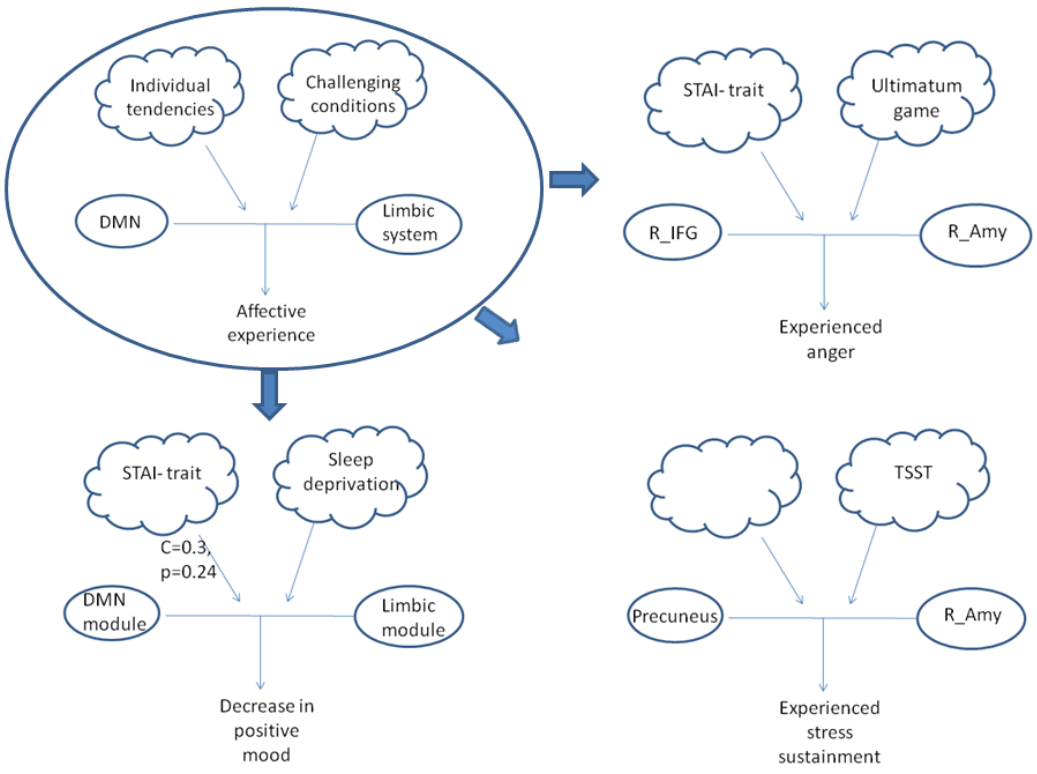

Figure 8-1: A model that summarizes our findings on rsFC changes that are associated with individual differences in emotional response: challenging conditions (e.g. social conflict) as well as by individual tendencies affect the interaction between the limbic system and regions of the default-mode network, which in turn effects the emotional experience

8.2. Methodological insights and contributions

Throughout this work we adopted a univariate approach for exploring changes in patterns of rsFC. However, in the case of SD, due to small sample size, we used an additional multivariate approach, which included LOOCV analysis and a graph modularity analysis. This integrated analysis produced new and

interesting findings that corresponded with inter-individual differences in subjective affective measures, and would not have been revealed in full, had we chosen only one of these approaches. In light of these results, we believe that a combined univariate-multivariate analysis may be beneficial for studying large-scale effects, as suggested in (Varoquaux and Craddock 2013).

The use of enrichment analysis to study patterns in fMRI, introduced in this work, offers a novel perspective on functional neural connectivity. This method addresses a basic problem in the field, by rigorously seeking the main signal within large-scale effects. In addition to providing an improved and more reliable mechanism of interpretation, extracting the main signal allows one to seek association with behavioral measures as well as other physiological measures with a low number of statistical tests, thus increasing statistical power of the analysis. To the best of our knowledge, enrichment analysis has not been used before for this purpose.

8.2. Study Limitations

In this study we examined the effect of different types of emotional challenges on patterns of neural coactivation at rest. Notably, this type of analysis overlooks region/parcel activity levels (amplitude). rsfMRI activity patterns have been shown to hold valuable information (Tian, Jiang et al. 2008, Wang, Jiang et al. 2008, Han, Wang et al. 2011, Liu, Hu et al. 2012), which in the context of the current study was overlooked. In addition, by using resting-state fMRI recorded immediately after an emotionally challenging task, our results provide a partial picture and do not reveal information on the chronometry of these modulations.

Our analysis was based on a predefined functional parcellation of the gray matter in order to reduce dimensionality. Though this parcellation has been tested and validated, the selection of parcellation template has been shown to effect subsequent results. Specifically high resolution templates provide reduced statistical power due to large number of tests, while low resolution templates may result in losing signals from small neural structures.

The use of enrichment analysis is always based on some previously established mapping that is used as an annotation. For this purpose, it would be ideal to use an established functional mapping of the brain that is accepted and acknowledged in the field as “common ground”. Such annotation systems exist in other fields for this type of analysis. E.g. the Gene Ontology system (Consortium 2004) or the KEGG pathway database (Kanehisa and Goto 2000) that are used as gene annotations in computational genomics analysis. However, due to the lack of such a common-ground in neuroscience, we adopted a functional annotation that was based on a previously published study, conducted on the 1000 connectomes data, and an anatomic annotation of lobe-laterality information that was based on the TD atlas. We believe that established mapping systems will be available in the near future, which will encourage and improve the use of enrichment analysis in the field.

REFERENCES

Adelstein, J. S., Z. Shehzad, M. Mennes, C. G. DeYoung, X.-N. Zuo, C. Kelly, D. S. Margulies, A. Bloomfield, J. R. Gray and F. X. Castellanos (2011). "Personality is reflected in the brain's intrinsic functional architecture." PloS one **6**(11): e27633-e27633.

Admon, R., D. Leykin, G. Lubin, V. Engert, J. Andrews, J. Pruessner and T. Hendler (2013). "Stress-induced reduction in hippocampal volume and connectivity with the ventromedial prefrontal cortex are related to maladaptive responses to stressful military service." Human brain mapping **34**(11): 2808-2816.

Admon, R., G. Lubin, O. Stern, K. Rosenberg, L. Sela, H. Ben-Ami and T. Hendler (2009). "Human vulnerability to stress depends on amygdala's predisposition and hippocampal plasticity." Proceedings of the National Academy of Sciences **106**(33): 14120-14125.

Admon, R., M. R. Milad and T. Hendler (2013). "A causal model of post-traumatic stress disorder: disentangling predisposed from acquired neural abnormalities." Trends in cognitive sciences **17**(7): 337-347.

Ames, D. L., C. J. Honey, M. A. Chow, A. Todorov and U. Hasson (2015). "Contextual Alignment of Cognitive and Neural Dynamics." Journal of cognitive neuroscience.

Andrade, E. B. and D. Ariely (2009). "The enduring impact of transient emotions on decision making." Organizational Behavior and Human Decision Processes **109**(1): 1-8.

Appelhans, B. M., Luecken, L. J. (2006). "Heart rate variability as an index of regulated emotional responding." Review of General Psychology **Vol 10**(3): 229-240.

Aron, A. R., T. W. Robbins and R. A. Poldrack (2004). "Inhibition and the right inferior frontal cortex." Trends in Cognitive Sciences **8**(4): 170-177.

Aron, A. R., T. W. Robbins and R. A. Poldrack (2014). "Inhibition and the right inferior frontal cortex: one decade on." Trends in Cognitive Sciences **18**(4): 177-185.

Attwell, D., A. M. Buchan, S. Charpak, M. Lauritzen, B. A. MacVicar and E. A. Newman (2010). "Glial and neuronal control of brain blood flow." Nature **468**(7321): 232-243.

Averill, J. R. (1983). "Studies on anger and aggression: Implications for theories of emotion." American psychologist **38**(11): 1145.

Banks, S. J., K. T. Eddy, M. Angstadt, P. J. Nathan and K. L. Phan (2007). "Amygdala–frontal connectivity during emotion regulation." Social cognitive and affective neuroscience **2**(4): 303-312.

Banks, S. J., K. T. Eddy, M. Angstadt, P. J. Nathan and K. L. Phan (2007). "Amygdala–frontal connectivity during emotion regulation." Soc Cogn Affect Neurosci **2**(4): 303-312.

Bar-Haim, Y., D. Lamy, L. Pergamin, M. J. Bakermans-Kranenburg and M. H. Van Ijzendoorn (2007). "Threat-related attentional bias in anxious and nonanxious individuals: a meta-analytic study." Psychological bulletin **133**(1): 1.

Beckmann, C. F., M. DeLuca, J. T. Devlin and S. M. Smith (2005). "Investigations into resting-state connectivity using independent component analysis." Philosophical Transactions of the Royal Society of London B: Biological Sciences **360**(1457): 1001-1013.

Beckmann, C. F. and S. M. Smith (2004). "Probabilistic independent component analysis for functional magnetic resonance imaging." Medical Imaging, IEEE Transactions on **23**(2): 137-152.

Beckmann, M., H. Johansen-Berg and M. F. Rushworth (2009). "Connectivity-based parcellation of human cingulate cortex and its relation to functional specialization." The Journal of neuroscience **29**(4): 1175-1190.

Behrmann, M., J. J. Geng and S. Shomstein (2004). "Parietal cortex and attention." Current Opinion in Neurobiology **14**(2): 212-217.

Bellec, P., P. Rosa-Neto, O. C. Lyttelton, H. Benali and A. C. Evans (2010). "Multi-level bootstrap analysis of stable clusters in resting-state fMRI." Neuroimage **51**(3): 1126-1139.

Benjamini, Y. and Y. Hochberg (1995). "Controlling the false discovery rate: a practical and powerful approach to multiple testing." Journal of the Royal Statistical Society. Series B (Methodological): 289-300.

Berkowitz, L. (1989). "Frustration-aggression hypothesis: examination and reformulation." Psychological bulletin **106**(1): 59.

Berkowitz, L. (1993). Towards a general theory of anger and emotional aggression: Implications of the cognitive-neoassociationistic perspective for the analysis of anger and other emotions, Lawrence Erlbaum Associates, Inc.

Biswal, B., F. Zerrin Yetkin, V. M. Haughton and J. S. Hyde (1995). "Functional connectivity in the motor cortex of resting human brain using echo-planar mri." Magnetic Resonance in Medicine **34**(4): 537-541.

Biswal, B. B., M. Mennes, X.-N. Zuo, S. Gohel, C. Kelly, S. M. Smith, C. F. Beckmann, J. S. Adelstein, R. L. Buckner and S. Colcombe (2010). "Toward discovery science of human brain function." Proceedings of the National Academy of Sciences **107**(10): 4734-4739.

Blair, R., J. S. Morris, C. D. Frith, D. I. Perrett and R. J. Dolan (1999). "Dissociable neural responses to facial expressions of sadness and anger." Brain **122**(5): 883-893.

Blanchard, D. C. and R. J. Blanchard (2003). "What can animal aggression research tell us about human aggression?" Hormones and Behavior **44**(3): 171-177.

Bluhm, R. L., P. C. Williamson, E. A. Osuch, P. A. Frewen, T. K. Stevens, K. Boksman, R. W. Neufeld, J. Théberge and R. A. Lanius (2009). "Alterations in default network connectivity in posttraumatic stress disorder related to early-life trauma." Journal of psychiatry & neuroscience: JPN **34**(3): 187.

Blumensath, T., T. E. Behrens and S. M. Smith (2012). Resting-state FMRI single subject cortical parcellation based on region growing. Medical Image Computing and Computer-Assisted Intervention–MICCAI 2012, Springer**:** 188-195.

Bosch, O. G., J. S. Rihm, M. Scheidegger, H.-P. Landolt, P. Stämpfli, J. Brakowski, F. Esposito, B. Rasch and E. Seifritz (2013). "Sleep deprivation increases dorsal nexus connectivity to the dorsolateral prefrontal cortex in humans." Proceedings of the National Academy of Sciences **110**(48): 19597-19602.

Buckner, R. L. and F. M. Krienen (2013). "The evolution of distributed association networks in the human brain." Trends in cognitive sciences **17**(12): 648-665.

Burghy, C. A., D. E. Stodola, P. L. Ruttle, E. K. Molloy, J. M. Armstrong, J. A. Oler, M. E. Fox, A. S. Hayes, N. H. Kalin and M. J. Essex (2012). "Developmental pathways to amygdala-prefrontal function and internalizing symptoms in adolescence." Nature neuroscience **15**(12): 1736-1741.

Camerer, C. (2003). Behavioral Game Theory: Experiments in Strategic Interaction, Princeton University Press.

Cannon, W. B. (1929). "Vob. IX JULY, 1929 No. 3 ORGANIZATION FOR PHYSIOLOGICAL HOMEOSTASIS." Physiological Reviews **9**(3).

Cavanna, A. E. and M. R. Trimble (2006). "The precuneus: a review of its functional anatomy and behavioural correlates." Brain **129**(3): 564-583.

Cicchetti, D., B. P. Ackerman and C. E. Izard (1995). "Emotions and emotion regulation in developmental psychopathology." Development and psychopathology **7**(01): 1-10.

Consortium, G. O. (2004). "The Gene Ontology (GO) database and informatics resource." Nucleic acids research **32**(suppl 1): D258-D261.

Craddock, R. C., P. E. Holtzheimer, X. P. Hu and H. S. Mayberg (2009). "Disease state prediction from resting state functional connectivity." Magnetic Resonance in Medicine **62**(6): 1619-1628.

Craddock, R. C., G. A. James, P. E. Holtzheimer, X. P. Hu and H. S. Mayberg (2012). "A whole brain fMRI atlas generated via spatially constrained spectral clustering." Human Brain Mapping **33**(8): 1914-1928.

Craddock, R. C., S. Jbabdi, C.-G. Yan, J. T. Vogelstein, F. X. Castellanos, A. Di Martino, C. Kelly, K. Heberlein, S. Colcombe and M. P. Milham (2013). "Imaging human connectomes at the macroscale." Nature methods **10**(6): 524-539.

Culham, J. C. and N. G. Kanwisher (2001). "Neuroimaging of cognitive functions in human parietal cortex." Current Opinion in Neurobiology **11**(2): 157-163.

Culham, J. C. and K. F. Valyear (2006). "Human parietal cortex in action." Current Opinion in Neurobiology **16**(2): 205-212.

Damasio, A. R., T. J. Grabowski, A. Bechara, H. Damasio, L. L. Ponto, J. Parvizi and R. D. Hichwa (2000). "Subcortical and cortical brain activity during the feeling of self-generated emotions." Nature neuroscience **3**(10): 1049-1056.

Damoiseaux, J., S. Rombouts, F. Barkhof, P. Scheltens, C. Stam, S. M. Smith and C. Beckmann (2006). "Consistent resting-state networks across healthy subjects." Proceedings of the national academy of sciences **103**(37): 13848-13853.

Davidson, R. J. (2004). "What does the prefrontal cortex "do" in affect: perspectives on frontal EEG asymmetry research." Biological psychology **67**(1): 219-234.

De Havas, J. A., S. Parimal, C. S. Soon and M. W. Chee (2012). "Sleep deprivation reduces default mode network connectivity and anti-correlation during rest and task performance." Neuroimage **59**(2): 1745-1751.

De Kloet, E. R., M. Joëls and F. Holsboer (2005). "Stress and the brain: from adaptation to disease." Nature Reviews Neuroscience **6**(6): 463-475.

Deco, G. and M. Corbetta (2011). "The dynamical balance of the brain at rest." The Neuroscientist **17**(1): 107-123.

Delorme, A. and S. Makeig (2004). "EEGLAB: an open source toolbox for analysis of single-trial EEG dynamics including independent component analysis." Journal of Neuroscience Methods **134**(1): 9-21.

Denson, T. F., W. C. Pedersen, J. Ronquillo and A. S. Nandy (2009). "The angry brain: Neural correlates of anger, angry rumination, and aggressive personality." Journal of Cognitive Neuroscience **21**(4): 734-744.

Depue, B., J. Orr, H. Smolker, F. Naaz and M. Banich (2015). "The Organization of Right Prefrontal Networks Reveals Common Mechanisms of Inhibitory Regulation Across Cognitive, Emotional, and Motor Processes." Cerebral Cortex: bhu324.

Dinstein, I., K. Pierce, L. Eyler, S. Solso, R. Malach, M. Behrmann and E. Courchesne (2011). "Disrupted neural synchronization in toddlers with autism." Neuron **70**(6): 1218-1225.

Dosenbach, N. U., B. Nardos, A. L. Cohen, D. A. Fair, J. D. Power, J. A. Church, S. M. Nelson, G. S. Wig, A. C. Vogel and C. N. Lessov-Schlaggar (2010). "Prediction of individual brain maturity using fMRI." Science **329**(5997): 1358-1361.

Dougherty, D. D., L. M. Shin, N. M. Alpert, R. K. Pitman, S. P. Orr, M. Lasko, M. L. Macklin, A. J. Fischman and S. L. Rauch (1999). "Anger in healthy men: a PET study using script-driven imagery." Biological psychiatry **46**(4): 466-472.

Drabant, E. M., K. McRae, S. B. Manuck, A. R. Hariri and J. J. Gross (2009). "Individual differences in typical reappraisal use predict amygdala and prefrontal responses." Biological psychiatry **65**(5): 367-373.

Drummond, S. P., A. Bischoff-Grethe, D. F. Dinges, L. Ayalon, S. C. Mednick and M. Meloy (2005). "The neural basis of the psychomotor vigilance task." SLEEP-NEW YORK THEN WESTCHESTER- **28**(9): 1059.

Efron, B. (2008). "Simultaneous inference: When should hypothesis testing problems be combined?" The annals of applied statistics: 197-223.

Engel, A. K., C. Gerloff, C. C. Hilgetag and G. Nolte (2013). "Intrinsic coupling modes: multiscale interactions in ongoing brain activity." Neuron **80**(4): 867-886.

Eryilmaz, H., D. Van De Ville, S. Schwartz and P. Vuilleumier (2011). "Impact of transient emotions on functional connectivity during subsequent resting state: a wavelet correlation approach." NeuroImage **54**(3): 2481-2491.

Etkin, A., T. Egner, D. M. Peraza, E. R. Kandel and J. Hirsch (2006). "Resolving Emotional Conflict: A Role for the Rostral Anterior Cingulate Cortex in Modulating Activity in the Amygdala." Neuron **51**(6): 871-882.

Fabiansson, E. C., T. F. Denson, M. L. Moulds, J. R. Grisham and M. M. Schira (2012). "Don't look back in anger: Neural correlates of reappraisal, analytical rumination, and angry rumination during recall of an anger-inducing autobiographical memory." NeuroImage **59**(3): 2974-2981.

Fehr, B. and J. A. Russell (1984). "Concept of emotion viewed from a prototype perspective." Journal of experimental psychology: General **113**(3): 464.

Feng, C., Y. J. Luo and F. Krueger (2015). "Neural signatures of fairness-related normative decision making in the ultimatum game: A coordinate-based meta-analysis." Human brain mapping **36**(2): 591-602.

Finn, E. S., X. Shen, J. M. Holahan, D. Scheinost, C. Lacadie, X. Papademetris, S. E. Shaywitz, B. A. Shaywitz and R. T. Constable (2014). "Disruption of functional networks in dyslexia: a whole-brain, data-driven analysis of connectivity." Biological psychiatry **76**(5): 397-404.

Fischl, B., D. H. Salat, E. Busa, M. Albert, M. Dieterich, C. Haselgrove, A. Van Der Kouwe, R. Killiany, D. Kennedy and S. Klaveness (2002). "Whole brain segmentation: automated labeling of neuroanatomical structures in the human brain." Neuron **33**(3): 341-355.

Foster, Brett L., V. Rangarajan, William R. Shirer and J. Parvizi (2015). "Intrinsic and Task-Dependent Coupling of Neuronal Population Activity in Human Parietal Cortex." Neuron **86**(2): 578-590.

Fox, M. D. and M. E. Raichle (2007). "Spontaneous fluctuations in brain activity observed with functional magnetic resonance imaging." Nat Rev Neurosci **8**(9): 700-711.

Fox, M. D., A. Z. Snyder, J. L. Vincent, M. Corbetta, D. C. Van Essen and M. E. Raichle (2005). "The human brain is intrinsically organized into dynamic, anticorrelated functional networks." Proceedings of the National Academy of Sciences of the United States of America **102**(27): 9673-9678.

Fox, P. T., M. E. Raichle, M. A. Mintun and C. Dence (1988). "Nonoxidative glucose consumption during focal physiologic neural activity." Science **241**(4864): 462-464.

Franceschini, A., D. Szklarczyk, S. Frankild, M. Kuhn, M. Simonovic, A. Roth, J. Lin, P. Minguez, P. Bork and C. von Mering (2013). "STRING v9. 1: protein-protein interaction networks, with increased coverage and integration." Nucleic Acids Research **41**(D1): D808-D815.

Fransson, P., U. Åden, M. Blennow and H. Lagercrantz (2011). "The functional architecture of the infant brain as revealed by resting-state fMRI." Cerebral Cortex **21**(1): 145-154.

Fredrikson, M. and T. Furmark (2003). "Amygdaloid regional cerebral blood flow and subjective fear during symptom provocation in anxiety disorders." Annals of the New York Academy of Sciences **985**(1): 341-347.

Friederici, A. D., S.-A. Rüschemeyer, A. Hahne and C. J. Fiebach (2003). "The role of left inferior frontal and superior temporal cortex in sentence comprehension: localizing syntactic and semantic processes." Cerebral cortex **13**(2): 170-177.

Frijda, N. H. (2009). "Emotions, individual differences and time course: reflections." Cognition and Emotion **23**(7): 1444-1461.

Gao, W., H. Zhu, K. S. Giovanello, J. K. Smith, D. Shen, J. H. Gilmore and W. Lin (2009). "Evidence on the emergence of the brain's default network from 2-week-old to 2-year-old healthy pediatric subjects." Proceedings of the National Academy of Sciences **106**(16): 6790-6795.

Genovese, C. R., N. A. Lazar and T. Nichols (2002). "Thresholding of statistical maps in functional neuroimaging using the false discovery rate." Neuroimage **15**(4): 870-878.

Gilam, G., T. Lin, G. Raz, S. Azrielant, E. Fruchter, D. Ariely and T. Hendler (2015). "Neural substrates underlying the tendency to accept anger-infused ultimatum offers during dynamic social interactions." NeuroImage.

Glaab, E., A. Baudot, N. Krasnogor, R. Schneider and A. Valencia (2012). "EnrichNet: network-based gene set enrichment analysis." Bioinformatics **28**(18): i451-i457.

Glahn, D. C., A. Winkler, P. Kochunov, L. Almasy, R. Duggirala, M. Carless, J. Curran, R. Olvera, A. Laird and S. Smith (2010). "Genetic control over the resting brain." Proceedings of the National Academy of Sciences **107**(3): 1223-1228.

Goldstein, A. N. and M. P. Walker (2014). "The role of sleep in emotional brain function." Annual review of clinical psychology **10**: 679-708.

Grecucci, A., C. Giorgetta, M. van't Wout, N. Bonini and A. G. Sanfey (2013). "Reappraising the ultimatum: an fMRI study of emotion regulation and decision making." Cerebral Cortex **23**(2): 399-410.

Greicius, M. D., B. Krasnow, A. L. Reiss and V. Menon (2003). "Functional connectivity in the resting brain: a network analysis of the default mode hypothesis." Proceedings of the National Academy of Sciences **100**(1): 253-258.

Gross, J. J. and O. P. John (2003). "Individual differences in two emotion regulation processes: implications for affect, relationships, and well-being." J Pers Soc Psychol **85**(2): 348-362.

Guidotti, R., C. Del Gratta, A. Baldassarre, G. L. Romani and M. Corbetta (2015). "Visual Learning Induces Changes in Resting-State fMRI Multivariate Pattern of Information." The Journal of Neuroscience **35**(27): 9786-9798.

Gujar, N., S.-S. Yoo, P. Hu and M. P. Walker (2010). "The unrested resting brain: sleep deprivation alters activity within the default-mode network." Journal of cognitive neuroscience **22**(8): 1637-1648.

Gujar, N., S.-S. Yoo, P. Hu and M. P. Walker (2011). "Sleep deprivation amplifies reactivity of brain reward networks, biasing the appraisal of positive emotional experiences." The Journal of neuroscience **31**(12): 4466-4474.

Güth, W., R. Schmittberger and B. Schwarze (1982). "An experimental analysis of ultimatum bargaining." Journal of economic behavior & organization **3**(4): 367-388.

Hampson, M., N. R. Driesen, P. Skudlarski, J. C. Gore and R. T. Constable (2006). "Brain connectivity related to working memory performance." The Journal of neuroscience **26**(51): 13338-13343.

Han, Y., J. Wang, Z. Zhao, B. Min, J. Lu, K. Li, Y. He and J. Jia (2011). "Frequency-dependent changes in the amplitude of low-frequency fluctuations in amnestic mild cognitive impairment: a resting-state fMRI study." Neuroimage **55**(1): 287-295.

Harmelech, T. and R. Malach (2013). "Neurocognitive biases and the patterns of spontaneous correlations in the human cortex." Trends in cognitive sciences **17**(12): 606-615.

Harmelech, T., S. Preminger, E. Wertman and R. Malach (2013). "The day-after effect: long term, Hebbian-like restructuring of resting-state fMRI patterns induced by a single epoch of cortical activation." The Journal of Neuroscience **33**(22): 9488-9497.

Harmon-Jones, E., P. A. Gable and C. K. Peterson (2010). "The role of asymmetric frontal cortical activity in emotion-related phenomena: A review and update." Biological psychology **84**(3): 451-462.

Harmon-Jones, E. and J. Sigelman (2001). "State anger and prefrontal brain activity: evidence that insult-related relative left-prefrontal activation is associated with experienced anger and aggression." Journal of personality and social psychology **80**(5): 797.

He, B. J., A. Z. Snyder, J. M. Zempel, M. D. Smyth and M. E. Raichle (2008). "Electrophysiological correlates of the brain's intrinsic large-scale functional architecture." Proceedings of the National Academy of Sciences **105**(41): 16039-16044.

Heller, W. (1993). "Neuropsychological mechanisms of individual differences in emotion, personality, and arousal." Neuropsychology **7**(4): 476.

Hermans, E. J., M. J. Henckens, M. Joëls and G. Fernández (2014). "Dynamic adaptation of large-scale brain networks in response to acute stressors." Trends in Neurosciences **37**(6): 304-314.

Hermans, E. J., H. J. van Marle, L. Ossewaarde, M. J. Henckens, S. Qin, M. T. van Kesteren, V. C. Schoots, H. Cousijn, M. Rijpkema and R. Oostenveld (2011). "Stress-related noradrenergic activity prompts large-scale neural network reconfiguration." Science **334**(6059): 1151-1153.

Herringa, R. J., R. M. Birn, P. L. Ruttle, C. A. Burghy, D. E. Stodola, R. J. Davidson and M. J. Essex (2013). "Childhood maltreatment is associated with altered fear circuitry and increased internalizing symptoms by late adolescence." Proceedings of the National Academy of Sciences **110**(47): 19119-19124.

Hopfinger, J., M. Buonocore and G. Mangun (2000). "The neural mechanisms of top-down attentional control." Nature Neuroscience **3**(3): 284-291.

Horne, J. A. (1985). "Sleep function, with particular reference to sleep deprivation." Annals of clinical research.

Hutchison, R. M., J. P. Gallivan, J. C. Culham, J. S. Gati, R. S. Menon and S. Everling (2012). "Functional connectivity of the frontal eye fields in humans and macaque monkeys investigated with resting-state fMRI." Journal of neurophysiology **107**(9): 2463-2474.

John, O. P. and J. J. Gross (2004). "Healthy and unhealthy emotion regulation: Personality processes, individual differences, and life span development." Journal of personality **72**(6): 1301-1334.

Jola, C., P. McAleer, M.-H. Grosbras, S. A. Love, G. Morison and F. E. Pollick (2013). "Uni-and multisensory brain areas are synchronised across spectators when watching unedited dance recordings." i-Perception **4**(4): 265.

Kanehisa, M. and S. Goto (2000). "KEGG: kyoto encyclopedia of genes and genomes." Nucleic acids research **28**(1): 27-30.

Kassinove, H., D. G. Sukhodolsky, S. V. Tsytsarev and S. Solovyova (1997). "Self-reported anger episodes in Russia and America." Journal of Social Behavior & Personality.

Keller, C. J., S. Bickel, C. J. Honey, D. M. Groppe, L. Entz, R. C. Craddock, F. A. Lado, C. Kelly, M. Milham and A. D. Mehta (2013). "Neurophysiological investigation of spontaneous correlated and anticorrelated fluctuations of the BOLD signal." The Journal of Neuroscience **33**(15): 6333-6342.

Kelly, C. and F. X. Castellanos (2014). "Strengthening connections: functional connectivity and brain plasticity." Neuropsychology review **24**(1): 63-76.

Kesler, M. L., A. H. Andersen, C. D. Smith, M. J. Avison, C. E. Davis, R. J. Kryscio and L. X. Blonder (2001). "Neural substrates of facial emotion processing using fMRI." Cognitive Brain Research **11**(2): 213-226.

Kimbrell, T. A., M. S. George, P. I. Parekh, T. A. Ketter, D. M. Podell, A. L. Danielson, J. D. Repella, B. E. Benson, M. W. Willis and P. Herscovitch (1999). "Regional brain activity during transient self-induced anxiety and anger in healthy adults." Biological psychiatry **46**(4): 454-465.

Kirk, D., P. J. Carnevale and P. M. Gollwitzer (2006). "Self-regulation in ultimatum bargaining: Controlling emotion with binding goals."

Kirk, U., J. Downar and P. R. Montague (2011). "Interoception drives increased rational decision-making in meditators playing the ultimatum game." Frontiers in neuroscience **5**.

Kirschbaum, C., J. C. Prüssner, A. A. Stone, I. Federenko, J. Gaab, D. Lintz, N. Schommer and D. H. Hellhammer (1995). "Persistent high cortisol responses to repeated psychological stress in a subpopulation of healthy men." Psychosomatic Medicine **57**(5): 468-474.

Koenigs, M. and D. Tranel (2007). "Irrational economic decision-making after ventromedial prefrontal damage: evidence from the Ultimatum Game." The Journal of neuroscience **27**(4): 951-956.

Lahnakoski, J. M., E. Glerean, I. P. Jääskeläinen, J. Hyönä, R. Hari, M. Sams and L. Nummenmaa (2014). "Synchronous brain activity across individuals underlies shared psychological perspectives." NeuroImage **100**: 316-324.

Lancaster, J. L., M. G. Woldorff, L. M. Parsons, M. Liotti, C. S. Freitas, L. Rainey, P. V. Kochunov, D. Nickerson, S. A. Mikiten and P. T. Fox (2000). "Automated Talairach atlas labels for functional brain mapping." Human brain mapping **10**(3): 120-131.

Lancichinetti, A. and S. Fortunato (2012). "Consensus clustering in complex networks." Scientific reports **2**.

Lanius, R., R. Bluhm, N. Coupland, K. Hegadoren, B. Rowe, J. Theberge, R. Neufeld, P. Williamson and M. Brimson (2010). "Default mode network connectivity as a predictor of post-traumatic stress

disorder symptom severity in acutely traumatized subjects." Acta Psychiatrica Scandinavica **121**(1): 33-40.

Lazarus, R. S. (1994). Emotion and Adaptation, Oxford University Press.

Lerner, J. S. and D. Keltner (2001). "Fear, anger, and risk." Journal of personality and social psychology **81**(1): 146.

Lewis, C. M., A. Baldassarre, G. Committeri, G. L. Romani and M. Corbetta (2009). "Learning sculpts the spontaneous activity of the resting human brain." Proceedings of the National Academy of Sciences **106**(41): 17558-17563.

Liao, W., C. Qiu, C. Gentili, M. Walter, Z. Pan, J. Ding, W. Zhang, Q. Gong and H. Chen (2010). "Altered Effective Connectivity Network of the Amygdala in Social Anxiety Disorder: A Resting-State fMRI Study." PLoS ONE **5**(12): e15238.

Lin, T., S. Vaisvaser, E. Fruchter, R. Admon, I. Wald, D. Pine, Y. Bar-Haim and T. Hendler (2015). "A neurobehavioral account for individual differences in resilience to chronic military stress." Psychological medicine **45**(05): 1011-1023.

Liu, B., M. Song, J. Li, Y. Liu, K. Li, C. Yu and T. Jiang (2010). "Prefrontal-related functional connectivities within the default network are modulated by COMT val158met in healthy young adults." The Journal of Neuroscience **30**(1): 64-69.

Liu, F., M. Hu, S. Wang, W. Guo, J. Zhao, J. Li, G. Xun, Z. Long, J. Zhang and Y. Wang (2012). "Abnormal regional spontaneous neural activity in first-episode, treatment-naive patients with late-life depression: a resting-state fMRI study." Progress in Neuro-Psychopharmacology and Biological Psychiatry **39**(2): 326-331.

Lu, H., Q. Zou, H. Gu, M. E. Raichle, E. A. Stein and Y. Yang (2012). "Rat brains also have a default mode network." Proceedings of the National Academy of Sciences **109**(10): 3979-3984.

Mackie, D. M., T. Devos and E. R. Smith (2000). "Intergroup emotions: explaining offensive action tendencies in an intergroup context." Journal of personality and social psychology **79**(4): 602.

Maldjian, J. A., P. J. Laurienti, R. A. Kraft and J. H. Burdette (2003). "An automated method for neuroanatomic and cytoarchitectonic atlas-based interrogation of fMRI data sets." NeuroImage **19**(3): 1233-1239.

Malik, M., J. T. Bigger, A. J. Camm, R. E. Kleiger, A. Malliani, A. J. Moss and P. J. Schwartz (1996). "Heart rate variability." Eur Heart J **17**(3): 354-381.

Manning, J. R., J. Jacobs, I. Fried and M. J. Kahana (2009). "Broadband shifts in local field potential power spectra are correlated with single-neuron spiking in humans." The Journal of neuroscience **29**(43): 13613-13620.

Margulies, D. S., A. C. Kelly, L. Q. Uddin, B. B. Biswal, F. X. Castellanos and M. P. Milham (2007). "Mapping the functional connectivity of anterior cingulate cortex." Neuroimage **37**(2): 579-588.

Margulies, D. S., J. L. Vincent, C. Kelly, G. Lohmann, L. Q. Uddin, B. B. Biswal, A. Villringer, F. X. Castellanos, M. P. Milham and M. Petrides (2009). "Precuneus shares intrinsic functional architecture in humans and monkeys." Proceedings of the National Academy of Sciences **106**(47): 20069-20074.

McEwen, B. S. (2003). "Mood disorders and allostatic load." Biological psychiatry **54**(3): 200-207.

McEwen, B. S. (2004). "Protection and damage from acute and chronic stress: allostasis and allostatic overload and relevance to the pathophysiology of psychiatric disorders." Annals of the New York Academy of Sciences **1032**(1): 1-7.

McEwen, B. S. (2006). "Sleep deprivation as a neurobiologic and physiologic stressor: allostasis and allostatic load." Metabolism **55**: S20-S23.

McFarlane, A. C. (1990). "Vulnerability to posttraumatic stress disorder."

Mennes, M., C. Kelly, X.-N. Zuo, A. Di Martino, B. B. Biswal, F. X. Castellanos and M. P. Milham (2010). "Inter-individual differences in resting-state functional connectivity predict task-induced BOLD activity." Neuroimage **50**(4): 1690-1701.

Milo, R., N. Kashtan, S. Itzkovitz, M. E. Newman and U. Alon (2003). "Uniform generation of random graphs with arbitrary degree sequences." arXiv preprint cond-mat/0312028 **106**: 1-4.

Moons, W. G., N. I. Eisenberger and S. E. Taylor (2010). "Anger and fear responses to stress have different biological profiles." Brain, behavior, and immunity **24**(2): 215-219.

Mueller, S. T. and B. J. Piper (2014). "The Psychology Experiment Building Language (PEBL) and PEBL test battery." Journal of neuroscience methods **222**: 250-259.

Niazy, R., C. Beckmann, G. Iannetti, J. Brady and S. Smith (2005). "Removal of FMRI environment artifacts from EEG data using optimal basis sets." Neuroimage **28**(3): 720-737.

Nir, Y., U. Hasson, I. Levy, Y. Yeshurun and R. Malach (2006). "Widespread functional connectivity and fMRI fluctuations in human visual cortex in the absence of visual stimulation." Neuroimage **30**(4): 1313-1324.

Nir, Y., R. Mukamel, I. Dinstein, E. Privman, M. Harel, L. Fisch, H. Gelbard-Sagiv, S. Kipervasser, F. Andelman and M. Y. Neufeld (2008). "Interhemispheric correlations of slow spontaneous neuronal fluctuations revealed in human sensory cortex." Nature neuroscience **11**(9): 1100-1108.

Nummenmaa, L., E. Glerean, M. Viinikainen, I. P. Jääskeläinen, R. Hari and M. Sams (2012). "Emotions promote social interaction by synchronizing brain activity across individuals." Proceedings of the National Academy of Sciences **109**(24): 9599-9604.

Ochsner, K. N., S. A. Bunge, J. J. Gross and J. D. Gabrieli (2002). "Rethinking feelings: An fMRI study of the cognitive regulation of emotion." Journal of Cognitive Neuroscience **14**(8): 1215-1229.

Pannekoek, J. N., I. M. Veer, M.-J. van Tol, S. J. A. van der Werff, L. R. Demenescu, A. Aleman, D. J. Veltman, F. G. Zitman, S. A. R. B. Rombouts and N. J. A. van der Wee (2013). "Aberrant limbic and salience network resting-state functional connectivity in panic disorder without comorbidity." Journal of Affective Disorders **145**(1): 29-35.

Patel, R., R. N. Spreng, L. M. Shin and T. A. Girard (2012). "Neurocircuitry models of posttraumatic stress disorder and beyond: a meta-analysis of functional neuroimaging studies." Neuroscience & Biobehavioral Reviews **36**(9): 2130-2142.

Pillutla, M. M. and J. K. Murnighan (1996). "Unfairness, anger, and spite: Emotional rejections of ultimatum offers." Organizational behavior and human decision processes **68**(3): 208-224.

Portas, C. M., G. Rees, A. Howseman, O. Josephs, R. Turner and C. D. Frith (1998). "A specific role for the thalamus in mediating the interaction of attention and arousal in humans." The Journal of Neuroscience **18**(21): 8979-8989.

Pradines, J. R., V. Farutin, S. Rowley and V. Dancík (2005). "Analyzing protein lists with large networks: edge-count probabilities in random graphs with given expected degrees." Journal of Computational Biology **12**(2): 113-128.

Pruessner, J. C., K. Dedovic, N. Khalili-Mahani, V. Engert, M. Pruessner, C. Buss, R. Renwick, A. Dagher, M. J. Meaney and S. Lupien (2008). "Deactivation of the limbic system during acute psychosocial stress: evidence from positron emission tomography and functional magnetic resonance imaging studies." Biological psychiatry **63**(2): 234-240.

Quaedflieg, C., T. Meyer, F. Smulders and T. Smeets (2015). "The functional role of individual-alpha based frontal asymmetry in stress responding." Biological psychology **104**: 75-81.

Rahnenführer, J., F. S. Domingues, J. Maydt and T. Lengauer (2004). "Calculating the statistical significance of changes in pathway activity from gene expression data." Statistical Applications in Genetics and Molecular Biology **3**(1).

Raichle, M. E. (2010). "The brain's dark energy." Scientific American **302**(3): 44-49.

Raichle, M. E. (2011). "The restless brain." Brain Connectivity **1**(1): 3-12.

Raichle, M. E. and M. A. Mintun (2006). "Brain work and brain imaging." Annu. Rev. Neurosci. **29**: 449-476.

Raz, A. and J. Buhle (2006). "Typologies of attentional networks." Nature Reviews Neuroscience **7**(5): 367-379.

Raz, G., Y. Winetraub, Y. Jacob, S. Kinreich, A. Maron-Katz, G. Shaham, I. Podlipsky, G. Gilam, E. Soreq and T. Hendler (2012). "Portraying emotions at their unfolding: a multilayered approach for probing dynamics of neural networks." NeuroImage **60**(2): 1448-1461.

Riedl, V., M. Valet, A. Wöller, C. Sorg, D. Vogel, T. Sprenger, H. Boecker, A. M. Wohlschläger and T. R. Tölle (2011). "Repeated pain induces adaptations of intrinsic brain activity to reflect past and predict future pain." Neuroimage **57**(1): 206-213.

Rissman, J., A. Gazzaley and M. D'Esposito (2004). "Measuring functional connectivity during distinct stages of a cognitive task." Neuroimage **23**(2): 752-763.

Roozendaal, B., B. S. McEwen and S. Chattarji (2009). "Stress, memory and the amygdala." Nature Reviews Neuroscience **10**(6): 423-433.

Rotemberg, J. J. (2008). "Minimally acceptable altruism and the ultimatum game." Journal of Economic Behavior & Organization **66**(3): 457-476.

Roy, A. K., Z. Shehzad, D. S. Margulies, A. M. C. Kelly, L. Q. Uddin, K. Gotimer, B. B. Biswal, F. X. Castellanos and M. P. Milham (2009). "Functional connectivity of the human amygdala using resting state fMRI." NeuroImage **45**(2): 614-626.

Rubinov, M. and O. Sporns (2010). "Complex network measures of brain connectivity: uses and interpretations." NeuroImage **52**(3): 1059-1069.

Rubinov, M. and O. Sporns (2011). "Weight-conserving characterization of complex functional brain networks." NeuroImage **56**(4): 2068-2079.

Sämann, P. G., C. Tully, V. I. Spoormaker, T. C. Wetter, F. Holsboer, R. Wehrle and M. Czisch (2010). "Increased sleep pressure reduces resting state functional connectivity." Magnetic Resonance Materials in Physics, Biology and Medicine **23**(5-6): 375-389.

Sanfey, A. G., J. K. Rilling, J. A. Aronson, L. E. Nystrom and J. D. Cohen (2003). "The neural basis of economic decision-making in the ultimatum game." Science **300**(5626): 1755-1758.

Sartory, G., J. Cwik, H. Knuppertz, B. Schürholt, M. Lebens, R. J. Seitz and R. Schulze (2013). "In search of the trauma memory: a meta-analysis of functional neuroimaging studies of symptom provocation in posttraumatic stress disorder (PTSD)." PloS one **8**(3): e58150.

Scherer, K. R. and P. H. Tannenbaum (1986). "Emotional experiences in everyday life: A survey approach." Motivation and Emotion **10**(4): 295-314.

Schiff, N. D. (2008). "Central thalamic contributions to arousal regulation and neurological disorders of consciousness." Annals of the New York Academy of Sciences **1129**(1): 105-118.

Shao, Y., L. Wang, E. Ye, X. Jin, W. Ni, Y. Yang, B. Wen, D. Hu and Z. Yang (2013). "Decreased Thalamocortical Functional Connectivity after 36 Hours of Total Sleep Deprivation: Evidence from Resting State fMRI." PloS one **8**(10): e78830.

Shaver, P., J. Schwartz, D. Kirson and C. O'connor (1987). "Emotion knowledge: further exploration of a prototype approach." Journal of personality and social psychology **52**(6): 1061.

Shehzad, Z., A. C. Kelly, P. T. Reiss, D. G. Gee, K. Gotimer, L. Q. Uddin, S. H. Lee, D. S. Margulies, A. K. Roy and B. B. Biswal (2009). "The resting brain: unconstrained yet reliable." Cerebral cortex **19**(10): 2209-2229.

Sherman, B. T. and R. A. Lempicki (2009). "Bioinformatics enrichment tools: paths toward the comprehensive functional analysis of large gene lists." Nucleic Acids Research **37**(1): 1-13.

Shirer, W., S. Ryali, E. Rykhlevskaia, V. Menon and M. Greicius (2012). "Decoding subject-driven cognitive states with whole-brain connectivity patterns." Cerebral Cortex **22**(1): 158-165.

Silvia, P. J., R. A. Henson and J. L. Templin (2009). "Are the sources of interest the same for everyone? Using multilevel mixture models to explore individual differences in appraisal structures." Cognition and Emotion **23**(7): 1389-1406.

Simon, E. B., N. Oren, H. Sharon, A. Kirschner, N. Goldway, H. Okon-Singer, R. Tauman, M. M. Deweese, A. Keil and T. Hendler (2015). "Losing Neutrality: The Neural Basis of Impaired Emotional Control without Sleep." The Journal of Neuroscience **35**(38): 13194-13205.

Smith, C. A. and P. C. Ellsworth (1985). "Patterns of cognitive appraisal in emotion." Journal of personality and social psychology **48**(4): 813.

Smith, C. A. and L. D. Kirby (2009). "Putting appraisal in context: Toward a relational model of appraisal and emotion." Cognition and Emotion **23**(7): 1352-1372.

Smith, C. A. and R. S. Lazarus (1990). "Emotion and adaptation."

Spielberger, C. D. (2010). State-Trait anxiety inventory, Wiley Online Library.

Spielberger, C. D. and S. J. Sydeman (1994). "State-Trait Anxiety Inventory and State-Trait Anger Expression Inventory."

Spielberger, C. D., S. J. Sydeman, A. E. Owen and B. J. Marsh (1999). "Measuring anxiety and anger with the State-Trait Anxiety Inventory (STAI) and the State-Trait Anger Expression Inventory (STAXI)."

Sporns, O. (2011). "The non-random brain: efficiency, economy, and complex dynamics." Frontiers in computational neuroscience **5**.

Sripada, C., D. Kessler, Y. Fang, R. C. Welsh, K. Prem Kumar and M. Angstadt (2014). "Disrupted network architecture of the resting brain in attention-deficit/hyperactivity disorder." Human brain mapping **35**(9): 4693-4705.

Srivastava, J., F. Espinoza and A. Fedorikhin (2009). "Coupling and decoupling of unfairness and anger in ultimatum bargaining." Journal of Behavioral Decision Making **22**(5): 475-489.

Stamatakis, E. A., R. M. Adapa, A. R. Absalom and D. K. Menon (2010). "Changes in resting neural connectivity during propofol sedation." PLoS One **5**(12): e14224.

Talairach, J. and P. Tournoux (1988). "Co-planar stereotaxic atlas of the human brain. 3-Dimensional proportional system: an approach to cerebral imaging."

Tambini, A., N. Ketz and L. Davachi (2010). "Enhanced Brain Correlations during Rest Are Related to Memory for Recent Experiences." Neuron **65**(2): 280-290.

Tarvainen, M. P., J. P. Niskanen, J. A. Lipponen, P. O. Ranta-aho and P. A. Karjalainen (2009). Kubios HRV — A Software for Advanced Heart Rate Variability Analysis

4th European Conference of the International Federation for Medical and Biological Engineering. J. Sloten, P. Verdonck, M. Nyssen and J. Haueisen, Springer Berlin Heidelberg. **22:** 1022-1025.

Thirion, B., G. Flandin, P. Pinel, A. Roche, P. Ciuciu and J. B. Poline (2006). "Dealing with the shortcomings of spatial normalization: Multi-subject parcellation of fMRI datasets." Human brain mapping **27**(8): 678-693.

Thomason, M. E., E. L. Dennis, A. A. Joshi, S. H. Joshi, I. D. Dinov, C. Chang, M. L. Henry, R. F. Johnson, P. M. Thompson and A. W. Toga (2011). "Resting-state fMRI can reliably map neural networks in children." Neuroimage **55**(1): 165-175.

Tian, L., T. Jiang, M. Liang, Y. Zang, Y. He, M. Sui and Y. Wang (2008). "Enhanced resting-state brain activities in ADHD patients: a fMRI study." Brain and Development **30**(5): 342-348.

Tunbridge, E. M., S. M. Farrell, P. J. Harrison and C. E. Mackay (2013). "Catechol-O-methyltransferase (COMT) influences the connectivity of the prefrontal cortex at rest." Neuroimage **68**: 49-54.

Tyszka, J. M., D. P. Kennedy, L. K. Paul and R. Adolphs (2014). "Largely typical patterns of resting-state functional connectivity in high-functioning adults with autism." Cerebral Cortex **24**(7): 1894-1905.

Tzourio-Mazoyer, N., B. Landeau, D. Papathanassiou, F. Crivello, O. Etard, N. Delcroix, B. Mazoyer and M. Joliot (2002). "Automated anatomical labeling of activations in SPM using a macroscopic anatomical parcellation of the MNI MRI single-subject brain." Neuroimage **15**(1): 273-289.

Uddin, L. Q., A. Clare Kelly, B. B. Biswal, F. Xavier Castellanos and M. P. Milham (2009). "Functional connectivity of default mode network components: correlation, anticorrelation, and causality." Human brain mapping **30**(2): 625-637.

Ulitsky, I., A. Maron-Katz, S. Shavit, D. Sagir, C. Linhart, R. Elkon, A. Tanay, R. Sharan, Y. Shiloh and R. Shamir (2010). "Expander: from expression microarrays to networks and functions." nature protocols **5**(2): 303-322.

Ulrich-Lai, Y. M. and J. P. Herman (2009). "Neural regulation of endocrine and autonomic stress responses." Nature Reviews Neuroscience **10**(6): 397-409.

Vahdat, S., M. Darainy, T. E. Milner and D. J. Ostry (2011). "Functionally specific changes in resting-state sensorimotor networks after motor learning." The Journal of Neuroscience **31**(47): 16907-16915.

Vaisvaser, S., T. Lin, R. Admon, I. Podlipsky, Y. Greenman, N. Stern, E. Fruchter, I. Wald, D. S. Pine, R. Tarrasch, Y. Bar-Haim and T. Hendler (2013). "Neural traces of stress: cortisol related sustained enhancement of amygdala-hippocampal functional connectivity." Frontiers in Human Neuroscience **7**.

van Kesteren, M. T. R., G. Fernández, D. G. Norris and E. J. Hermans (2010). "Persistent schema-dependent hippocampal-neocortical connectivity during memory encoding and postencoding rest in humans." Proceedings of the National Academy of Sciences **107**(16): 7550-7555.

Van Marle, H. J., E. J. Hermans, S. Qin and G. Fernández (2010). "Enhanced resting-state connectivity of amygdala in the immediate aftermath of acute psychological stress." NeuroImage **53**(1): 348-354.

Van Mechelen, I. and K. Hennes (2009). "The appraisal basis of anger occurrence and intensity revisited." Cognition and Emotion **23**(7): 1373-1388.

Van't Wout, M., R. S. Kahn, A. G. Sanfey and A. Aleman (2006). "Affective state and decision-making in the ultimatum game." Experimental brain research **169**(4): 564-568.

Varoquaux, G. and R. C. Craddock (2013). "Learning and comparing functional connectomes across subjects." NeuroImage.

Veer, I. M., N. Y. Oei, P. Spinhoven, M. A. van Buchem, B. M. Elzinga and S. A. Rombouts (2011). "Beyond acute social stress: increased functional connectivity between amygdala and cortical midline structures." NeuroImage **57**(4): 1534-1541.

Vigneau, M., V. Beaucousin, P.-Y. Herve, H. Duffau, F. Crivello, O. Houde, B. Mazoyer and N. Tzourio-Mazoyer (2006). "Meta-analyzing left hemisphere language areas: phonology, semantics, and sentence processing." Neuroimage **30**(4): 1414-1432.

Vincent, J., G. Patel, M. Fox, A. Snyder, J. Baker, D. Van Essen, J. Zempel, L. Snyder, M. Corbetta and M. Raichle (2007). "Intrinsic functional architecture in the anaesthetized monkey brain." Nature **447**(7140): 83-86.

Waites, A. B., A. Stanislavsky, D. F. Abbott and G. D. Jackson (2005). "Effect of prior cognitive state on resting state networks measured with functional connectivity." Human brain mapping **24**(1): 59-68.

Wang, J., H. Rao, G. S. Wetmore, P. M. Furlan, M. Korczykowski, D. F. Dinges and J. A. Detre (2005). "Perfusion functional MRI reveals cerebral blood flow pattern under psychological stress." Proceedings of the National Academy of Sciences of the United States of America **102**(49): 17804-17809.

Wang, J., L. Wang, Y. Zang, H. Yang, H. Tang, Q. Gong, Z. Chen, C. Zhu and Y. He (2009). "Parcellation-dependent small-world brain functional networks: A resting-state fMRI study." Human brain mapping **30**(5): 1511-1523.

Wang, J., X. Zuo, Z. Dai, M. Xia, Z. Zhao, X. Zhao, J. Jia, Y. Han and Y. He (2013). "Disrupted functional brain connectome in individuals at risk for Alzheimer's disease." Biological psychiatry **73**(5): 472-481.

Wang, K., T. Jiang, C. Yu, L. Tian, J. Li, Y. Liu, Y. Zhou, L. Xu, M. Song and K. Li (2008). "Spontaneous activity associated with primary visual cortex: a resting-state FMRI study." Cerebral cortex **18**(3): 697-704.

Wang, Z., J. Liu, N. Zhong, Y. Qin, H. Zhou and K. Li (2012). "Changes in the brain intrinsic organization in both on-task state and post-task resting state." Neuroimage **62**(1): 394-407.

Watson, D., Clark, L. A., and Tellegen, A. (1988). "Development and validation of brief measures of positive and negative affect: the PANAS scales." Journal of Personality and Social Psychology **54(6)**: 1063-1070.

Whalen, P. J., L. M. Shin, S. C. McInerney, H. Fischer, C. I. Wright and S. L. Rauch (2001). "A functional MRI study of human amygdala responses to facial expressions of fear versus anger." Emotion **1**(1): 70.

Wiggins, J. L., J. K. Bedoyan, S. J. Peltier, S. Ashinoff, M. Carrasco, S.-J. Weng, R. C. Welsh, D. M. Martin and C. S. Monk (2012). "The impact of serotonin transporter (5-HTTLPR) genotype on the

development of resting-state functional connectivity in children and adolescents: a preliminary report." Neuroimage **59**(3): 2760-2770.

Wildgruber, D., I. Hertrich, A. Riecker, M. Erb, S. Anders, W. Grodd and H. Ackermann (2004). "Distinct frontal regions subserve evaluation of linguistic and emotional aspects of speech intonation." Cerebral cortex **14**(12): 1384-1389.

Xia, M., J. Wang and Y. He (2013). "BrainNet Viewer: a network visualization tool for human brain connectomics." PLoS One **8**(7): e68910.

Yan, X., A. D. Brown, M. Lazar, V. L. Cressman, C. Henn-Haase, T. C. Neylan, A. Shalev, O. M. Wolkowitz, S. P. Hamilton and R. Yehuda (2013). "Spontaneous brain activity in combat related PTSD." Neuroscience Letters **547**: 1-5.

Yehuda, R. and J. LeDoux (2007). "Response variation following trauma: a translational neuroscience approach to understanding PTSD." Neuron **56**(1): 19-32.

Yeo, B. T., F. M. Krienen, J. Sepulcre, M. R. Sabuncu, D. Lashkari, M. Hollinshead, J. L. Roffman, J. W. Smoller, L. Zöllei and J. R. Polimeni (2011). "The organization of the human cerebral cortex estimated by intrinsic functional connectivity." Journal of Neurophysiology **106**(3): 1125-1165.

Yeo, B. T., J. Tandi and M. W. Chee (2015). "Functional connectivity during rested wakefulness predicts vulnerability to sleep deprivation." NeuroImage **111**: 147-158.

Zalesky, A., A. Fornito and E. T. Bullmore (2010). "Network-based statistic: identifying differences in brain networks." Neuroimage **53**(4): 1197-1207.

Zeng, L.-L., H. Shen, L. Liu, L. Wang, B. Li, P. Fang, Z. Zhou, Y. Li and D. Hu (2012). "Identifying major depression using whole-brain functional connectivity: a multivariate pattern analysis." Brain **135**(5): 1498-1507.

Zhang, S. and C.-s. R. Li (2012). "Functional connectivity mapping of the human precuneus by resting state fMRI." NeuroImage **59**(4): 3548-3562.

Zohar, D., O. Tzischinsky, R. Epstein and P. Lavie (2005). "The effects of sleep loss on medical residents' emotional reactions to work events: a cognitive-energy model." Sleep: Journal of Sleep and Sleep Disorders Research.

איזור (parcel) שמרכזו באמיגדלה הימנית הראה שינוי ב-ק"ת ב-מ"מ גם בעקבות מטלת קונפליקט בינאישי (גרסה מעוררת כעס של משחק האולטימטום).במקרה זה נצפתה עליה בק"ת עם איזור בודד שמרכזו בג'ירוס הפרונטלי הימני התחתון. רמת ק"ת הכוללת של אזור זה היו במתאם חיובי עם הרווח שהושג לאחר מכן במשחק, כמו גם עם רמת הכעס שדווחה בעקבות המשחק.

בעקבות חסך שינה זיהינו תבנית רחבת היקף של ירידה ב-ק"ת ב-מ"מ בין התלמוס לאוסף גדול של אזורים קורטיקלים ועליה ב-ק"ת ב-מ"מ בין האופרקולום הפרונטלי השמאלי התחתון למספר אזורים קורטיקלים. תבנית ההתחזקות לעיל הייתה במתאם שולי עם השינוי המדווח במצב- רוח שלילי. בנוסף לכך עוצמת השינוי על פני כל הקשרים המעורבים בתבנית הייתה במתאם עם מידת החרדה התכונתית, כפי שנמדדה בתחילת הניסוי.

ניתוח למידה חישובית מסוג אימות צולב בהשארת נבדק אחד בחוץ (leave one out cross validation) העלה כי תבנית רחבת היקף זו אפשרה להבחין בין מצב חסך שינה למצב מנוחה רגיל ברמת דיוק של 94.1%. בנוסף, ניתוח מודולריות שבוצע על נתוני ה-ק"מ ב-מ"מ הממוצעים על פני הקבוצה בשילוב עם ניתוח העשרה גילה שינוי בארגון המודולרי, שבו היו מעורבים אזורים המיוחסים לרשת מצב ברירת המחדל (default mode network), רשת הבקרה הפרונטו-פריאלית וכן למערכת הלימבית. שינוי זה נמצא במתאם עם השינוי במצב הרוח המדווח.

מסקנות:

השימוש החדשני שנעשה פה בניתוח העשרה לאפיון שינויים ב-ק"ת הביא לשיפור היכולת להבין ולאפיין שינויים, כאשר אלה מתרחשים בקנה מידה רחב. שיפור כזה נצפה בניתוח תוצאות המחקרים בעקבות חסך שינה וכן לאחר מטלה מעוררת מתח חברתי. השינויים שנמצאו בעקבות כל אחת מהמטלות השונות היו שונים במהותם, אך עם זאת, ניתן לומר כי הן חולקות מכנה משותף לפיו הקשר בין המערכת הלימבית לרשת מצב ברירת המחדל מושפע מהבדלים אישיותיים ומחוויות העבר, ומשפיע על החוויה הרגשית הסובייקטיבית.

במישור המתודולוגי אנו מאמינים כי ניתוח מוכוון נתונים בשילוב עם ניתוח העשרה מהווה כלי בעל פוטנציאל אבחוני לחקירת שינויים בקישוריות תפקודית מוחית.

מטרות:

1) פיתוח אמצעים משופרים לאפיון ופירוש של שינויים רחבי היקף בק"ת של נתוני fMRI.
2) חקירה מוכוונת נתונים של שינויים ב-ק"ת בעקבות מספר סוגים שונים של "אתגר רגשי".
3) זיהוי הבדלים בין אישיים בשינויי ק"ת אשר נמצאים במתאם עם הבדלים בין אישיים במדדי חוויה רגשית.

שיטות:

לצורך ניתוח העשרה בתוך קבוצות אזורים מוחיים אימצנו את המבחן הסטטיסטי ההיפר-גאומטרי, אשך מעריך את ההסתברות לראות לפחות x אלמנטים בעלי תכונה מסוימת בתוך מדגם מקרי בגודל k, תוך התחשבות בשכיחות התכונה באוכלוסייה הנדגמת. מבחן זה שימש אותנו גם לצורך חישוב העשרה בתוך קבוצות של קשרים מוחיים, אך לצורך מקרה זה הוספנו גם מבחן פרמוטציות א-פרמטרי, המתחשב בשונות במידת ק"ת באיזורי המוח השונים. שני המבחנים שולבו בחבילת Matlab בשם RichMind. בהינתן אוסף תוצאות (אזורי עניין או קשרים מוחיים) ומיפוי מוחי ידוע, RichMind בוחן את מידת העשרה בקלט, ומספק הן דוחות סטטיסטיים והן תצוגה של ההעשרות שזוהו על המוח. התוכנה נבדקה על ממצאים שהתקבלו בשני מחקרים שפורסמו בעבר, הראשון בדק הבדלי ק"ת במ"מ בין נבדקים עם ליקוי קוגניטיבי אמנסטי קל לבין נבדקים בריאים, והשני שבדק משתתפים בריאים אשר צפו בקטעי סרטים מעוררי רגשות. בהמשך ניתחנו נתוני דימות במ"מ לפני ואחרי שלוש פרדיגמות שונות המציבות אתגר רגשית: מטלה המעוררת מתח חברתי, מטלת קונפליקט בינאישי המעוררת כעס (משחק האולטימטום) ולילה ללא שינה. מחקרים אלו הכילו נתונים עבור 57, 44 ו -17 נבדקים בהתאמה. בכל שלושת המקרים נעשה שימוש בחלוקה פונקציונלית (פרצלציה) מוגדרת מראש של המוח אשר יושמה על הנתונים לפני הניתוח לצורך הפחתת ממדים. קנה המידה של הפרצלציה נבחר בהתאם למספר הנבדקים במטרה למקסם את הכח סטטיסטי. השתמשנו בגישה של ניתוח חד-משתני כדי לזהות שינויים ב-ק"ת ב-מ"מ. במחקר על חסך שינה השמשנו בשילוב בין גישה חד משתנית לרב משתנית בשל מספר הנבדקים הנמוך. ממצאים בקנה מידה רחב אופיינו בעזרת ניתוח העשרה. החוויה הרגשית נמדדה באמצעות מספר שאלוני דיווח עצמי ובחלק מהמקרים גם בעזרת מדד פיסיולוגי של קצב הלב והשונות בקצב הלב.

תוצאות עיקריות:

בעקבות מטלת לחץ (stress) חברתי זיהינו שינוי רחב היקף ב-ק"ת ב-מ"מ אשר כלל התחזקות ק"ת בין התלמוס לאזורים קורטיקליים שונים, והחלשות בין-המיספריאלית של ק"ת בין האונה הטמפורלית לפריאטלית. שינויים אלה עמדו במתאם עם שינוי בדיווחי לחץ סובייקטיבי. הוספת מדע לגבי שימור הלחץ 20 דקות מאוחר יותר הביא לגילוי הקשר בודד בין האמיגדלה הימנית לפרקונאוס, אשר ניבא במהופך את מידת ההחלמה בחוויה הסובייקטיבית.

רקע:

בעשור וחצי האחרון למדה קהילת חוקרי המוח כי גם במצב מנוחה מתרחשת פעילות מתמדת במוח אשר צורכת משאבים רבים. נמצא כי כאשר מתמקדים בתדירויות נמוכות של אותות דימות מוחי, פעילות זו מתרחשת באופן מסונכרן בתוך רשתות תפקודיות ידועות. עוד נמצא כי למרות שימורן הכללי של תבניות מסונכרנות אלה לאורך זמן, הן משתנות יחד עם שינויים במצב הקוגניטיבי והרגשי, והועלתה ההשערה כי הן מכילות בתוכן מידע על חוויות העבר של הפרט כמו גם נטיותיו הרגשיות והקוגניטיביות.

חקירת השונות בקישוריות תפקודית (ק"ת) מוחית במצב מנוחה (מ"מ) על ידי הדמיה מגנטית תיפקודית (fMRI) בוצעה בעבר באמצעות ניתוח מוכוון היפותזה, תוך התמקדות במספר מועט של אזורי עניין. גישה זו מוגבלת בכך שהיא מאפשרת לגלות רק חלק מהתופעה המתרחשת, בשל התבססותה על ידע קיים בנוגע לתהליך הנחקר. גישה חלופית היא לבצע ניתוח כלל מוחי מבוסס ווקסלים, שהוא תובעני יותר מבחינה חישובית ורגיש יותר לרעש. פשרה אפשרית בין הגישות היא התמקדות באוסף של אזורי עניין המספקים כיסוי טוב של המוח (פרצלציה). הפחתת ממדים שכזאת מאפשרת לבצע ניתוח ק"ת כלל מוחי במ"מ, תוך התייחסות לנתונים כאוסף של קשרים עצמאיים, ולבצע ניתוח סטטיסטי על כל קשר כזה בנפרד. לחלופין, שיטות רבות-משתנים מאפשרות להעריך את היחסים בין מטריצות שלמות של ערכי ק"מ ואת המשתנים הפנוטיפים הקשורים אליהם במבחן סטטיסטי בודד. עם זאת גישה זו לא מגלה מידע אודות מעורבותם של קשרים ספציפים בתהליך הנחקר.

למרות ההתקדמות המתודולוגית שנעשתה בלימוד שונות בק"ת במ"מ, נכון להיום, ממצאים אשר מתקבלים מניתוח רחב היקף כזה מפורשים לרוב על ידי השוואה איכותית למיפוי מוחי המבוסס על ספרות קודמת. מתודולוגיה שכזאת, אשר לא עושה שימוש בכלים סטטיסטים, טומנת בחובה סיכון לדיווח על תוצאות שווא וכן להחמצת ממצאים רלוונטים. על מנת לפרש את הממצאים באופן מדוייק, יש להשתמש בכלים סטטיסטים. דרך טבעית לעשות זאת היא לבדוק האם קשר בין שני אזורים מוחיים מופיע בתוצאות בכמות גדולה מהצפוי באופן מובהק סטטיסטית (כלומר מועשר). ניתוח העשרה שכזה נמצא בשימוש נרחב מזה זמן רב בתחום הביואינפורמטיקה, והוא הדרך המקובלת לאפיון קבוצות גנים אשר מזוהים בניתוח גנטי מוכוון נתונים.

בעבודה זו נעשה שימוש בנתוני דימות מוחי תפקודי במ"מ על מנת לבחון את האופן שבו סוגים שונים של חוויות מאתגרות רגשית משפיעים על תבניות הק"ת המוחית במצב המנוחה שלאחר החוויה. לצורך כך נעשה שימוש במספר שיטות מוכוונות נתונים, בשילוב עם ניתוחי העשרה כדרך מבוססת לפירוש הממצאים. בהנחה שק"ת במ"מ מכילה בתוכה מידע על נטיות אישיות וכן על חוויות העבר, אנו בוחנים את ההבדלים הבין אישיים בתבניות אלה ואת הקשר ביניהם לבין מדדים התנהגותיים של תגובה רגשית וויסות רגשי. שיערנו כי חוויות מאתגרות רגשית יגרמו לשינוים רחבי היקף בתבניות ק"ת במזמן מנוחה. בנוסף שיערנו כי חלק משינויים אלה יהיו במתאם עם הבדלים בינאישיים במדדים סובייקטיביים של החוויה הרגשית.

אוניברסיטת תל-אביב

הפקולטה לרפואה ע"ש סאקלר

המדרשה לתארים מתקדמים ע"ש מרים ושלדון ג 'אדלסון

החוג :פיסיולוגיה

אפיון בלתי מונחה של רשתות מוחיות המעורבות בעיבוד וויסות רגשי באדם

חיבור לשם קבלת התואר
"דוקטור לפילוסופיה"
מאת עדי מרון-כץ

הוגש לסנאט של אוניברסיטת תל-אביב

אוקטובר 2015